Report
P-16-16
October 2017

KBS-3H – Second data report for the Multi-Purpose Test

Xavier Pintado
Tim Schatz
José-Luis García-Siñeriz
Cristina de la Rosa

SVENSK KÄRNBRÄNSLEHANTERING AB

SWEDISH NUCLEAR FUEL
AND WASTE MANAGEMENT CO

Box 3091, SE-169 03 Solna
Phone +46 8 459 84 00
skb.se

SVENSK KÄRNBRÄNSLEHANTERING

ISSN 1651-4416
SKB P-16-16
ID 1552434
October 2017

KBS-3H – Second data report for the Multi-Purpose Test

Xavier Pintado, Tim Schatz
B+Tech Oy

José-Luis García-Siñeriz, Cristina de la Rosa
Aitemin

Keywords: KBS-3H, Instrumentation, Sensors, Total pressure, Pore water pressure, Gas pressure, Degree of saturation, Volumetric water content, Displacement, Inclination, Strain measurement, Distance blocks, Supercontainer, Transition zone, Compartment plug.

Abstract

The Multi Purpose Test (MPT), currently underway at the Äspö HRL, is a full-scale, demonstration of the KBS-3H reference design. The test is conducted without heating and includes the main KBS-3H components in a partial deposition drift configuration. The test installation was carried out according to the Drainage, Artificial Watering and air Evacuation (DAWE) procedure and the system behaviour is now being monitored through in situ instrumentation. Dismantling and post-mortem analysis will be carried out at a later stage and the timing for this will be dependent on the measured data. MPT activities were started in 2011 as part of the KBS-3H project development (SKB 2012). The MPT is also affiliated with the LucoeX project and is partly funded by the European Commission.

This report presents measurement data from the in situ instrumentation in the MPT during the period from December 7, 2013 to December 31, 2015. A total of 227 sensors were initially installed in the MPT. The pressure development is monitored as total pressure in the rock (27 sensors), bentonite blocks (13 sensors) and plug (3 sensors). Additionally, pore pressure is measured in the rock (27 sensors) and bentonite blocks (23 sensors). The saturation process is followed by measuring the relative humidity (34 sensors), suction (32 sensors) and volumetric water content (13 sensors). The movements of the components are determined with extensometers (13 sensors) and inclinometers (6 sensors). The outflow through the plug is measured outside the drift. The strains on the Supercontainer and the plug are measured with strain gauges (8 on the Supercontainer and 24 on the plug). A set of three gas pressure sensors were also installed.

Some of the sensors (33) were enabled to transmit signals wirelessly. Seven transmitters and two receivers were installed for this purpose. Wireless signal transmission is a novel technique in nuclear waste management and its development is advanced in the MPT.

This is the second data report for the MPT, which includes monitored output to 31 December 2015 for the majority of the sensors; psychrometer data through January 2016 is also presented. The first data report contained monitored output to 30 June 2014.

The KBS-3H design has been developed jointly by SKB and Posiva since 2002. This report has been prepared within the project phase “KBS-3H – System Design 2011–2016”.

Sammanfattning

Multi Purpose Test (MPT) är en fullskaledemonstration utav horisontell deponering, KBS-3H, vilket installerats i enlighet med aktuell referensdesign, Drainage, Artificial Watering and air Evacuation (DAWE). MPT inkluderar huvudkomponenterna i KBS-3H designen men utförs utan värmare. Testet installerades 2013 i Äspö HRL och moniteras sedan dess med in situ instrumentering.

Aktuell plan är att bryta testet om ett antal år och analysera hur det har utvecklats. Tidpunkten för brytningen kommer att avgöras baserat på mätdata från testet.

Arbetet med MPT påbörjades 2011 inom ramen för KBS-3H projektet (SKB 2012). Testet är även en del utav EU projektet LucoeX och därigenom delvis finansierat utav Europeiska kommissionen.

Denna rapport presenterar data från in situ instrumenteringen mellan teststart den 7:e december 2013 och den 31:e december 2015. Totalt har 227 sensorer installerats i MPT. Tryckutvecklingen moniteras som totaltryck i berget (27 sensorer), i bentonitblocken (13 sensorer) och vid pluggen (3 sensorer). Dessutom mäts portrycket i berget (27 sensorer) och i bentonitblocken (23 sensorer). Mättnadsprocessen följs genom att mäta vatteninnehållet (34 sensorer), sug (32 sensorer) och volymetriskt vatteninnehåll (13 sensorer). Komponenternas rörelser mäts med extensometrar (13 sensorer) och inklinometrar (6 sensorer). Eventuellt läckage genom pluggen moniteras med mätvall direkt utanför pluggen. Spänningen i metallkomponenterna mäts med töjningsgivare (8 st på Supercontainern och 24 st på pluggen). Tre gastrycksgivare är också installerade i testet.

Ett antal sensorer (33) utnyttjar ett trådlöst system för att skicka sina signaler. Sju sändare och två mottagare är installerade för detta ändamål. Trådlös teknik är relativt ny i denna typ av installation och har tagit ett steg framåt i samband med MPT.

Detta är den andra datarapporten från MPT, och den inkluderar data fram till den 31:e december 2015 för huvuddelen av sensorerna med något undantag där även data för januari 2016 är inkluderat. Den första datarapporten innehöll data fram till den 30:e juni 2014.

KBS-3H designen utvecklas gemensamt av SKB och Posiva Oy sedan 2002 och denna rapporten har skrivits inom ramen för projektfas ”KBS-3H – System Design 2011–2016”.

Contents

1 Introduction

1.1 General

The common goal of SKB and Posiva is the disposal of spent nuclear fuel from Swedish and Finnish nuclear power plants at depth in crystalline bedrock while ensuring the safety of the surface living environment well into the future. The method selected for the final repository is the KBS-3 multi-barrier approach (Figure 1-1).

The KBS-3V reference design employs vertical disposal of the spent nuclear fuel canisters whereas the KBS-3H alternative design considers horizontal disposal of the canisters. Both design options are being examined. The current SKB and Posiva repository R&D programmes are described in the RD&D Programme (SKB 2013) and YJH-2015 (Posiva 2015) reports, respectively.

The Multi-Purpose Test (MPT), currently underway at the Äspö HRL, is a full-scale, demonstration of the KBS-3H design carried out at −220 m. The test is conducted without heating and includes the main KBS-3H components in a partial deposition drift configuration (Figure 1-2). The test installation was carried out according to the Drainage, Artificial Watering and air Evacuation (DAWE, see Section 1.2) procedure and the system behaviour is now being monitored through in situ instrumentation. Dismantling and post-mortem analysis will be carried out at a later stage and the timing for these activities will be dependent on the measured data.

MPT activities were started in 2011 as part of the KBS-3H project development (SKB 2012). The MPT is also affiliated with the LucoeX project and is partly funded by the European Commission.

The initial conditions of the bentonite components used in the MPT are described in Table 1-1 (Johanesson 2014).

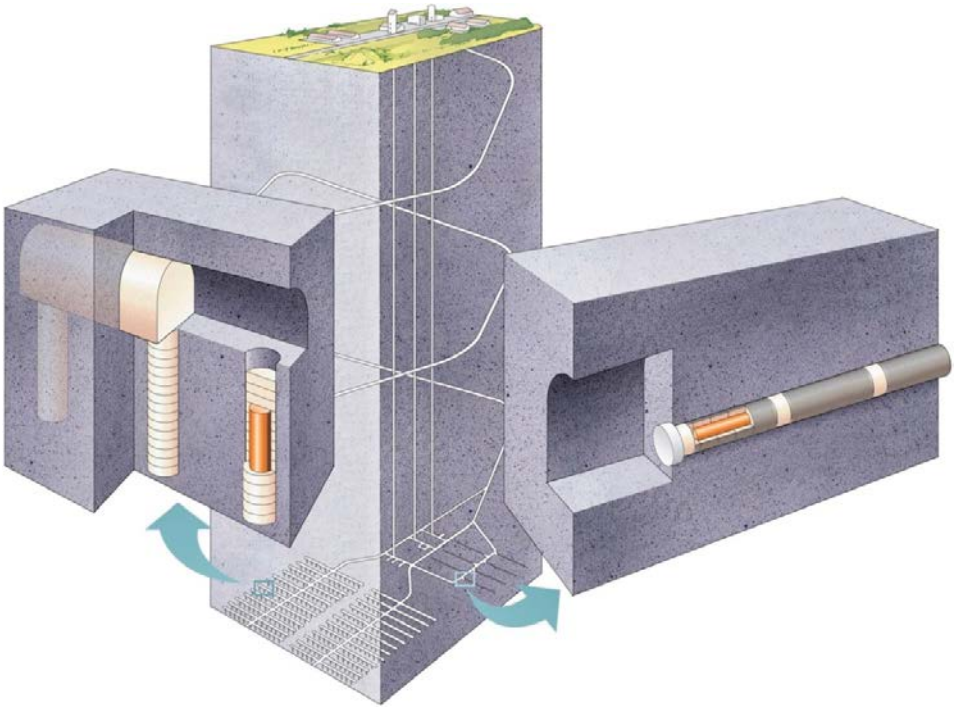

Figure 1-1. *Schematic illustration of the KBS-3 method with its three barriers: the canister, the buffer and the rock. The vertical reference design (KBS-3V) is illustrated to the left and the horizontal alternative (KBS-3H) to the right.*

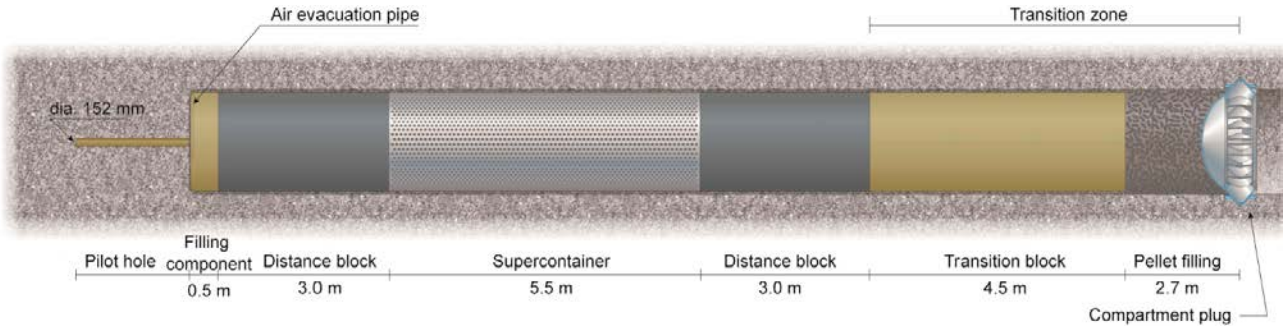

Figure 1-2. *The main KBS-3H components (Supercontainer, distance blocks and a compartment plug with transition zone) as configured in the Multi-Purpose Test. The filling component has the same properties as the distance and transition blocks. The diameter of the drift is 1 850 mm.*

Table 1-1. Initial conditions of the MPT bentonite components.

Type	Bulk density (kg/m^3)	Gravimetric water content (%)	Degree of saturation (%)	Dry density (kg/m^3)	Volumetric water content (m^3/m^3)
Distance Blocks/Transition blocks/Filling component	2 071	20.6	92.4	1 718	0.35
SC ring blocks	2 106	11.0	65.6	1 898	0.21
SC end blocks	2 069	17.2	83.2	1 766	0.30
Pellet filling	1 000	21.0	32.8	826	0.17

Inflow into the 95-meter drift has been monitored since it was excavated in 2005 up to the point the test was assembled. Initially, the inflow was approximately 12 l/min but by 2007 it had naturally come down to around 5 l/min. In 2007–2008 the five positions of highest inflows into the drift were grouted. As a result, the inflow was reduced to approximately 0.4 l/min (Eriksson and Lindström 2008). By 2011 the inflow had naturally decreased to roughly 0.25 l/min.

In order to monitor the inflow into the MPT drift, a set of wooden weirs were installed along its length (Figure 1-3). The weirs were placed where the rock conditions allowed it, but the positions match up quite well with the component lengths. Inflow data is presented in Table 1-2.

A summary of the inflow data is provided below:

Full MPT section two months prior to installation: ~32 l/day (22.2 ml/min).

Supercontainer section in 2012: ~19 l/day (13.2 ml/min).

Inner distance block section in 2012: ~8 l/day (5.6 ml/min).

Outer distance block, transition block and pellets section in 2012: ~3 l/day (2.1 ml/min).

It can be noted that the inflow into the MPT drift is well below 0.1 l/min which is the KBS-3H limit for emplacement of a Supercontainer.

Figure 1-3. *Wooden weir used to enable monitoring of groundwater inflow into the MPT drift.*

Table 1-2. Inflows (l/min) into the MPT drift by position from end of drift during 2011–2013, possible outliers are marked in red. Measurements were limited in 2013 due to development work on the deposition machine.

Date	4.07 m from end of drift	9.07 m from end of drift	11.17 m from end of drift	17.87 m from end of drift	19.27 m from end of drift	34.47 m from end of drift	94.47 m from end of drift	Date	18.47 m from end of drift
2011-09-20	0.0060	0.0140		0.0240		0.1480	0.2200	2013-08-23	0.0228
2011-09-21	0.0060	0.0230	0.0290	0.0220		0.1460	0.2200	2013-08-26	0.0220
2011-09-22	0.0065	0.0215	0.0215	0.0225		0.1470	0.2100	2013-09-09	0.0216
2011-10-06	0.0062	0.0182	0.0212	0.0217		0.1560	0.2100	2013-09-10	0.0236
2011-10-20	0.0058	0.0200	0.0202	0.0215		0.1500	0.2130	2013-09-12	0.0230
2011-11-08	0.0060	0.0200	0.0205	0.0205		0.1540	0.1980	2013-09-16	0.0232
2011-11-21	0.0055	0.0195	0.0205	0.0210		0.1360	0.1930	2013-09-18	0.0224
2011-12-06	0.0060	0.0194	0.0197	0.0205		0.1330	0.1930	2013-09-19	0.0224
2012-01-10	0.0060	0.0195	0.0195	0.0205		0.1350	0.1930	2013-09-23	0.0224
2012-05-22	0.0056	0.0190	0.0190	0.0205		0.1700		2013-09-25	0.0200
2012-06-07	0.0053	0.0186	0.0190	0.0193		0.1330	0.1830	2013-09-30	0.0280
2012-06-28	0.0056	0.0190	0.0190	0.0198	0.0202	0.1330	0.1900	2013-10-04	0.0228
2012-07-18	0.0055	0.0190	0.0190	0.0200	0.0260	0.1300	0.1830		
2012-09-27	0.0050	0.0162			0.0162	0.1280			
2012-10-17	0.0050	0.0180	0.0180	0.0180	0.0200	0.1280	0.1800		

* Inflows tend towards lower rates over time.

Average inflows along the test section of the drift are presented in Figure 1-4.

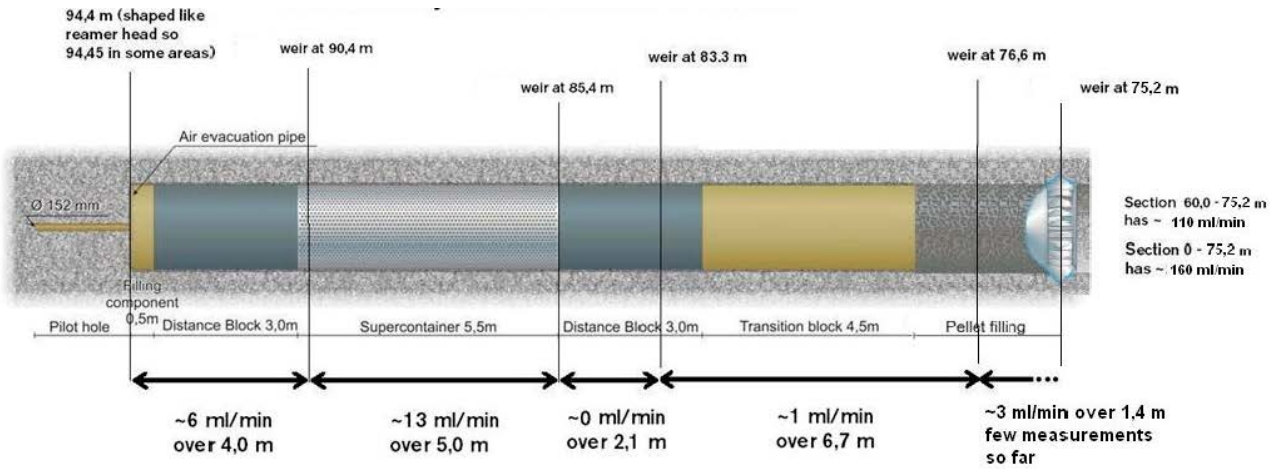

Figure 1-4. *Average inflows into different sections of the drift since 2011.*

1.2 Purpose and scope

The objective of the MPT instrumentation is to study the buffer and filling component behavior during the early evolution of the system.

This report presents the MPT instrumentation scheme and the associated set of data from December 7, 2013 at 08:30 (day 1, initiation of DAWE procedures) to December 31, 2015 at 23:55 (day 754). At 14:50 on December 7, 2013, increasing pressure due to the DAWE filling was observed and a maximum pressure of 235 kPa was reached at 15:15 after which the filling was stopped.

Practical details of the sensor and component installation procedures were reported previously (Kronberg 2016) and a first report of the data measured during the first six months was also published (Pintado et al. 2015). A set of key dates for the MPT are shown in Table 1-3.

Table 1-3. Key dates for the MPT.

Activity	Date
1st FAT in Madrid	19.04.2013
2nd FAT in Madrid	25.07.2013
3rd FAT in Äspö (wireless sensors)	21.10.2013
SAT	03.12.2013
DAWE procedure	07.12.2013
First inspection	27.01.2014
Second inspection	10.03.2015
Change of power supply in Datalogger	05.06.2015
Initial data report	01.09.2015

FAT: Factory Acceptance Test.
SAT: Site Acceptance Test.

2 Geometry and coordinate system

Given that the Supercontainer, distance and transition blocks are assembled in a facility above ground and installed as full components (packages), the sensor coordinates cannot be ascertained upon installation in their final location. Instead, the position of each drift component is determined and the sensor coordinates calculated based on these determinations and the engineering schematics. Adding to the complexity is that the sections are mirrored when comparing the above ground sensor installation with the below ground installed component, i.e. when looking at a sensor being installed to the left side on top of a bentonite block in the assembly facility that sensor will eventually be located to the right inside the drift (when looking from the outside and into the drift).

The MPT instrumentation was set up according to the coding system presented in Section 2.1 with regard to the onsite Data Acquisition System (DAS). From this standpoint the center of the plug collar is regarded as the zero position.

Data from the DAS is fed into SKB's Sicada database under a different coding system, which is described in Section 2.2. For this purpose, the drift end is considered to be position zero.

2.1 Data Acquisition System (DAS)

The frame of reference for the positions of the sensors in the MPT is indicated in Figure 2-1.

Three coordinates are used to identify specific positions in the drift:

r = radial distance (mm) from the center of the sensor to the drift axis,

α = clockwise angle (degrees) from the drift axis for the rock sensors and counterclockwise angle from the drift axis for the block sensors, relative to the vertical diameter of the drift,

d = distance (mm) from the origin of the test area (middle of the plug collar) towards the rear of the drift.

This is a relative coordinate system referenced to the drift axis with origin in the plug. The absolute (topographic) coordinate system is given by the position of the drift in the Äspö HRL.

It should be noted that the total pressure sensors in bentonite blocks coded as 0990 do not follow the reference coordinate system described above. This discontinuity results from two of the total pressure sensors being moved to the plug after it was decided that more information about the pressure on the plug would be necessary. It was not possible to add these sensors prior to drift component installation because the delivery time did not fit with the schedule of the test.

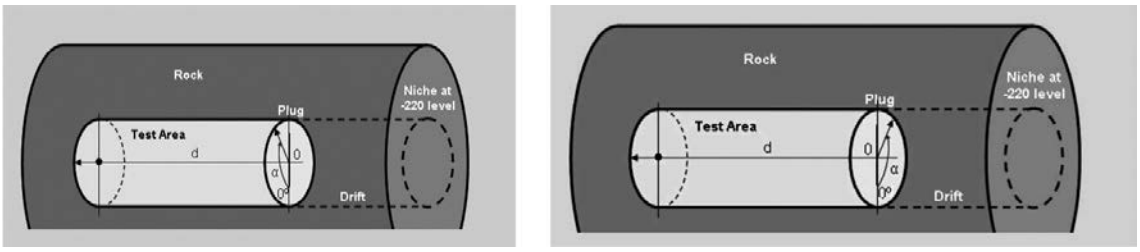

Figure 2-1. *Frame of reference for MPT rock sensors (left) and frame of reference for MPT block sensors (right).*

Coding system

The sensors are identified according to the following code:

SS-DDDD-N where:

- SS refers to sensor type (see Table 2-1).
- DDDD refers to the position at which the sensor is installed (depth in cm from the center of the plug collar).
- N refers to sensor ordering and is only necessary in cases where several sensors of the same type are installed in the same zone and at the same depth. Sensor ordering starts by 1 and increases with the radius r. For the same radius, it increases with the value of angle α taking into account that the view is towards the drift entrance.

Table 2-1. Codes for types of sensors.

Code	Sensor
TP	Total pressure
PP	Pore pressure
WC	Water content capacitive
WP	Water content psychometric
WF	Water content soil moisture
DS	Displacement Supercontainer
DB	Displacement bentonite
DC	Displacement collar
IS	Inclination Supercontainer
IB	Inclination bentonite
SG	Strain Gauge
GP	Gas Pressure
FM	Flow Meter

2.2 Sicada

Sicada is SKB's main database, and the associated codification for the MPT sensors is as follows:

P XK DDD S N where:

- P refers to object point.
- XK refers to KBS-3H experiment.
- DDD refers to position at which the sensor is installed (depth in dm from the drift front).
- S refers to type of sensor (see Table 2.2).
- N refers to sensor ordering.

Table 2-2. Codes for types of sensors in Sicada codification.

Code	Sensor
T	Total pressure
U	Pore pressure
W	Water content capacitive/psychrometric
D	Displacement Supercontainer/bentonite
I	Inclination Supercontainer/bentonite
S	Strain Gauge

3 Description of the sensors

The different sensors that are placed in the blocks, pellets, Supercontainer, plug and rock are described in this chapter. The sensors have been installed in ten sections (Figure 3-1). The chapter also includes background information regarding sensor distribution and placement.

3.1 Sensor types

Total pressure measurement

Total pressure is the sum of the swelling pressure and the pore water pressure. It is measured with the following sensors:

- Geokon total pressure cells with vibrating wire transducers were installed in the rock wall for measuring axial stress (S1) and radial stress (S2, S4, S7, S8, S9 and S9+) relative to the tunnel axis. Additionally, one of these sensors was placed in the axial direction at the S8/S9 block/block interface. The configuration of this type of sensor in the rock wall is presented in Figure 3-2.
- Geokon total pressure cells with piezo resistive transducers (custom modified by ÅF, Sweden) were installed in bentonite block drift components. Specifically, these cells were placed in ring blocks and end blocks at block/canister interfaces, measuring radially to the drift axis for the former and along the drift axis for the latter, in distance blocks at the Supercontainer endplate/block interface measuring along the drift axis and at the pellet-filling/plug interface measuring along the drift axis. These sensors may not be properly grounded as signals have become rather noisy.
  - The braided shields or screens of the sensor cables in blocks were cut in all cases to be able to place the cables inside the protective housing. Therefore, they are not connected to ground and the signals are relatively noisy. The sensors in the plug have intact screens but their signals are also noisy.

Pore water pressure measurement

Pore water pressure is measured with the following sensors:

- Keller pore pressure piezo resistive sensors were installed outside the test area and the pressure is transmitted through tubing connected to the borehole measurement locations. The tubing is equipped with porous stainless steel filters at the sampling ends. The tubes were filled and purged manually. The configuration of this type of sensor in the rock wall is presented in Figure 3-3. The boreholes are isolated with packer assemblies in Section 9.
- Measurement Specialities 4 arm Wheatstone bridge sensors were installed in the blocks and pellets-filled zones. The measurement of positive pore pressures in the blocks are not expected before several years due to the low hydraulic conductivity of the compacted bentonite (Karnland et al. 2006, Kiviranta et al. 2016) and also due to the time necessary for filling the sensor cavities. Positive pore pressures measured in the early stages of the test are likely due to unanticipated hydraulic connection to the sensors through, e.g., cracks in the blocks.

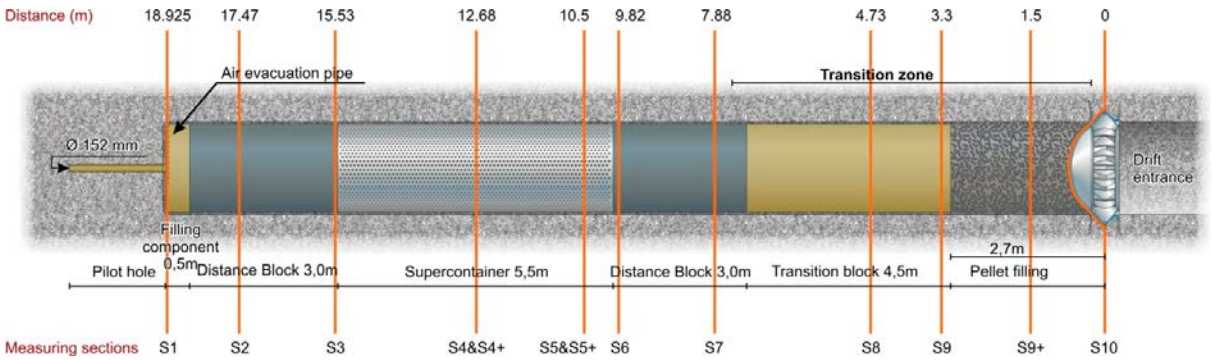

Figure 3-1. *Measurement section locations along the MPT drift (DAS coding, with the plug as position 0).*

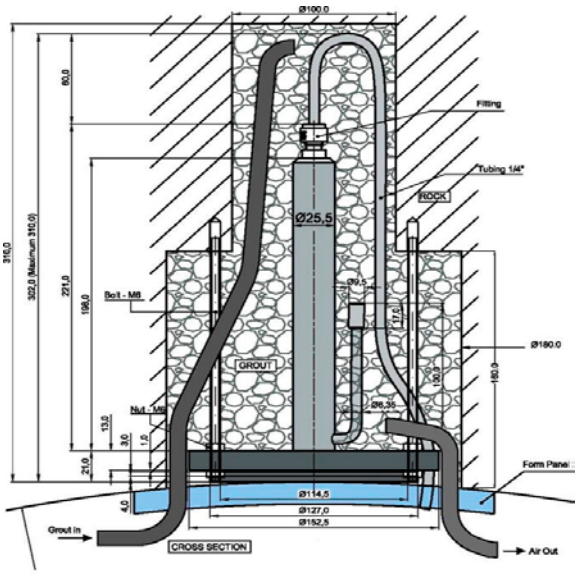

Figure 3-2. *Configuration of Geokon total pressure sensor in the rock wall.*

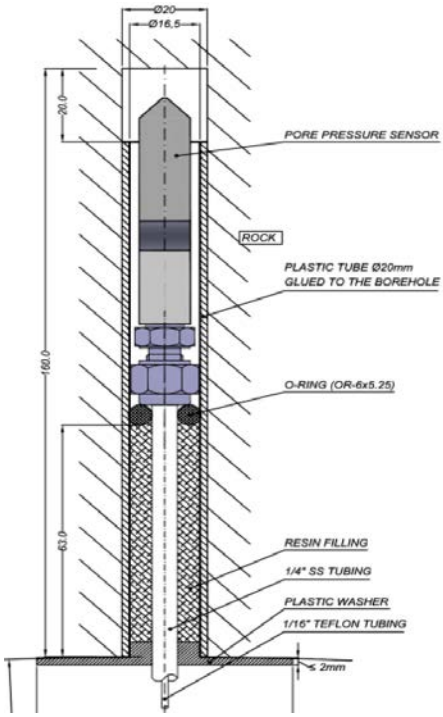

Figure 3-3. *Configuration of Keller pore pressure sensor in the rock wall.*

Gas pressure measurement

Gas pressure is measured with the following sensors:

- Keller pore pressure sensors piezo resistive sensors were installed outside the test area and the pressure is transmitted through tubing connected to the measurement location. The tubing has a porous stainless steel filter at the end.

The main aim for installing these sensors was for measuring the evolution of gas pressure if the DAWE procedure was not used. Essentially these sensors did end up measuring the water pressure in the gap and, as this pressure rose quite quickly after the DAWE procedure, the sensors were over ranged almost from the beginning of the test. For this reason, the sensors were changed to new ones with higher range. The new range was 0–3 MPa absolute and the change was made on 12 December 2014, 370 days after starting the test.

Water saturation measurement

The water saturation in the bentonite blocks is recorded by measuring the relative humidity in the pore system, which can be converted to total suction (negative water pressure). The following techniques and devices are used:

- Aitemin SHT75 v3 capacitive hygrometer were installed. The measuring range for these sensors is from 0 to 100 % RH but they are not accurate enough for measuring the saturation process when the suction is low (above 95 % RH). For this reason, psychrometers were also installed.
- Wescor type PST-55 thermocouple psychrometer with modification by Aitemin were installed. The effective measuring range for these sensors is from 95 to 99.6 % RH corresponding to suction between 54 to 6 916 kPa at 20 °C. The psychrometer response (Figure 3-4) is not the same for all soils and changes as function of the soil and the environment. In particular, the plateau region can be narrower or wider and appear at different times. Interpretation of the psychrometer signals requires parameter values in order to represent the different regions of the output trace versus time. The signal corresponding to the plateau region is explicitly used for suction calculation. Therefore, it is important to check the consistency of the input parameters and time constants over long periods of signal collection. More information about this sensor can be found in Wescor (2014).

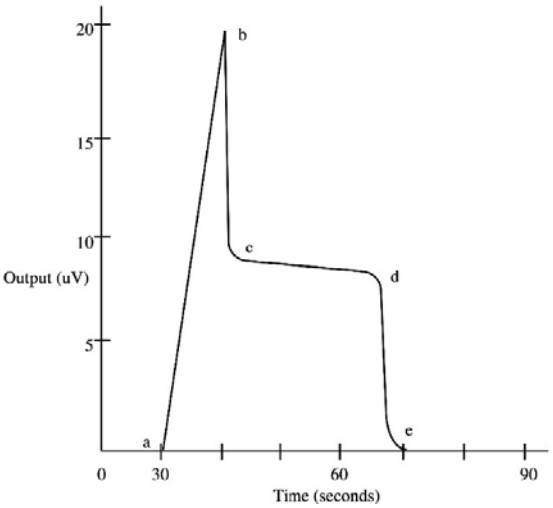

Figure 3-4. *General psychrometer response during the measurement process (Gensler 1986).*

Volumetric water content measurement

The volumetric water is defined as V_ω/V_T (volume of water/total volume) and is measured in the MPT drift as follows:

- Soil moisture sensors (ThetaProbe type ML2x, Delta-T Devices with custom modification by Aitemin) were installed in the bentonite blocks. The measuring range should cover all possible volumetric water contents. These sensors consist of a waterproof PVC housing, which contains the electronics, and, at the other end, four sharpened stainless steel rods that are inserted into the material to be analyzed. Given the swelling capacity of the bentonite buffer, the standard housing of the units was reinforced with a SS316L casing provided with a fitting for ¼" OD tubing (to protect the cable). Any remaining empty space in the casings was filled with resin. The output signal of these sensors is 0 to 1 V DC (Figure 3-5) for a range of soil dielectric constants, ε, from 1 to 32, which corresponds to a linear range of 0 to approximately 0.6 m^3/m^3 volumetric moisture content for generalized mineral soils.

In order to explicitly determine the relationship between the measured signal and the volumetric water content, soil-specific calibrations were carried out with compacted bentonite samples for three different sensors (Table 3-1 and Figure 3-6). The following linear relationship was found:

$$\frac{V_\omega}{V_T} = 0.601 \times signal\ (V) - 0.163 \qquad (3\text{-}1)$$

The sensor calibrations were performed for samples that were compacted with the sensor needles in place. This approach was not possible for the MPT blocks as the sensor probe needles could not be installed/pushed into the compacted MPT blocks. For this reason, holes were drilled in the blocks. The sensor probe needles were inserted into these holes and bentonite powder was added to fill the holes as completely as possible. As such, the sensors are not in direct contact with the MPT blocks in their initial state (see Table1-1) or further evolved states to known degree, and the resulting measurements may not reflect actual block conditions.

The soil moisture sensors were functioning adequately to around day 500. At this time the power supply in the datalogger failed and was changed. The signals from these sensors became unstable thereafter.

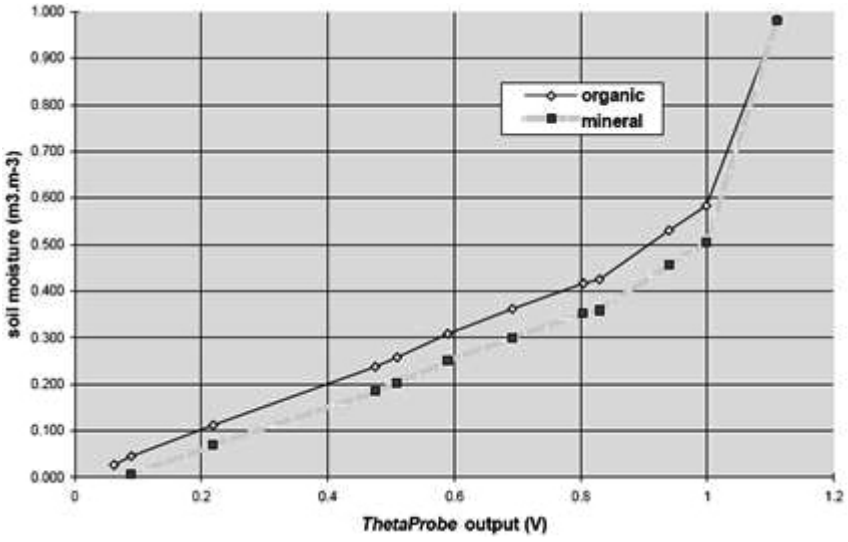

Figure 3-5. *Relationship between ThetaProbe output and soil moisture content for generalized mineral and organic soils (Delta-T Devices 1999).*

Table 3-1. Soil moisture sensor calibration test results.

Sample	Volumetric water content	ML2x-397/025	ML2x-397/046	ML2x-397/022	Average
1	0.426	0.953 V	0.975 V	0.959 V	0.962 V
2	0.299	0.885 V	0.886 V	0.887 V	0.886 V
3	0.304	0.875 V	0.885 V	0.864 V	0.874 V
4	0.251	0.679 V	0.673 V	0.696 V	0.696 V
5	0.305	0.776 V	0.779 V	0.789 V	0.781 V
6	0.370	0.903 V	0.908 V	0.909 V	0.907 V
7	0.122	0.438 V	–	0.437 V	0.437 V
8	0.157	0.508 V	–	0.513 V	0.510 V

Strain measurement

Strains on the Supercontainer and plug face are measured with the following strain gauges:

- HBM 1-LY41-3/350 with a range of 0–50 000 µm/m (plug face).
- HBM 1-XY101-3/350 with a range of 0–50 000 µm/m (Supercontainer).

Displacement measurement

Displacements within the MPT drift are measured as follows:

- RDP LVDT sensors with a range ±25 mm were installed inside the drift to measure displacements of the Supercontainer with respect to the rock wall (Figure 3-7). In these cases, positive displacements indicate movement of the Supercontainer away from the rock. LVDT sensors were also installed in drift section 5 to measure the displacement of bentonite blocks with respect to the canister where positive displacements indicate movement away from the canister. Finally, in drift section 9, LVDT sensors were installed to measure the displacement between two blocks and where any positive increase indicates that the space between the blocks is increasing.
- RDP LVDT sensors with a range ±12.5 mm were installed outside the drift on the plug face to measure displacement of the plug along the drift axis. Positive displacements indicate movement of the plug toward the drift.

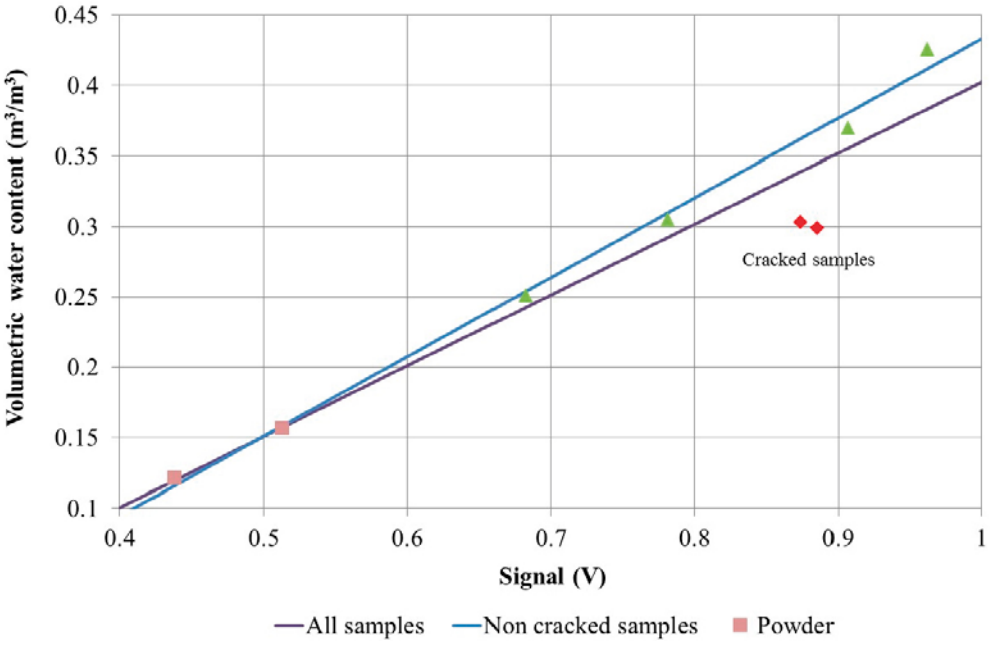

Figure 3-6. *Soil moisture sensor calibration test results. Points plotted as green triangles represent intact calibration samples and points plotted as red diamonds represent cracked samples. The latter were not used to determine the calibration relationship.*

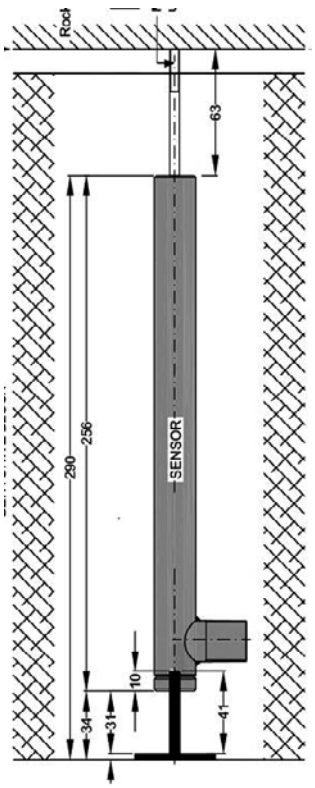

Figure 3-7. *LVDT installation for measuring the displacements of the Supercontainer respect the rock wall.*

Ideally these sensors would be installed measuring zero displacement but they were configured in a workshop and it is possible that they experienced some movement during emplacement of the blocks and Supercontainer.

Inclination measurement

Inclinations of the Supercontainer and bentonite blocks are measured as follows:

- Measurement Specialities DPL series inclinometers with a range of ±5° were installed in bentonite blocks in sections S2 and S7. The x-axis for the inclinometers corresponds to the longitudinal direction along the bottom of the drift and a positive angle response indicates an incline (counter clockwise rotation) away from the plug face. The y-axis for the inclinometers corresponds to the lateral direction of the drift and a positive response indicates an incline (clockwise rotation) away from the rock wall as drawn in Figure 2-1.

In section S4, the inclinometers were installed completely opposite to those in sections S2 and S7. As such, the y-axis for the inclinometers corresponds to the longitudinal direction along the bottom of the drift and a positive response indicates an incline (clockwise rotation) away from the rear of the drift and the x-axis corresponds to the lateral direction of the drift and a positive response indicates a decline (counter clockwise rotation) toward the rock wall as drawn in Figure 2-1.

3.2 Installed sensors

The locations of the measurement sections along the drift are presented in Figure 3-1 and the type and number of sensors are presented in Table 3-2.

Table 3-2. Distribution of sensors by sections showing the distribution between those that are read by means of conventional cables (wired), wireless or tubing that transmits pressure.

	Sections												
Sensors	**S1**	**S2**	**S3**	**S4**	**S5**	**S6**	**S7**	**S8**	**S9**	**S9+**	**S10**	**Out**	**Tot**
TP rock	5	4		2			4	4	2	6			**27**
TP plug											2+1		**3**
TP buffer				4	4	4			1				**13**
PP rock short	1	4					4						**9**
PP rock borehole									18				**18**
PP buffer		1+3		4	2+3		1+3				3+3		**23**
WC		3+3		4	2+3		3+3	4+3	3+3				**34**
WP		6		4	4		6	6	6				**32**
WF	1	2		2	2		2	2	2				**13**
DS				4	4								**8**
DB									2				**2**
DC												3	**3**
IS				2									**2**
IB		1					1		1+1				**4**
GP	1					1					1		**3**
SG					8							24	**32**
FM												1	**1**
Total	**8**	**27**	**0**	**26**	**32**	**5**	**27**	**19**	**39**	**6**	**10**	**28**	**227**
Tubings	**2**	**4**	**0**	**0**	**0**	**1**	**4**	**0**	**0**	**0**	**1**	**0**	**12**
Wireless	**0**	**6**	**0**	**0**	**6**	**0**	**6**	**5**	**6**	**0**	**4**		**33**
Wired	**8**	**21**	**0**	**26**	**26**	**5**	**21**	**14**	**33**	**6**	**6**	**28**	**194**

3.3 Reasoning behind the distribution of sensors

This section introduces the reasoning behind the instrumentation in each section.

Section S1

This section is in contact with the rock at the end of the drift. The instrumentation was installed to provide an indication of the swelling pressure evolution at five points in contact with the rock. A pore pressure transducer was installed to measure the drain effect inside the rock. A soil moisture sensor was installed to yield information about the evolution of the water content of the buffer (inner filling block).

A filter connected with steel tubing was installed to be able to measure the remaining gas pressure at the upper part of the drift as well as to take samples for compositional analysis. Due to the DAWE procedure, this system was flooded early on and as a result no gas pressure was measured.

Sections S2

Section S2 corresponds to the distance block on the back end of the Supercontainer. Four pore pressure transducers were installed to measure the drain effect inside the rock walls and four total pressure cells were installed to track the swelling pressure evolution in contact with the rock. Within the block, the distribution of the sensors varies radially in order to study the evolution of the saturation process from the rock to the inner part of the block. The capacitive hygrometer and the psychrometers were installed to monitor the saturation process over the full range. The soil moisture sensors were installed to measure the volumetric water content. Pore pressure transducers were installed to monitor the positive pressure when the buffer is saturated. An inclinometer was installed to provide information about possible block tilting.

Section S3

This section only has a radio module to aid in wireless signal transmission through the Supercontainer.

Sections S4 & S4+

Located in the middle of the Supercontainer, the instrumentation in this section was designed to monitor the swelling pressure development from the ring blocks against the Supercontainer shell and the canister surface. Capacitive hygrometers and psychrometers were emplaced to follow the evolution of the saturation process in the blocks from the rock to the inner part of the buffer. Two soil moisture sensors were installed to measure the volumetric water content and four pore pressure transducers were installed to follow the positive pressure when the buffer saturates. Two inclinometers were included to provide information about package tilting (one close to the shell and the other close to the canister) and four extensometers were installed to monitor movements.

Sections S5 & S5−

This section, located close to the canister end, was instrumented with pore pressure transducers, capacitive hygrometers, psychrometers and soil moisture sensors for a variety of purposes: 1) to follow the saturation process inside the Supercontainer, 2) to track swelling pressure developments against the canister, 3) to measure the saturation process in the block and 4) to monitor canister movements with respect to the Supercontainer shell.

Instrumentation in this section is also devoted to monitoring the mechanical behavior of the Supercontainer courtesy of eight strain gauges which were fixed to the Supercontainer shell to detect failures.

Section S6

The instrumentation in this section was installed to monitor the development of swelling pressure against the front end of the Supercontainer from the adjacent distance block. A filter connected with a steel tube was installed to be able to measure the gas pressure due the possible corrosion of the Supercontainer as well as to collect samples for compositional analysis. Due to the DAWE procedure, this sensor was flooded from the beginning of the test.

Section S7

Section S7 corresponds to the distance block on the front end of the Supercontainer. This section was instrumented similarly to that of S2.

Section S8

This section corresponds to the transition block and it was instrumented to follow the saturation process by means of suction and water content sensors inside the block and total pressure cells installed at the rock walls.

Section S9

The instrumentation in this section was installed to monitor the influence of pellet-filled zone on the transition block. A total pressure sensor is installed for assessing the swelling pressure developed by the pellets on the block. Soil moisture sensors and suction instruments were installed in the last block on the side opposite to the pellets in order to avoid quick saturation of the sensors during the DAWE. The swelling pressure development against the rock is also monitored in this section. Sensors were installed in the block to monitor possible movements. Pore pressure sensors were installed in the three boreholes in this drift section to provide information about groundwater flow.

Section S9+

Section S9+ in the pellet-filled zone is located 0.9 m from the plug and was added in order to install the six total pressure cells that could not fit in sections S9 & S10 for practical reasons.

Section S10

This section is mainly for studying the swelling pressure development against the plug. The instrumentation has a dual purpose. On the one hand it provides information about the stresses against the plug (total pressure in some locations) and on the other it provides information to compare with the swelling pressure developed in the Supercontainer side (from section 4 to the plug) for studying the development of friction between the bentonite and the rock. In order to be able to measure the effective pressure, pore pressure sensors were installed. There was also a gas pressure sensor in this section but it was flooded from the beginning due to the DAWE procedure.

Plug Face

Sixteen strain gauges were installed on the external plug face to monitor the stress state. A temperature sensor was installed to allow for temperature correction of the strain gauge measurements. Three displacement transducers were installed to provide information about plug movements.

A flow monitoring system was installed on the drift floor just outside the plug face to measure water leakage through the plug.

In the following Chapters (4–6), outer sensor positions refer to those sensors located at the interface between the MPT drift boundaries (i.e. rock wall or plug) and drift components whereas inner sensor positions refer to those sensors located within MPT drift components.

4 Distance blocks

The sensors in the distance blocks are located in drift sections S-1, S-2, S-6 and S-7 (Figure 3-1).

4.1 Inner sensor positions

The location of the inner sensors and other information is presented in Table 4-1 (drift section 1), Table 4-2 (drift section 2), Table 4-3 (drift section 6) and Table 4-4 (drift section 7).

Table 4-1. Numbering and position of inner distance block sensors in drift section 1.

	Coordinate system ÄSPÖ 96							
Point No.	Easting [m]	Northing [m]	Point Elevation [m]	Drawing label	Sensor code in SICADA	Sensor code in SCADA	Assembly tag label	Manufacturer
1	1904.721	7253.178	−217.881	WF	PXK003WF1	WF-1867	ML2x377/048	Delta-T
2	1904.870	7253.179	−216.447	GP	PXK004GP1	GP-1856	GP 1892-1	Keller

Table 4-2. Numbering and position of inner distance block sensors in drift section 2.

	Coordinate system ÄSPÖ 96							
Point No.	Easting [m]	Northing [m]	Point Elevation [m]	Drawing label	Sensor code in SICADA	Sensor code in SCADA	Assembly tag label	Manufacturer
1	1906.208	7253.179	−216.564	WF2	PXK017WF2	WF-1722-2	WF 1722-2	Delta-T
2	1906.208	7252.972	−216.592	WP4	PXK017WP4	WP-1722-4	WP 1722-4	Wescor
3	1906.207	7253.386	−216.591	WC5	PXK017WC5	WC-1722-5	WC 1722-5	Aitemin
4	1906.082	7253.179	−216.809	IB1	PXK016IB1	IB-1722	IB 1722-1	Measurement specialities
5	1906.203	7252.613	−216.798	PP3	PXK017PP3	PP-1722-3	Wireless	Measurement specialities
6	1906.202	7253.745	−216.798	PP2	PXK017PP2	PP-1722-2	Wireless	Measurement specialities
7	1906.195	7253.114	−217.123	WP1	PXK017WP1	WP-1722-1	WP 1722-1	Wescor
8	1906.195	7253.244	−217.123	WC2	PXK017WC2	WC-1722-2	Wireless	Aitemin
9	1906.191	7252.380	−217.314	WP5	PXK017WP5	WP-1722-5	WP 11722-5	Wescor
10	1906.189	7252.381	−217.414	WC6	PXK017WC6	WC-1722-6	WC 1722-6	Aitemin
11	1905.940	7253.842	−217.303	WSU	Transmitter	WSU-S2	Wireless	Aitemin
12	1906.189	7253.978	−217.314	WP3	PXK017WP3	WP-1722-3	WP 1722-3	Wescor
13	1906.187	7253.978	−217.414	WC4	PXK017WC4	WC-1722-4	Wireless	Aitemin
14	1906.184	7253.054	−217.581	WP2	PXK017WP2	WP-1722-2	WP 1722-2	Aitemin
15	1906.184	7253.304	−217.581	WC1	PXK017WC1	WC-1722-1	Wireless	Wescor
16	1906.173	7252.779	−218.057	PP4	PXK017PP4	PP-1722-4	PP 1722-4	Measurement specialities
17	1906.171	7252.972	−218.137	WP6	PXK017WP6	WP-1722-6	WP 1722-6	Wescor
18	1906.170	7253.179	−218.163	WF1	PXK017WF1	WF-1722-1	WF 1722-1	Delta-T
19	1906.170	7253.386	−218.137	WC3	PXK017WC3	WC-1722-3	WC 1722-3	Aitemin
20	1906.172	7253.580	−218.057	PP1	PXK017PP1	PP-1722-1	Wireless	Measurement specialities

Table 4-3. Numbering and position of inner distance block sensors in drift section 6.

	Coordinate system ÄSPÖ 96							
Point No.	Easting [m]	Northing [m]	Point Elevation [m]	Drawing label	Sensor code in SICADA	Sensor code in SCADA	Assembly tag label	Manufacturer
1	1913.463	7252.635	−217.644	TP3	PXK090TP3	TP-0990-2	TP 0990-3	Geokon / ÅF
2	1913.461	7253.745	−217.644	TP5	PXK090TP5	TP-0990-4	TP 0990-5	Geokon / ÅF
3	1913.449	7253.190	−218.199	TP2	PXK090TP2	TP-0990-1	TP 0990-2	Geokon / ÅF
4	1913.704	7253.190	−216.787	GP1	PXK092GP1	GP-0967	GP 0967-1	Keller
5	1913.462	7253.190	−217.088	TP4	PXK092TP4	TP-0990-3	TP 0990-4	Geokon / ÅF

Table 4-4. Numbering and position of inner distance block sensors in drift section 7.

	Coordinate system ÄSPÖ 96							
Point No.	Easting [m]	Northing [m]	Point Elevation [m]	Drawing label	Sensor code in SICADA	Sensor code in SCADA	Assembly tag label	Manufacturer
1	1915.653	7252.628	−217.158	PP3	PXK112PP3	PP-0820-3	Wireless	Measurement specialities
2	1915.657	7252.986	−216.952	WP4	PXK112WP4	WP-0820-4	WP 0820-4	Wescor
3	1915.658	7253.193	−216.924	WF2	PXK112WF2	WF-0820-2	WF 0820-2	Delta-T
4	1915.657	7253.401	−216.951	WC5	PXK112WC5	WC-0820-5	WC 0820-5	Aitemin
5	1915.651	7253.759	−217.158	PP2	PXK112PP2	PP-0820-2	Wireless	Measurement specialities
6	1915.645	7253.128	−217.483	WP1	PXK112WP1	WP-0820-1	WP 0820-1	Wescor
7	1915.644	7253.258	−217.483	WC2	PXK112WC2	WC-0820-2	Wireless	Aitemin
8	1915.641	7252.395	−217.673	WP5	PXK112WP5	WP-0820-5	WP 0820-5	Wescor
9	1915.639	7252.395	−217.773	WC6	PXK112WC6	WC-0820-6	WC 0820-6	Aitemin
10	1915.634	7253.068	−217.940	WP2	PXK112WP2	WP-0820-2	WP 0820-2	Wescor
11	1915.633	7253.319	−217.940	WC1	PXK112WC1	WC-0820-1	Wireless	Aitemin
12	1915.639	7253.992	−217.673	WP3	PXK112WP3	WP-0820-3	WP 0820-3	Wescor
13	1915.636	7253.992	−217.773	WC4	PXK112WC4	WC-0820-4	Wireless	Aitemin
14	1915.623	7252.793	−218.416	PP4	PXK112PP4	PP-0820-4	PP 0820-4	Measurement specialities
15	1915.621	7252.986	−218.496	WP6	PXK112WP6	WP-0820-6	WP 0820-6	Wescor
16	1915.620	7253.193	−218.522	WF1	PXK112WF1	WF-0820-1	WF 0820-1	Delta-T
17	1915.620	7253.401	−218.496	WC3	PXK112WC3	WC-0820-3	WC 0820-3	Aitemin
18	1915.622	7253.594	−218.416	PP1	PXK112PP1	PP-0820-1	Wireless	Measurement specialities
19	1915.532	7253.193	−217.175	IB1	PXK109IB1	IB-0820	IB 0820-1	Measurement specialities
20	1915.449	7253.856	−217.664	WSUS7	Transmitter	WSU-S7	Wireless	Aitemin

4.2 Inner sensor results and comments

4.2.1 Relative humidity

The relative humidity sensors in the peripheral positions of the blocks at sections S-2 and S-7 have measured fast increases in the relative humidity with all of them reaching 100 % within the first 300 days. The process was faster on the right hand side (WC-6 in both sections showing less than 50 days to reach 100 % humidity in S-2 and less than 100 days in S-7) and slower at the remaining positions.

Sudden changes in RH and noise observed after reaching saturation are typical from sensors that are damaged by flooding and such affected data is not presented. Asymmetric wetting is apparent from the psychrometer results and these sensors, with the exception of sensor WP-5 in section 2, are still collecting viable data.

Much slower RH increases were registered by the sensors at more inward locations of the blocks, specifically wireless sensors (WC-1, WC-2 and WC-4). Unfortunately, signals were lost after 100 days in S-2 and was only observed from day 90 to day 100 in S-7. The results are presented in Figures 4-1 (S-2) and 4-2 (S-7). The psychrometers in the inner position of the blocks (WP-1 and WP-2 in both sections) were not in range, so the suction was still over the threshold range measurement.

It should be taken into account that the capacitive hygrometers lose accuracy above 95 % RH so relative humidity measurements of 100 % do not necessarily imply that the material is fully saturated.

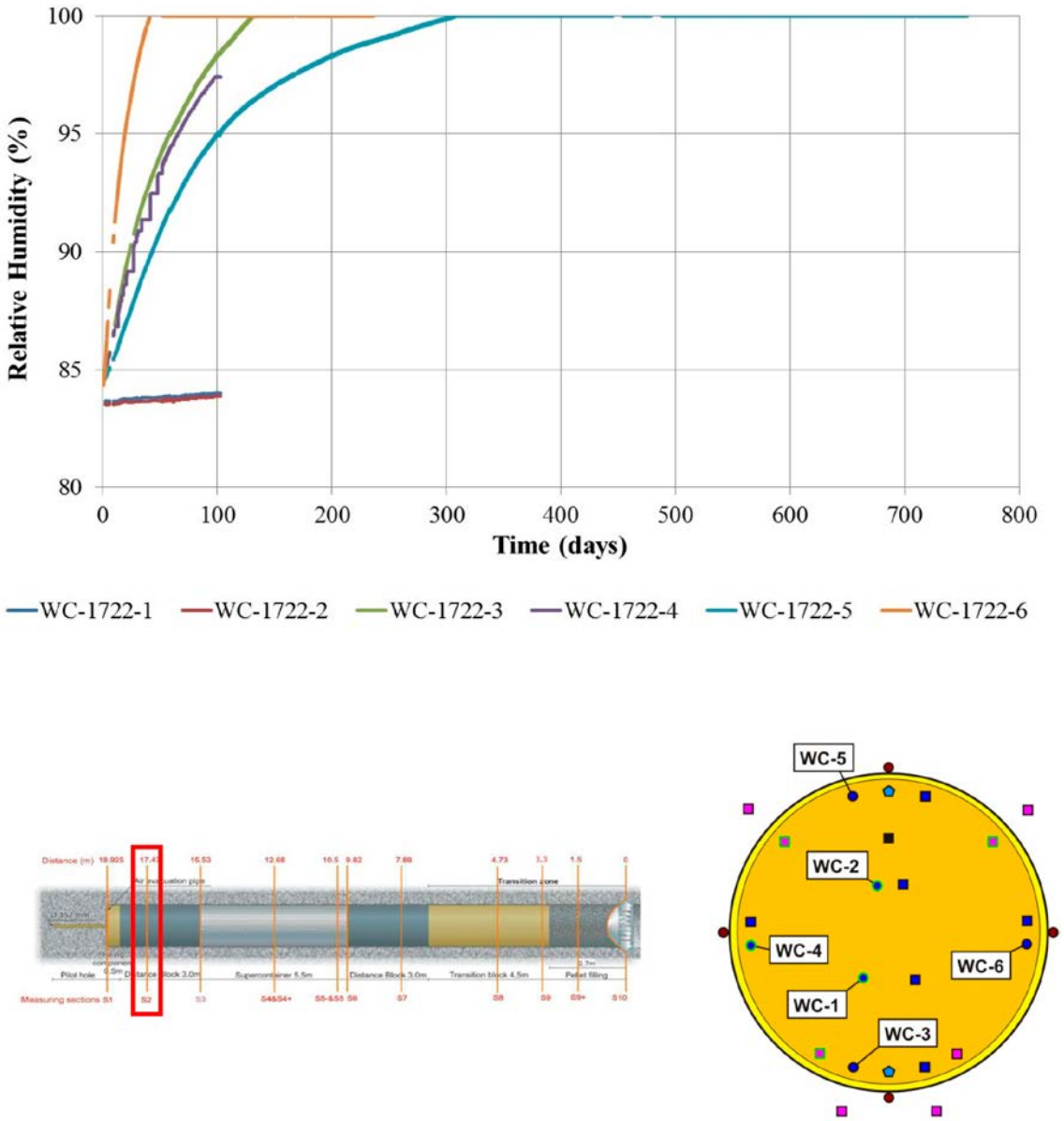

Figure 4-1. *Response of capacitive hygrometers at inner distance block positions (in the bentonite block) in drift section S-2. A total of six such sensors were installed in this section (bottom-right inset; WC-1 corresponds to WC-1772-1, etc.). The radial distance of sensors WC-1 and WC-2 to the rock wall is 675 mm and that of sensors WC-3 to WC-6 to the rock wall is 125 mm.*

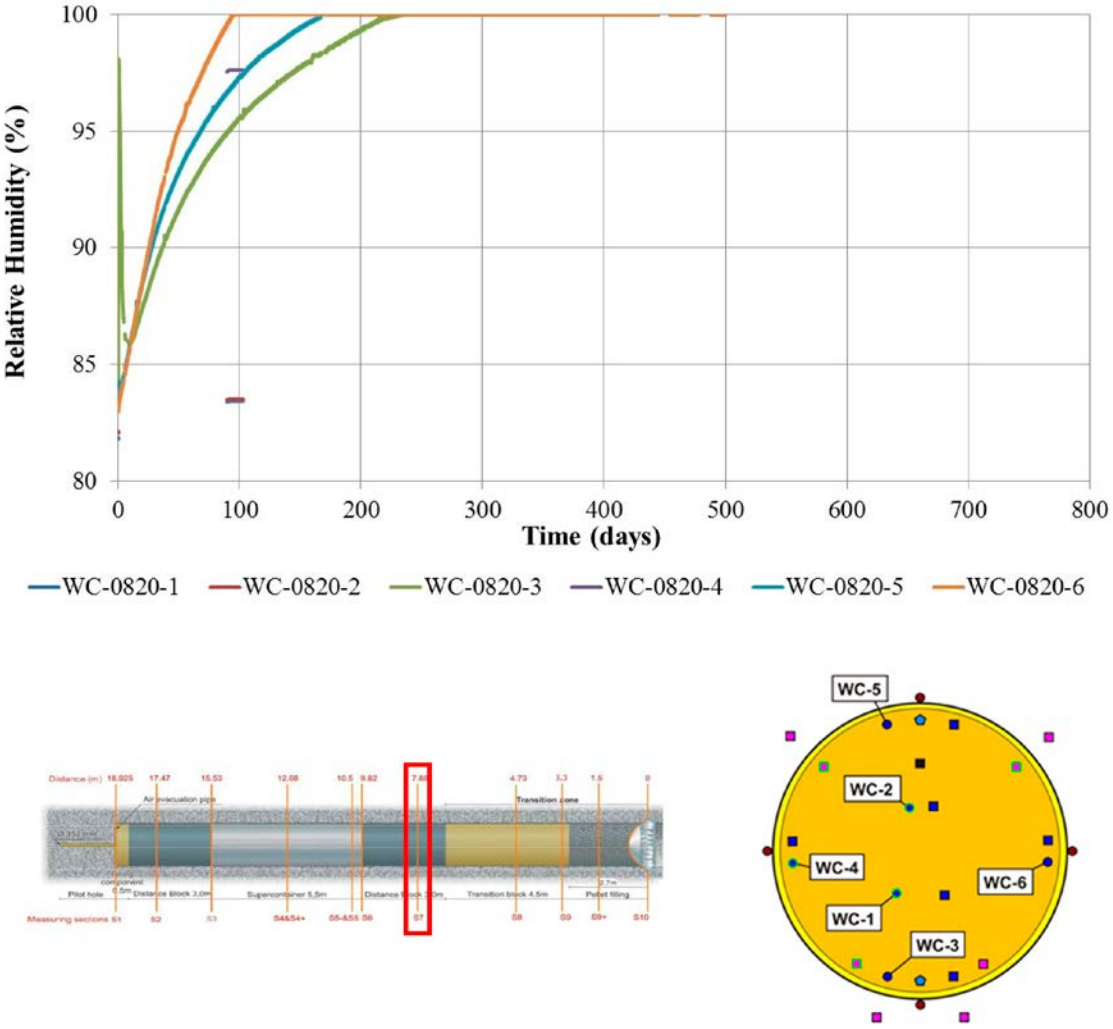

Figure 4-2. *Response of capacitive hygrometers at inner distance block positions (in the bentonite block) in drift section S-7. A total of six such sensors were installed in this section (bottom-right inset; WC-1 corresponds to WC-0820-1, etc.). Sensor WC-3 showed an early spike in relative humidity perhaps due to the initial water filling of the gap. The radial distance of sensors WC-1 and WC-2 to the rock wall is 675 mm and that of sensors WC-3 to WC-6 to the rock wall is 125 mm.*

4.2.2 Suction

In-range signals from the psychrometers correspond only to suction established at 95 % relative humidity. For temperatures between 5 °C and 15 °C, the suction at 95 % relative humidity should be between 6.6 and 6.8 MPa based on the psychometric law. Results are presented in Figures 4-3 and 4-4 for S-2 and S-7, respectively.

A total of six such sensors were installed in each section (see insets in Figures 4-3 and 4-4; WP-1 corresponds to WP-1722-1, etc for S-2 and to WP-0820-1, etc for S-7). Sensors WP-3, WP-4, WP-5 and WP-6 in peripheral locations have reached in-range suction limits in both sections. Again those sensors located on the right hand side developed signal growth faster in concert with the humidity sensors described above. Those sensors located at the bottom and on the left hand side reacted at almost the same time. The signal from the topmost sensors lagged behind. Full saturation was reached only on the right hand side (suction values close to zero) while the remaining sensors indicate saturation to be ongoing (low suction but still decreasing). The signals for sensors closer to the center have not yet started to approach in-range limits. All signals were lost after day 551 (11 June 2015) due to hardware malfunctioning but they were reestablished on 17 January 2016 (day 767).

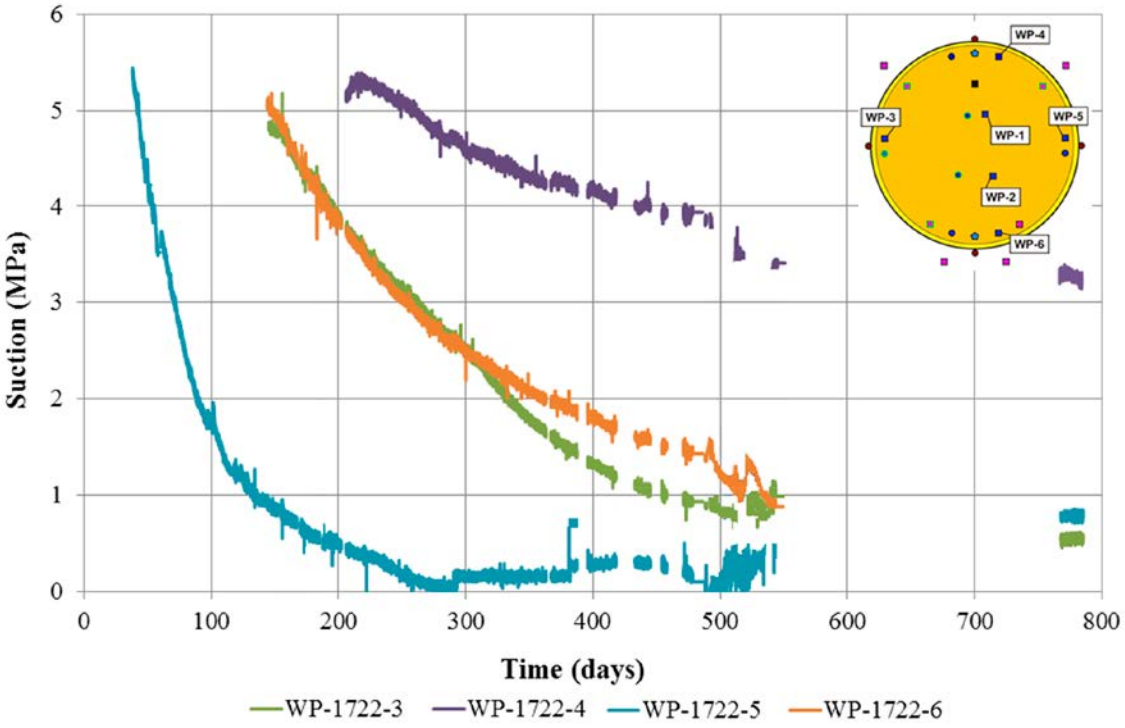

Figure 4-3. *Decay in psychrometer signal for sensors WP-3, WP-4, WP-5 and WP-6 at inner distance block positions in drift section 2 after reaching in-range suction limits. The radial distance of sensors WP-1 and WP-2 to the rock wall is 675 mm and that of sensors WP-3 to WP-6 to the rock wall is 125 mm.*

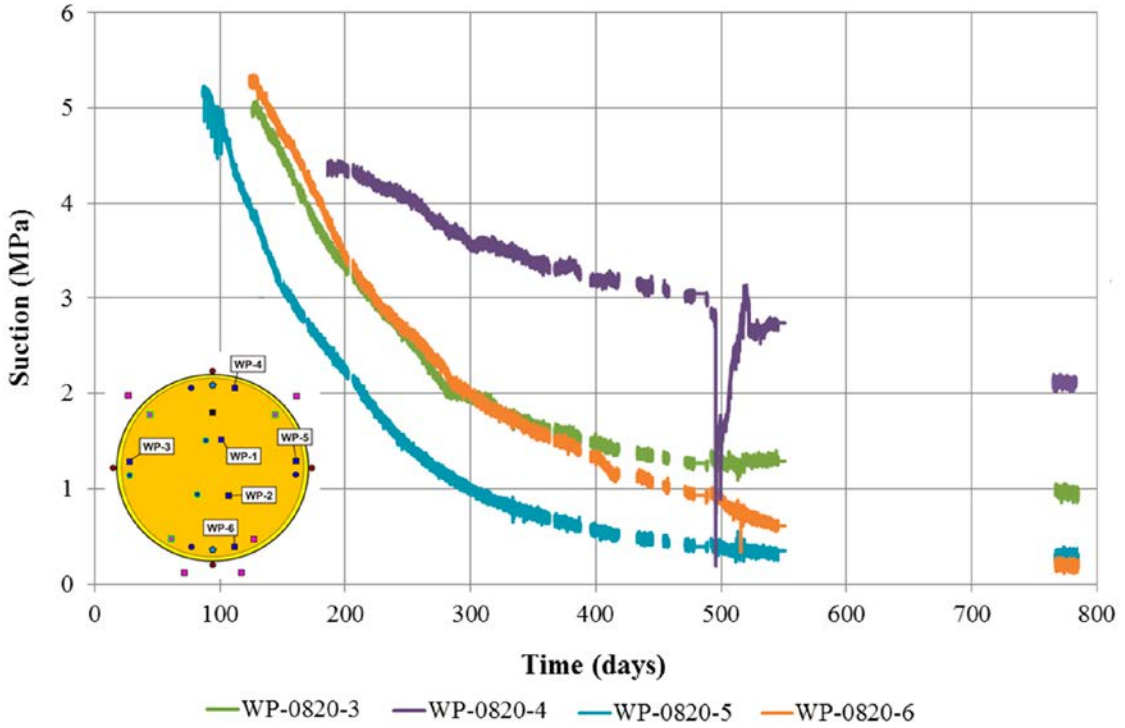

Figure 4-4. *Decay in psychrometer signal for sensors WP-3, WP-4, WP-5 and WP-6 in inner distance block positions in drift section 7 after reaching in-range suction limits. The radial distance of sensors WP-1 and WP-2 to the rock wall is 675 mm and that of sensors WP-3 to WP-6 to the rock wall is 125 mm.*

4.2.3 Pore pressure

Pore pressures in the blocks were measured with four pore pressure sensors in S-2 and S-7 (see insets in Figures 4-5 and 4-6; PP-1 corresponds to PP-1722-1, etc for S-2 and to PP-0820-1, etc for S-7).

Again, wireless sensor signals (PP-1, PP-2 and PP-3) were lost after 100 days in S-2 and lasted only from around day 90 to day 100 in S-7. Therefore, only signal from sensor PP-4 is registered after day 100. Pore pressure started to increase in S-2 after 140 days and more clearly after day 200, the peak registered after day 650 (up to 1.3 MPa) could be related with a purge of the sensor. Sensor PP-4 in S-7 displayed an unreasonably large signal from the beginning of the test and may be malfunctioning. Signal was lost from this sensor before day 500.

The pore pressure increase shown by sensor PP-4 in S-2 is quite clear. It could be expected that the suction measured by sensor WP-6 in that section (close to PP-4) should be close to zero but it is close to 4 MPa when the pore pressure starts to increase after 200 days. These contradictory results could be due to local effects.

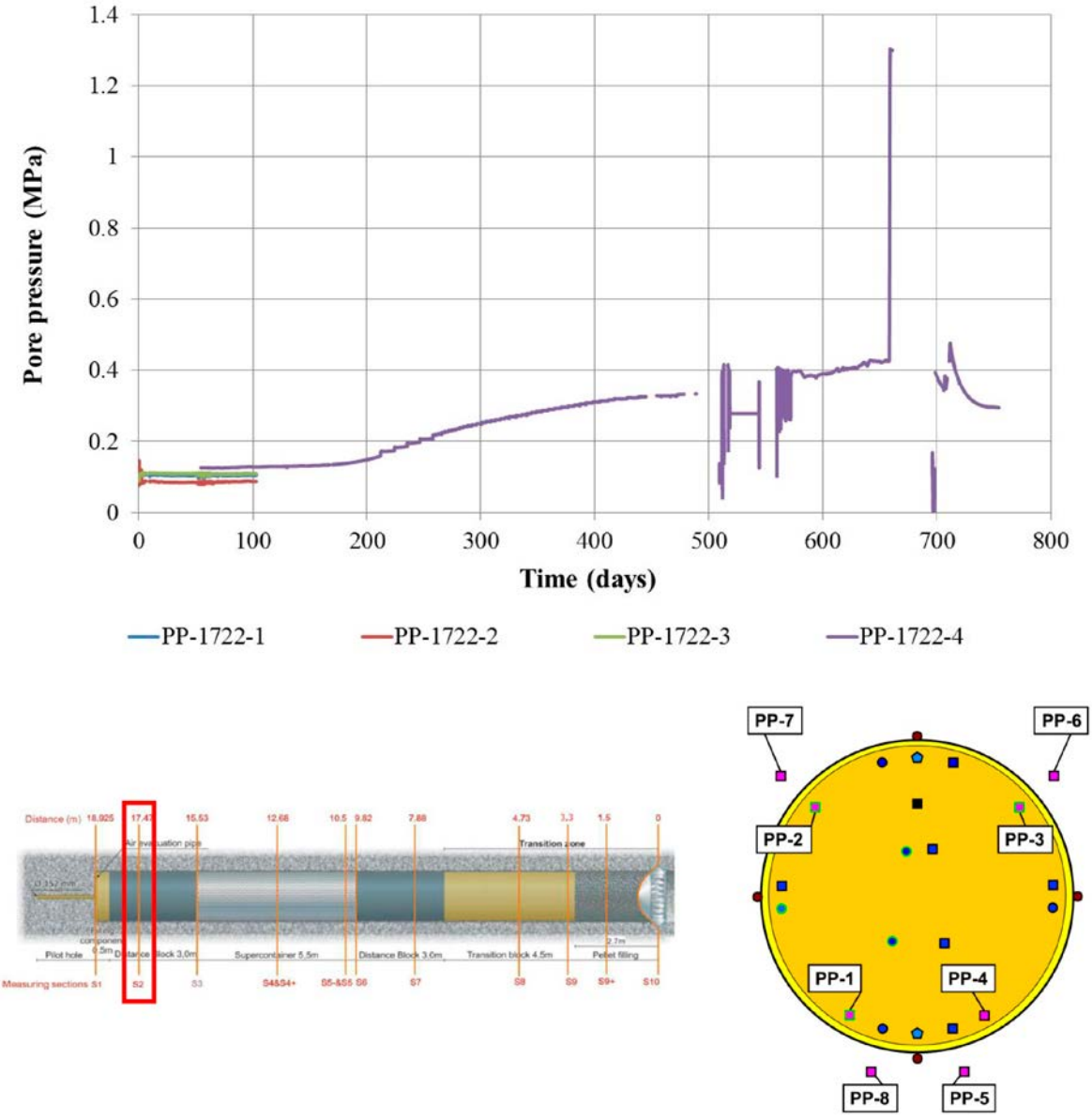

Figure 4-5. *Response of pore pressure sensors at inner distance block positions (in the bentonite block) in drift section S-2. The radial distance of sensors PP-1 to PP-4 to the rock wall is 125 mm.*

In previous, in situ experiments, pore pressure sensors in the blocks did not measure any increase in pore pressure. This observation may be due to the low hydraulic conductivity of the bentonite. Similarly, the BRIE test, also conducted in the Äspö HRL, was instrumented with pore pressure sensors and pressure increases were not observed. Other examples indicating delays in the development of measurable pore pressures in bentonite blocks include the FEBEX, which was an "in situ" test carried out during 20 years in Grimsel, Switzerland. The test was done in a horizontal gallery of 17.4 m length and 2.28 m diameter with two heaters surrounded with bentonite blocks test (ENRESA 2000) and the ESDRED test also performed at the Grimsel Test Site (Switzerland).

The density of the bentonite close to the sensors can be determined during the dismantling process and compared to data from swelling pressure measurements in oedometer cells, the Big Bertha tests, which are tests made in steel cells with an inner diameter of 800 mm and different lengths depending the number of blocks tested (the length of each block is 350 mm. The diameter of the blocks is 715 mm in order to leave a gap of 42.5 mm. Big Bertha tests can be done with or without continuous water supply and the cell has sensors for measuring the water pressure and the swelling pressure (Sandén et al. 2008, SKB 2012). Comparison can also be made to earlier perforation hole tests (Asensio Sánchez 2013, Pintado et al. 2016).

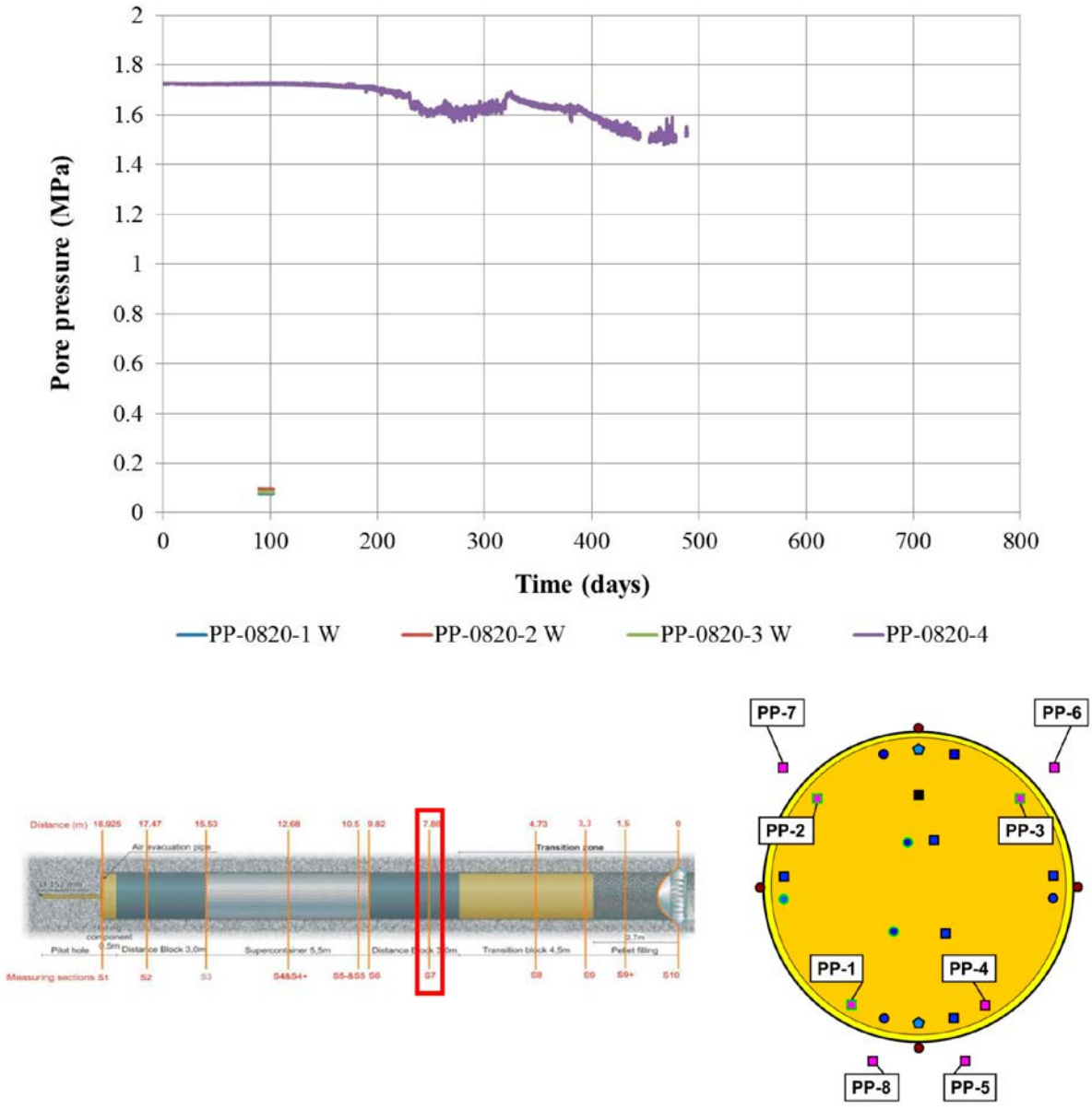

Figure 4-6. *Response of pore pressure sensors at inner distance block positions (in the bentonite block) in drift section S-7. The radial distance of sensors PP-1 to PP-4 to the rock wall is 125 mm.*

The pressure in the gap between the rock wall and the drift components was measured with a gas pressure sensor in S-1 (Figure 4-7). The range of the initial sensor was 250 kPa and it was installed for the purposes of measuring gas pressure if the DAWE procedure was not followed. As the DAWE procedure was followed, the sensor was flooded in less than 10 days, and essentially measured water pressure. This sensor was changed to a higher range pore pressure sensor at day 369. Peak pressures were observed at day 466 (peak pressure to almost 1 MPa) and around day 550 (pressures reached more than 1.0 MPa). The peak at around day 550 was followed by a decrease in pressure to 0.5 MPa by day 600 afterwhich pressures then increased steadily until stabilizing at around 1.22 MPa by day 699.

4.2.4 Water content

Volumetric water content was measured with soil moisture sensors in sections S-1 (one sensor), S-2 (two sensors) and S-7 (two sensors). The sensor measurements are shown in Figures 4-8 to 4-10.

In S-1 (Figure 4-8) the sensor registered a decrease in volumetric water content measurement from an initial value of around 0.41 m^3/m^3 until a constant value was reached after 100 days (around 0.10 m^3/m^3). The volumetric water content then started to slowly increase reaching 0.17 m^3/m^3 by day 465, when it then dropped to a much lower value. At this point the signal became exceedingly noisy. The initial decrease in volumetric water content (to day 100) could be related to an expansion/ fracturing of the bentonite block which could lead to new voids in the vicinity of the measuring rods resulting in lower measurements. The block in question is in the rear of the drift and may be more prone to suffer expansion/breaking.

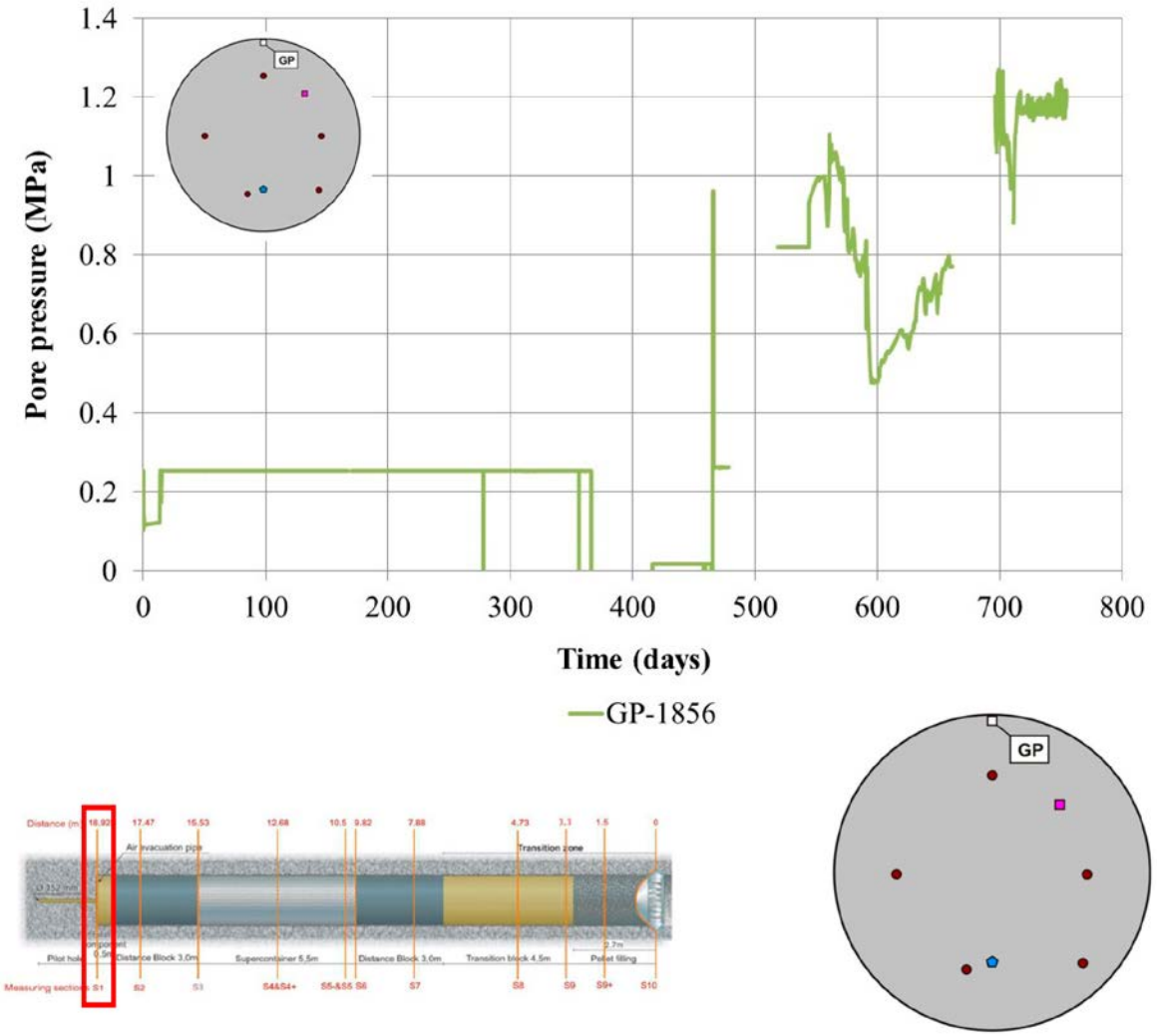

Figure 4-7. *Response of gas pressure sensor in drift section S-1 (bottom-right inset). The sensor was installed at the rock wall at the end of the drift.*

In S-2 (see Figure 4-9) both installed sensors showed similar development with increasing volumetric water content stabilizing at approximately 0.40 m^3/m^3. Sharp drops in signal were observed thereafter which may indicate some malfunctioning. After day 543 the signals became exceedingly noisy and were removed from the graph for clarity.

In S-7 (see Figure 4-10) sensor WF-2 showed a similar trend to that of the sensor in S-1 (see Figure 4-8) but the volumetric water content decreased less and a faster increase in water content was also observed. The explanation for this behavior could be the same, i.e. an expansion/fracturing of the bentonite but to a lesser extent due to higher confinement of the blocks.

Sensor WF-1, on the other hand, displayed a constant signal of 0.45 V throughout which indicates it may be malfunctioning or surrounded by bentonite with high water content. Signals from both sensors became very noisy (oscillating) after day 543.

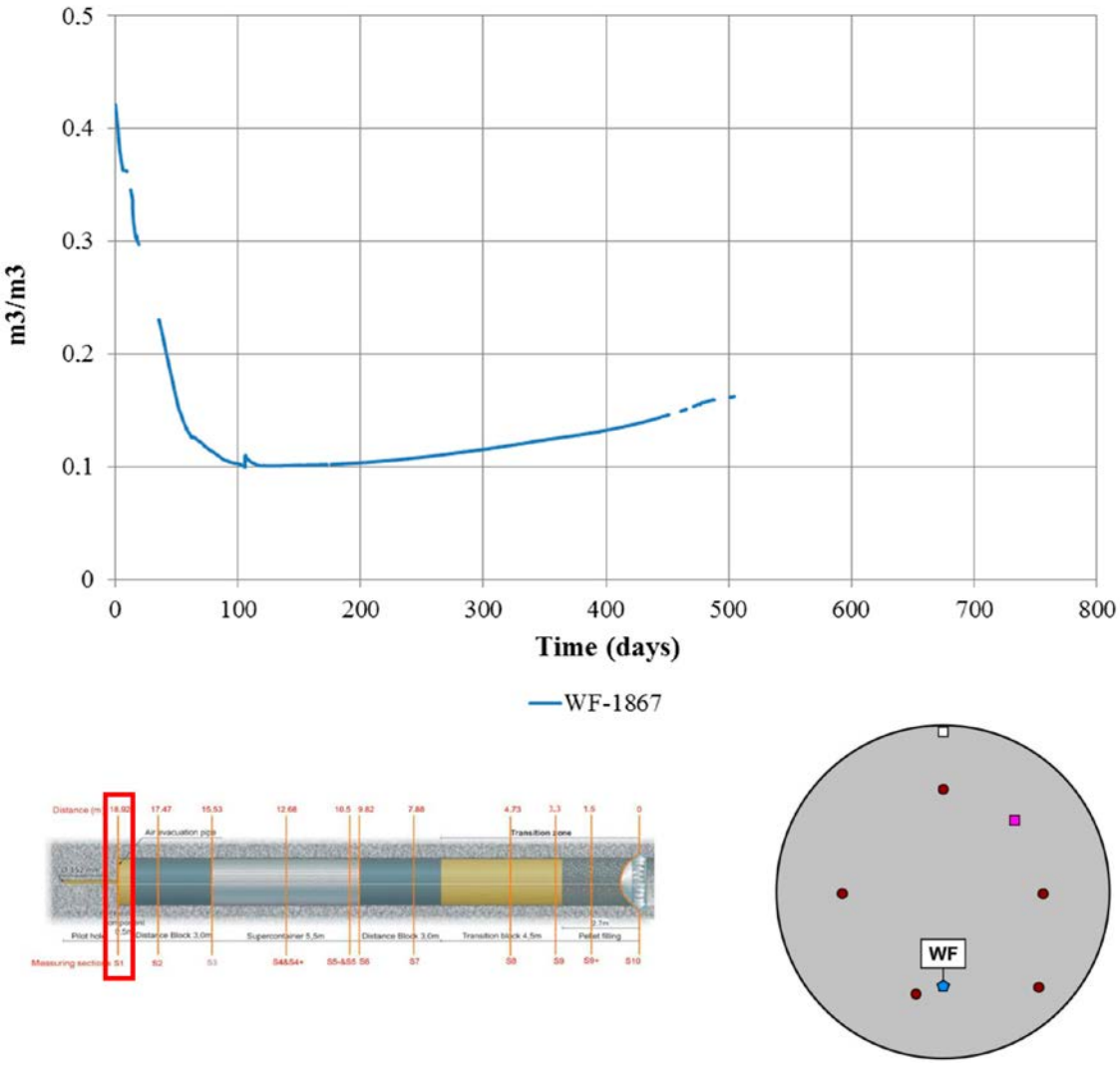

Figure 4-8. *Response of soil moisture sensor at inner distance block position in drift section S-1. The radial distance of the sensor to the rock wall is 358.5 mm.*

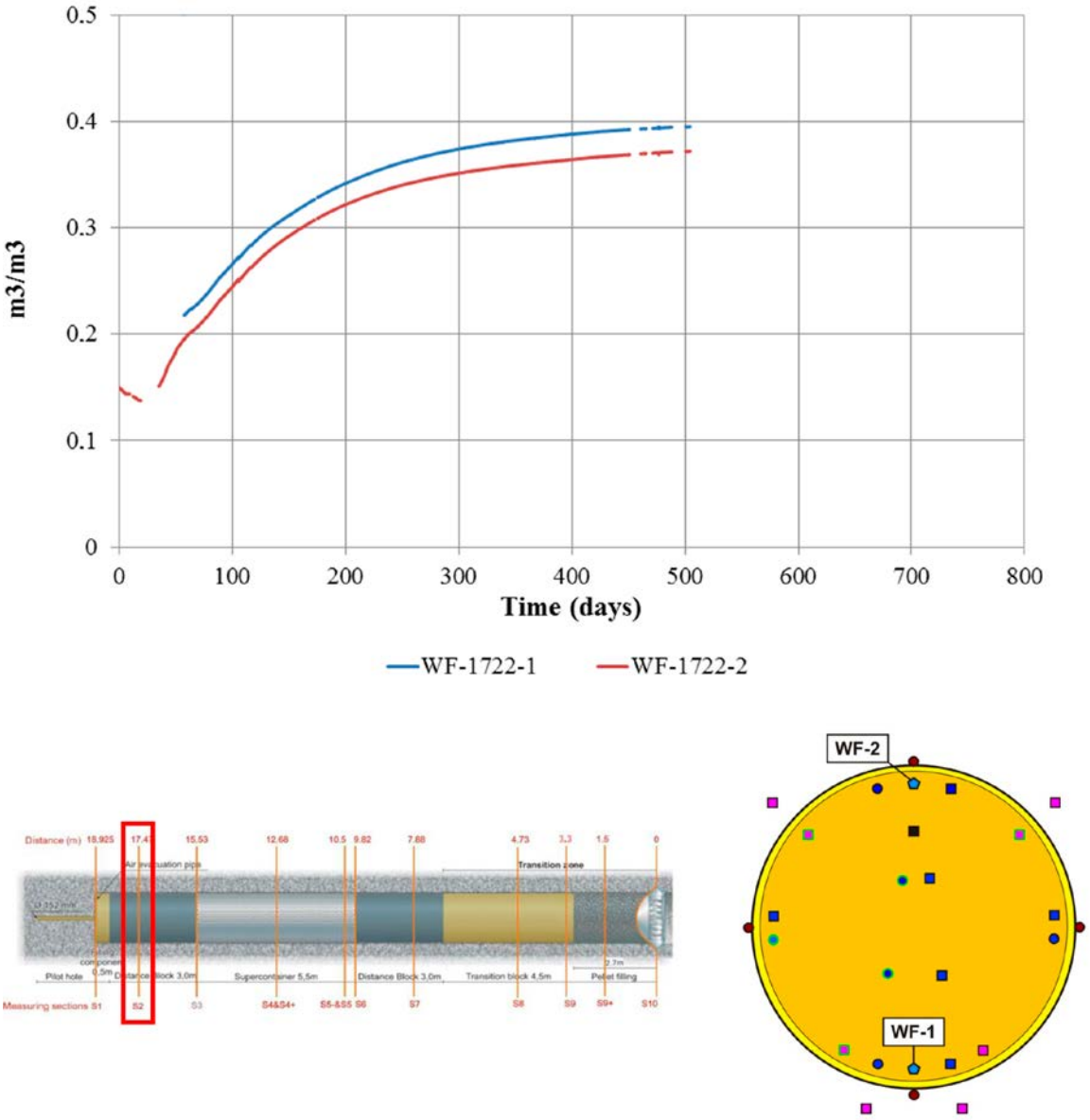

Figure 4-9. *Response of soil moisture sensors at inner distance block positions in drift section S-2. The radial distance of the sensors to the rock wall is 125 mm.*

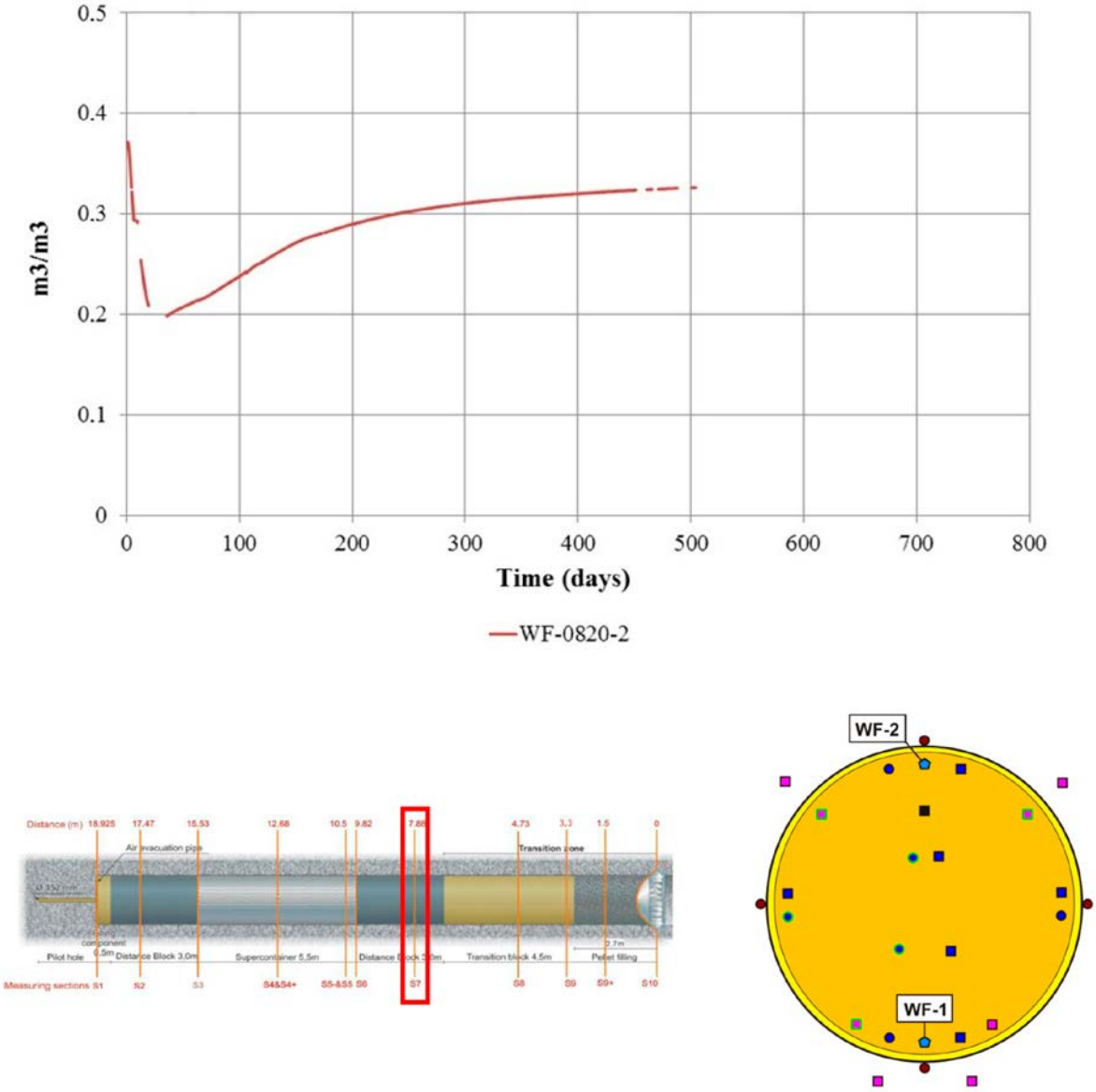

Figure 4-10. *Response of soil moisture sensors at inner distance block positions in drift section S-7. The radial distance of the sensors to the rock wall is 125 mm.*

4.2.5 Inclination

Results from the inclinometer sensors, one sensor installed in S-2 and another in S-7, are presented in Figures 4-11 and 4-12. The reference inclination is that after emplacement and only inclinations along the x-axis were measured.

In S-2, a sudden change in inclination after the first 3 days to a constant value of 2.5° (corresponding to half of the sensor range) was measured suggesting a sudden rotation of the block towards the pilot borehole possibly due to asymmetric block swelling. This sensor output remained constant up to day 489 when a slight decrease in inclination angle was registered.

In S-7, the signal from the inclinometer sensor was first recorded after 54 days. The measured signal appears to indicate a slow inclination towards the plug (negative inclination angle) until day 600 when the signal started increasing.

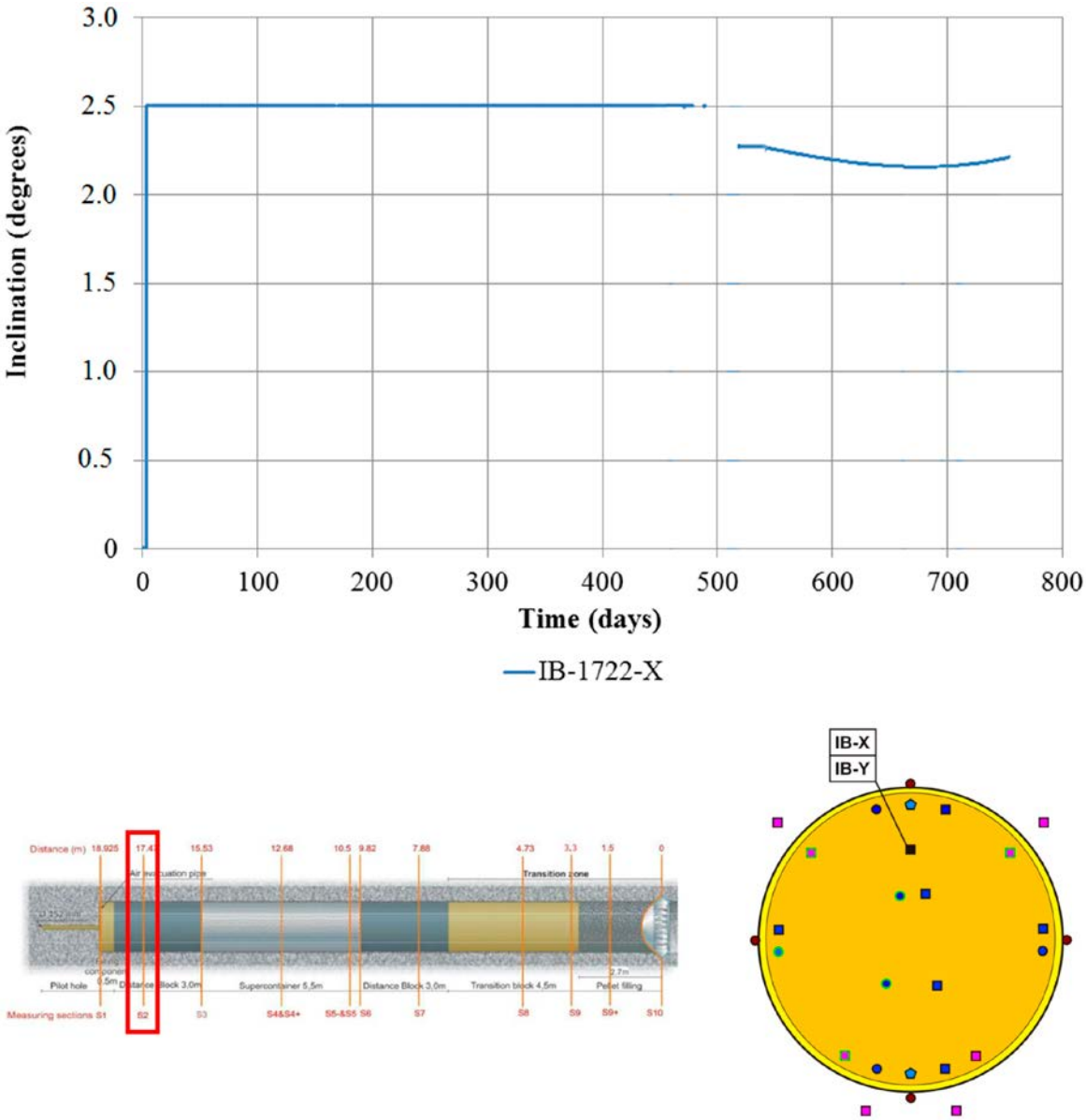

Figure 4-11. *Response of the inclinometer sensor at inner distance block position in drift section S-2.*

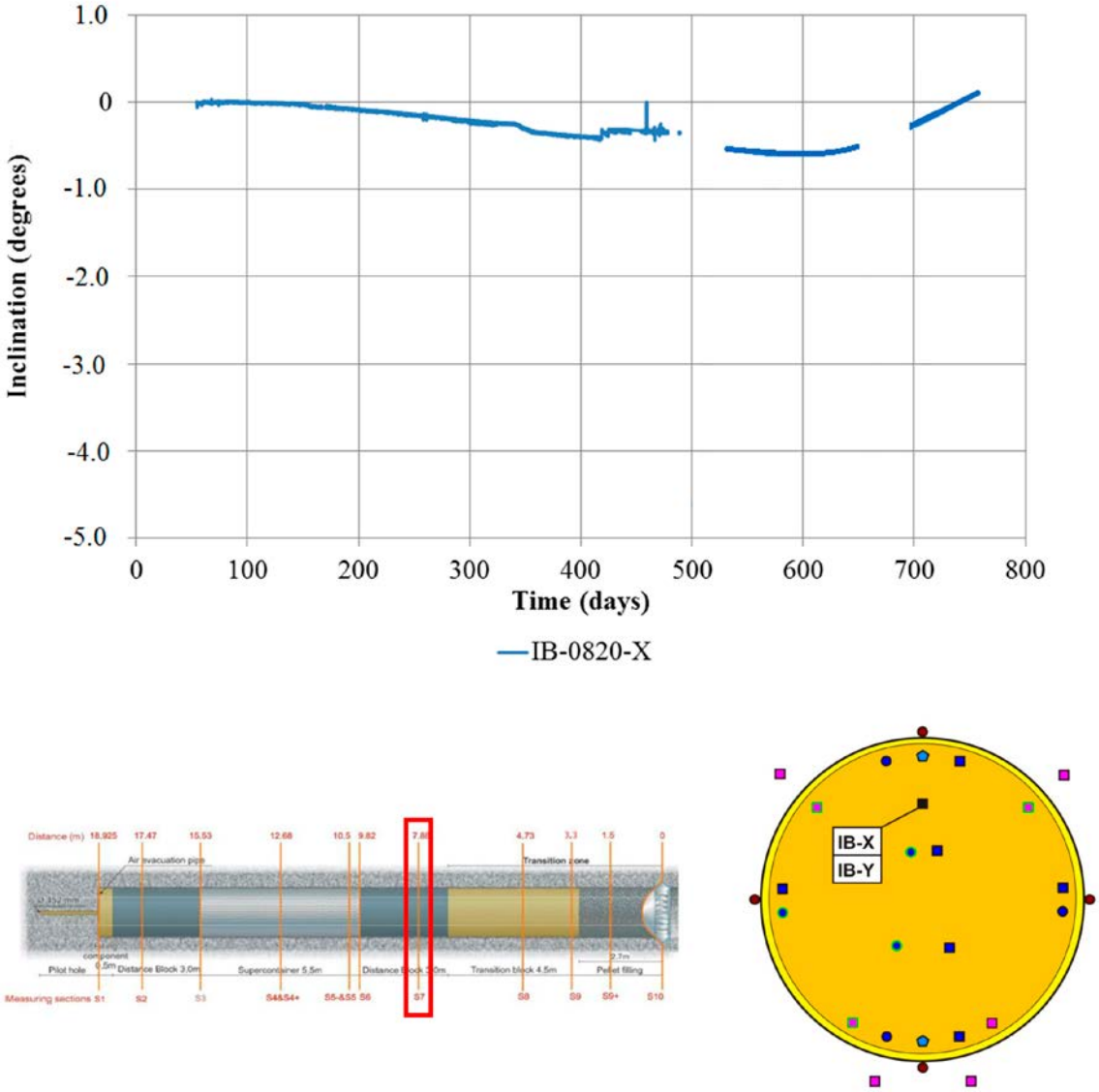

Figure 4-12. *Response of inclinometer sensor at inner distance block position in drift section S-7.*

4.3 Outer sensor positions

The location of the outer sensors and other information is presented in Tables 4-5 (section 1), 4-6 (section 2) and 4-7 (section 7).

Table 4-5. Numbering and position of outer distance block sensors in drift section 1.

	Coordinate system ÄSPÖ 96							
Point No.	**Easting [m]**	**Northing [m]**	**Point Elevation [m]**	**Drawing label**	**Sensor code in SICADA**	**Sensor code in SCADA**	**Assembly tag label**	**Manufacturer**
4	1 904.504	7 252.779	−216.885	PP-1	PXK000PP1	PP-1877-1	PP-1877-1	Keller
6	1 904.509	7 253.186	−216.724	TP-2	PXK000TP2	TP-1877-2	TP-1877-2	Geokon
5	1 904.483	7 253.754	−217.303	TP-3	PXK000TP3	TP-1877-3	TP-1877-3	Geokon
3	1 904.460	7 253.329	−217.857	TP-4	PXK000TP4	TP-1877-4	TP-1877-4	Geokon
1	1 904.465	7 252.656	−217.820	TP-5	PXK000TP5	TP-1877-5	TP-1877-5	Geokon
2	1 904.483	7 252.601	−217.302	TP-1	PXK000TP1	TP-1877-1	TP-1877-1	Geokon

Table 4-6. Numbering and position of outer distance block sensors in drift section 2.

	Coordinate system ÄSPÖ 96							
Point No.	Easting [m]	Northing [m]	Point Elevation [m]	Drawing label	Sensor code in SICADA	Sensor code in SCADA	Assembly tag label	Manufacturer
10	1905.955	7252.519	−216.707	PP-6	PXK015PP6	PP-1732-6	PP-1732-6	Keller
12	1905.954	7252.950	−218.239	PP-5	PXK015PP5	PP-1732-5	PP-1732-5	Keller
14	1905.951	7253.424	−218.236	PP-8	PXK015PP8	PP-1732-8	PP-1732-8	Keller
8	1905.950	7253.849	−216.708	PP-7	PXK015PP7	PP-1732-7	PP-1732-7	Keller
11	1905.954	7252.261	−217.359	TP-2	PXK015TP2	TP-1732-2	TP-1732-2	Geokon
13	1905.957	7253.180	−218.268	TP-1	PXK015TP1	TP-1732-1	TP-1732-1	Geokon
9	1905.946	7254.106	−217.365	TP-4	PXK015TP4	TP-1732-4	TP-1732-4	Geokon
7	1905.950	7253.186	−216.425	TP-3	PXK015TP3	TP-1732-3	TP-1732-3	Geokon

Table 4-7. Numbering and position of outer distance block sensors in drift section 7.

Point No.	Easting [m]	Northing [m]	Point Elevation [m]	Drawing label	Sensor code in SICADA	Sensor code in SCADA	Assembly tag label	Manufacturer
17	1915.376	7252.533	−217.076	PP-6	PXK109PP6	PP-0788-6	PP-0788-6	Keller
19	1915.372	7252.956	−218.613	PP-5	PXK109PP5	PP-0788-5	PP-0788-5	Keller
21	1915.381	7253.433	−218.610	PP-8	PXK109PP8	PP-0788-8	PP-0788-8	Keller
23	1915.373	7253.853	−217.075	PP-7	PXK109PP7	PP-0788-7	PP-0788-7	Keller
18	1915.376	7252.270	−217.712	TP-2	PXK109TP2	TP-0788-2	TP-0788-2	Geokon
20	1915.387	7253.201	−218.642	TP-1	PXK109TP1	TP-0788-1	TP-0788-1	Geokon
24	1915.387	7254.114	−217.715	TP-4	PXK109TP4	TP-0788-4	TP-0788-4	Geokon
22	1915.376	7253.198	−216.796	TP-3	PXK109TP3	TP-0788-3	TP-0788-3	Geokon

4.4 Outer sensor results and comments

4.4.1 Total pressure

Total pressure is measured in sections S-1, S-2 and S-7 (see Figures 4-13 to 4-15).

In S-1, a total of five such sensors were installed between the back-end of the drift and the last bentonite block (see Figure 4-13). The sensors showed increasing pressure almost from the beginning, with a short drop for all of them by day 57 that was recovered rapidly afterwards. The readings from each sensor are described in more detail below.

The signal from sensor TP-1892-1, leveled off after 512 days to 3.43 MPa followed by a minimal decline. The reading at the end of the measurement period is around 3.26 MPa.

The signal from sensor TP-1892-2, leveled off after 304 days to 3.6 MPa followed by minimal decline. At day 509 a sharp drop in signal to approximately 2 MPa was observed after which it began to slowly increase. A second, sharp drop in signal was observed at day 700 to 1.4 MPa.

The signal from sensor TP-1892-3 showed an increasing trend during the entire period up to a value of 4.32 MPa.

The signal from sensor TP-1892-4, leveled off after almost 600 days to 3.6 MPa. At day 700 a sharp drop in signal to almost 2 MPa was observed which continued decreasing steeply thereafter to 1.34 MPa at the end of the period.

The signal from sensor TP-1892-5 steadily increased to almost 2 MPa by day 640 at which point a sudden, shallow drop to ~1.5 MPa was observed followed by an increasing trend thereafter.

The signals recorded by sensors TP-1 to TP-4 were similar up to the sudden drop experienced by sensor TP-2. The rapid pressure increases indicate that wetting is occurring at the interface between the end of the drift and the block filling component. During the DAWE procedure, any open space between the rock surface of the drift end and the block filling component may have been filled. The signal recorded by TP-1892-5 was clearly lower than that of the other sensors which may indicate that this part of the block was completely flush against the drift end and had less opportunity to take up water. The observed loss in signal by sensors TP-2 and TP-4 could be due to a rearrangement of the blocks during the swelling process.

In S-2, four total pressure sensors were installed at the rock wall (see Figure 4-14). All sensors showed initially increasing pressures which levelled off after 100 days to values below1 MPa. Around day 200 pressures began to slowly increase except for those measured by sensor TP-1947-3 located at the top of the drift. Abrupt increases in signal for sensors TP-1 and TP-3 were observed after day 500 whereas the measured pressures from sensors TP-2 and TP-4 continued on their slowly increasing trajectories. At the end of the measurement period, signals from sensors TP-1, TP-2, TP-3 and TP-4 in S-2 were at approximately 1.8, 1.2, 2.4 and 1.2 MPa, respectively.

In S-7, four total pressure sensors were installed at the rock wall (see Figure 4-15). The observed signals were similar to those of the sensors installed in S-2 except only sensor TP-3 showed an abrupt increase around day 500. At the end of the measurement period, signals from sensors TP-1, TP-2, TP-3 and TP-4 in S-7 were at approximately 1.1, 1.2, 1.6 and 1.3 MPa, respectively.

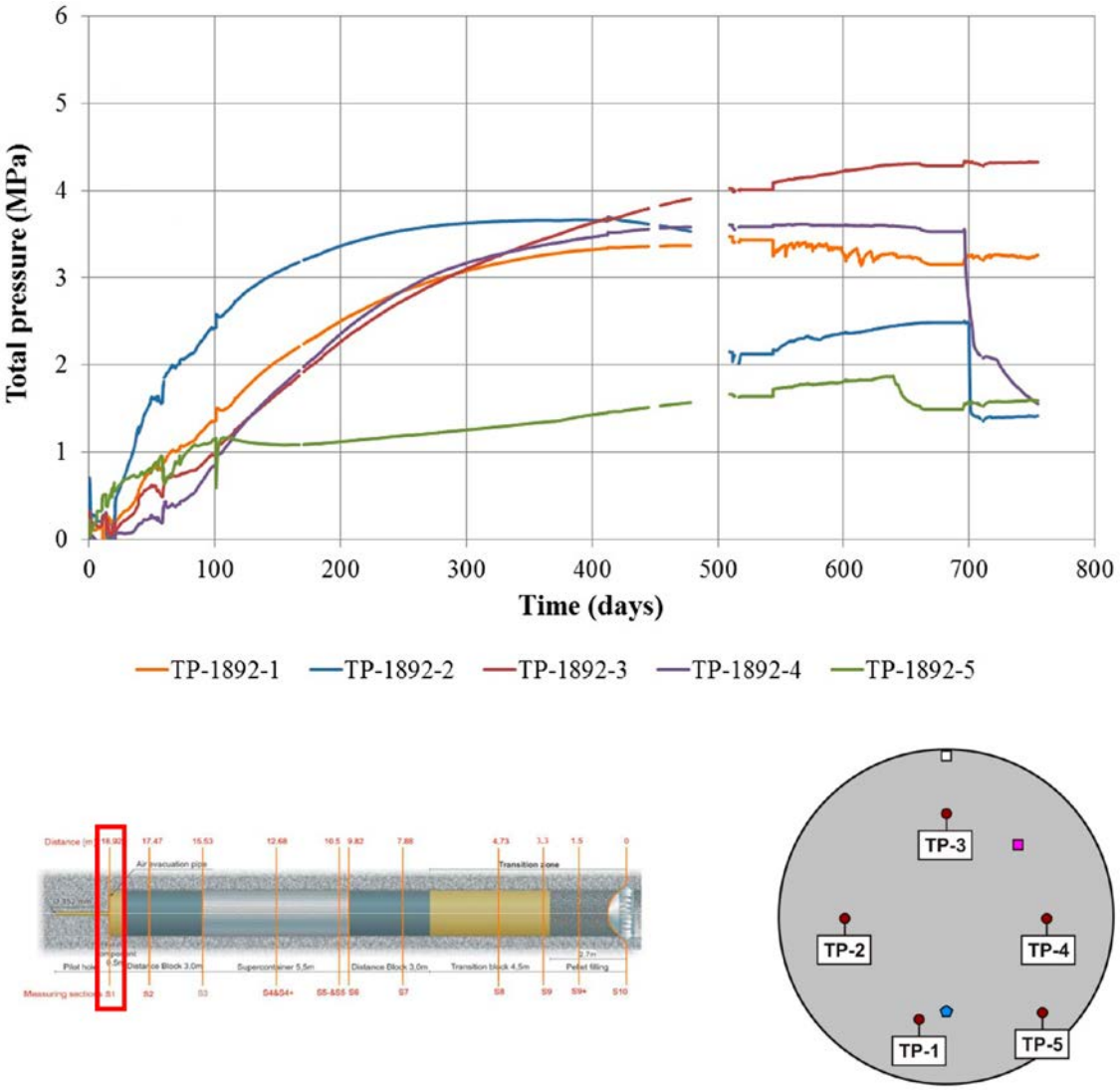

Figure 4-13. *Response of total pressure sensors at outer distance block positions (measuring axial pressures at the rock wall surface) in drift section S-1.*

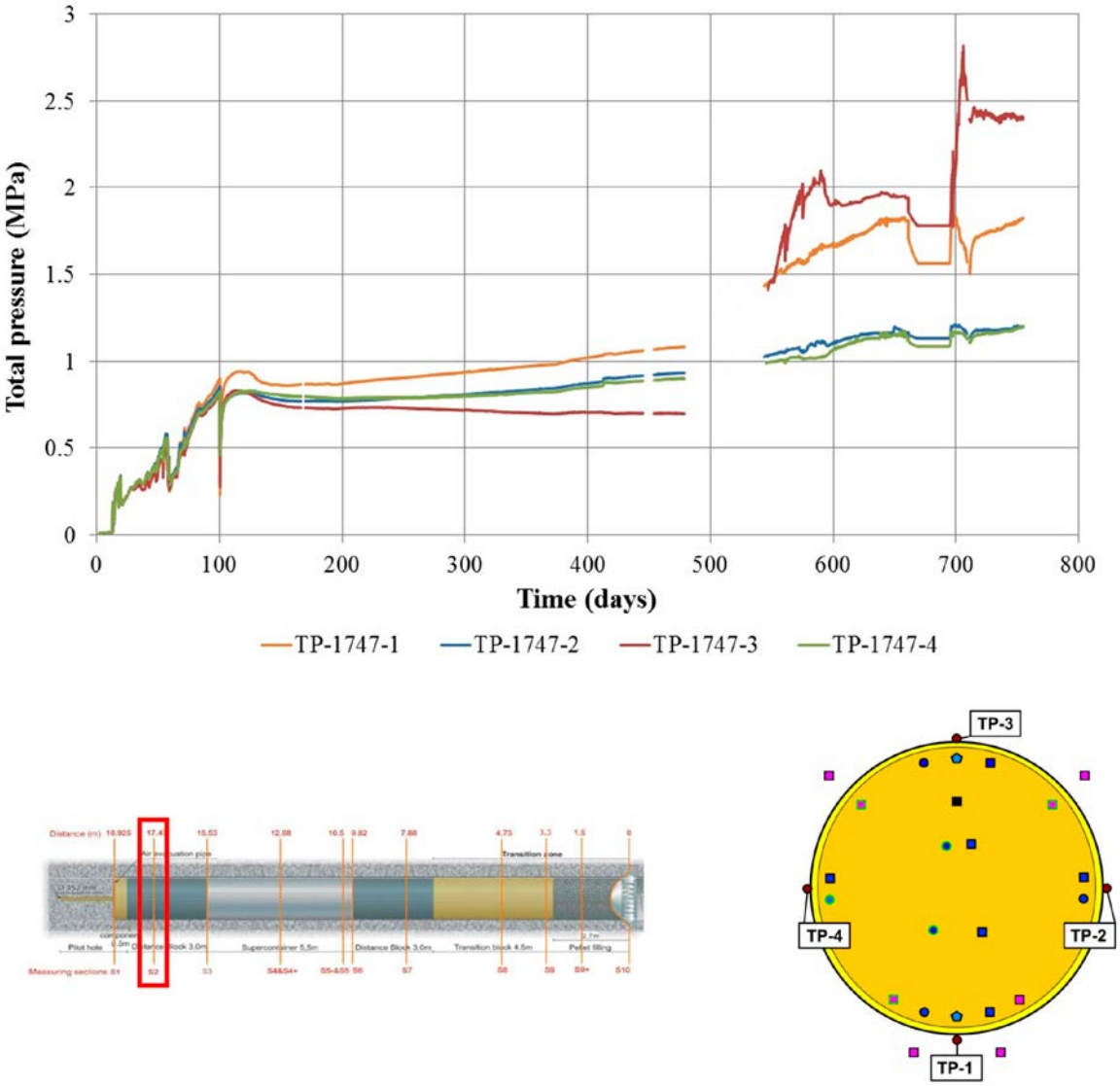

Figure 4-14. *Response of total pressure sensors at outer distance block positions (measuring radial pressures at the rock wall surface) in drift section S-2.*

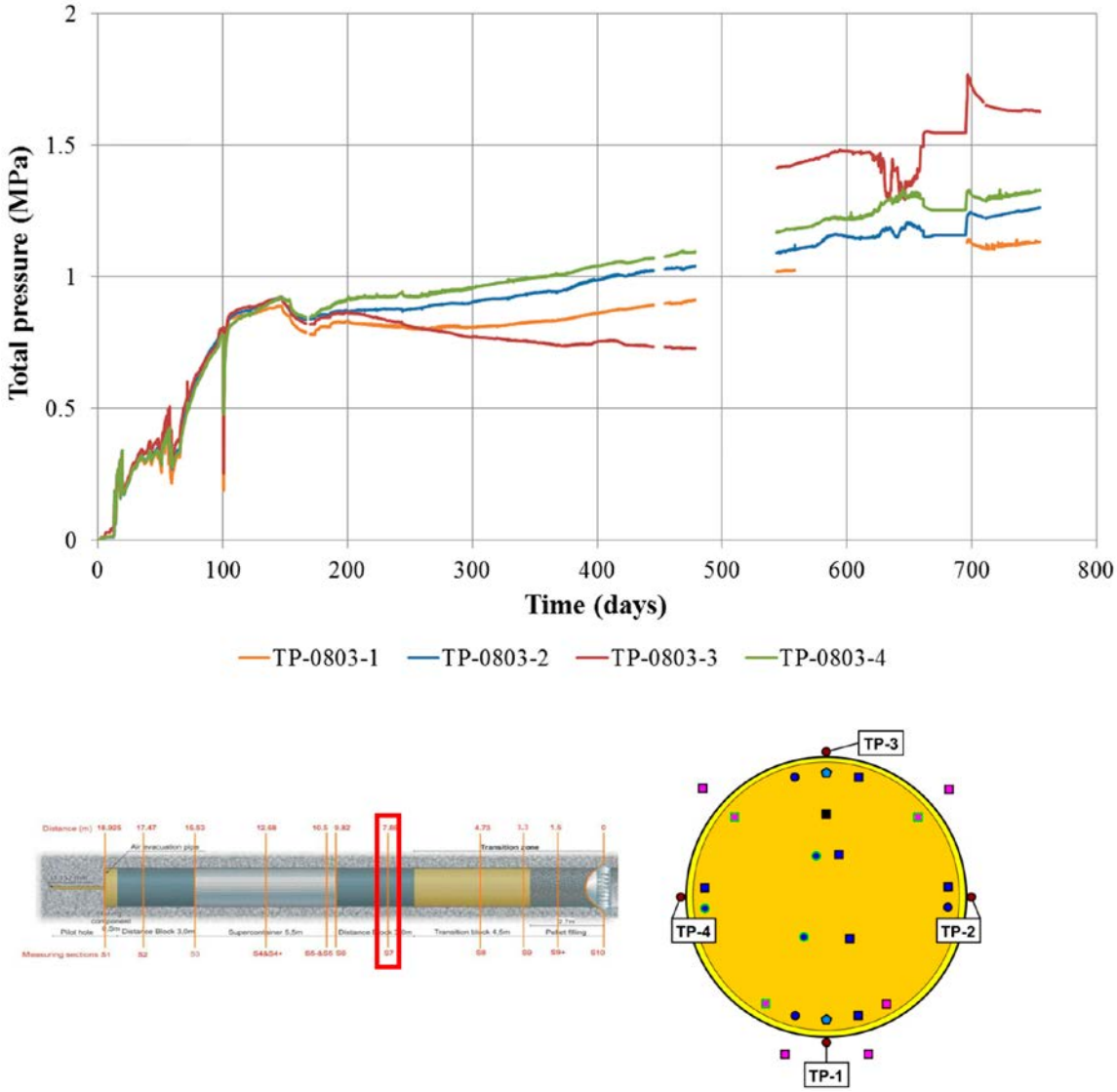

Figure 4-15. *Response of total pressure sensors at outer distance block positions (measuring radial pressures at the rock wall surface) in drift section 7.*

4.4.2 Pore pressure

Pore pressure is measured in drift sections S-1, S-2 and S-7 (see Figures 4-16 to 4-18).

The sensor in S-1 was located between the rock and the bentonite block at the end of the drift. The sensor remained at a constant value of around 0.1 MPa from near the beginning of the test indicating it may not have been fully purged of air. At day 513 it increased sharply to over 0.2 MPa followed by a decrease shortly thereafter. After day 700 a fast pressure increase reaching up to almost 0.7 MPa was observed.

Four sensors were installed at the rock wall of the drift in S-2 (see Figure 4-17). Only two of the sensors registered changes in signal during the measurement period (sensors PP-6 and PP-8) while the other two (PP-5 and PP-8) remained at a value of 0.1 MPa from the beginning indicating they may not have been fully purged of air or were isolated in some way. Both active sensors showed pressure increases which stabilized at almost 0.5 MPa by day 56 for sensor PP-6 (upper right position) and at 1.0 MPa by day 111 for sensor PP-8 (bottom left position). Thereafter, slowly decreasing signals were observed for both sensors out to day 400 for sensor PP-6 and day 500 for sensor PP-8. Signals from both sensors showed an abrupt increase to similar pressures at day 511 and behaved somewhat comparably afterwards. Towards the end of the measurement period, sensor PP-8 stabilized at 1.1 MPa and sensor PP-6 continued increasing to reach 1.8 MPa. The signals from these sensors behaved with a pattern similar to those of the total pressure cells (see Figures 4-14).

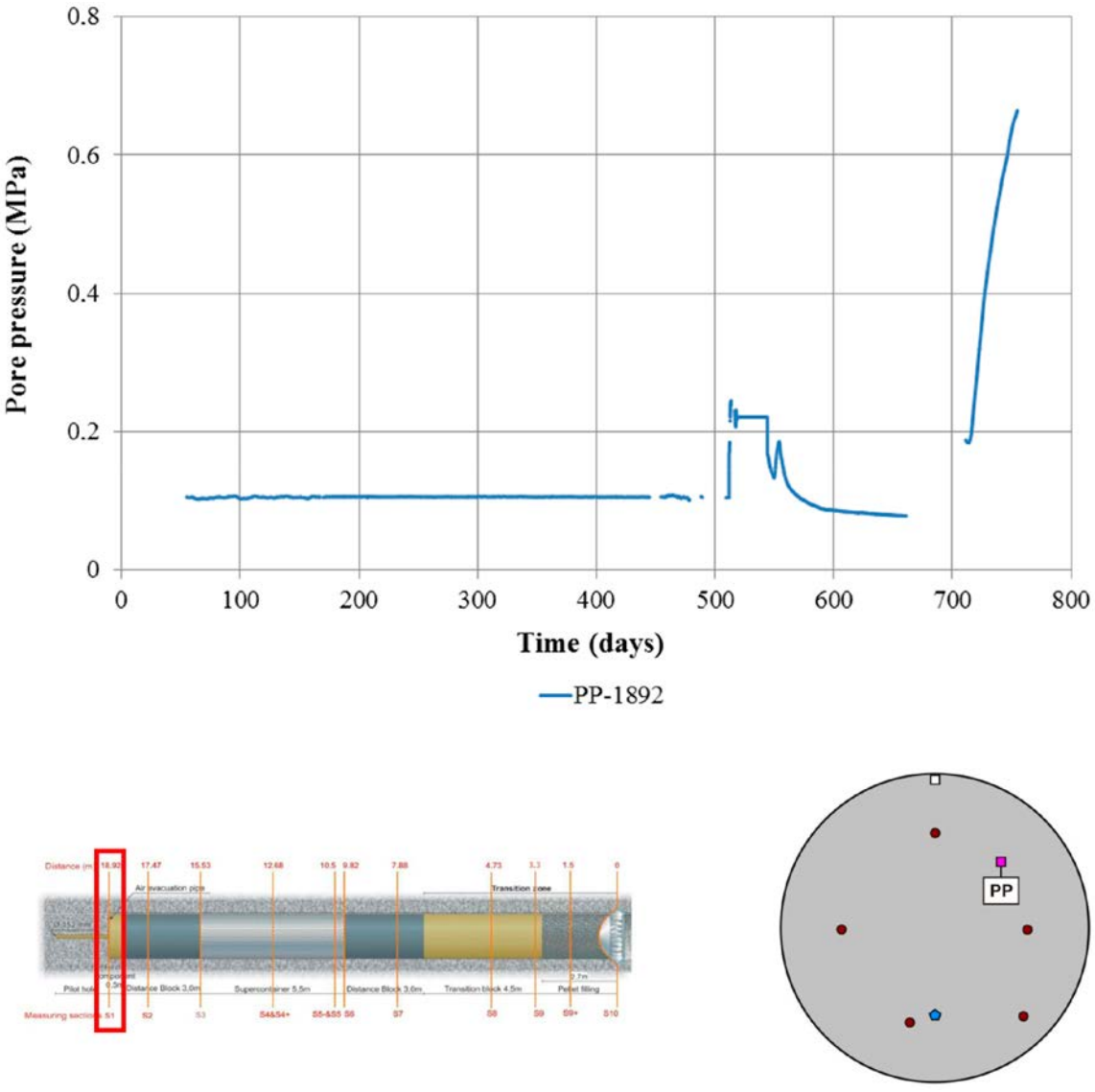

Figure 4-16. *Response of outer pore pressure sensor in drift section 1.*

Four sensors were also installed at the rock wall of the drift in S-7 (see Figure 4-18). Three of the sensors (PP-5, PP-6 and PP-8) showed activity during the measurement period while sensor PP-7 remained at a value of 0.1 MPa from the beginning indicating that it may not have been fully purged of air or was otherwise isolated in some way.

Sensor PP-8 showed a clear pressure increase during first 100 days which then stabilized at almost 1.0 MPa. The signal remained at this level until day 488 when it started to increase slowly again up to day 645 when it reached 1.13 MPa and started to decrease. Currently, the signal seems to be leveled at a value slightly above 1 MPa.

The pressure measured by sensor PP-6 stabilized quickly to values below 0.2 MPa. On day 551 it showed a sudden increase up to 0.6 MPa and continued sharply increasing and decreasing to overall higher pressures until day 646 when it fell to 0.1 MPa.

Sensor PP-5 showed no activity until day 115 when the measured signal increased suddenly up to 0.45 MPa and remained steadily increasing to 0.7 MPa at day 457 when it dropped down to 0.2 MPa and started increasing again up to the end of the period reaching 0.92 MPa.

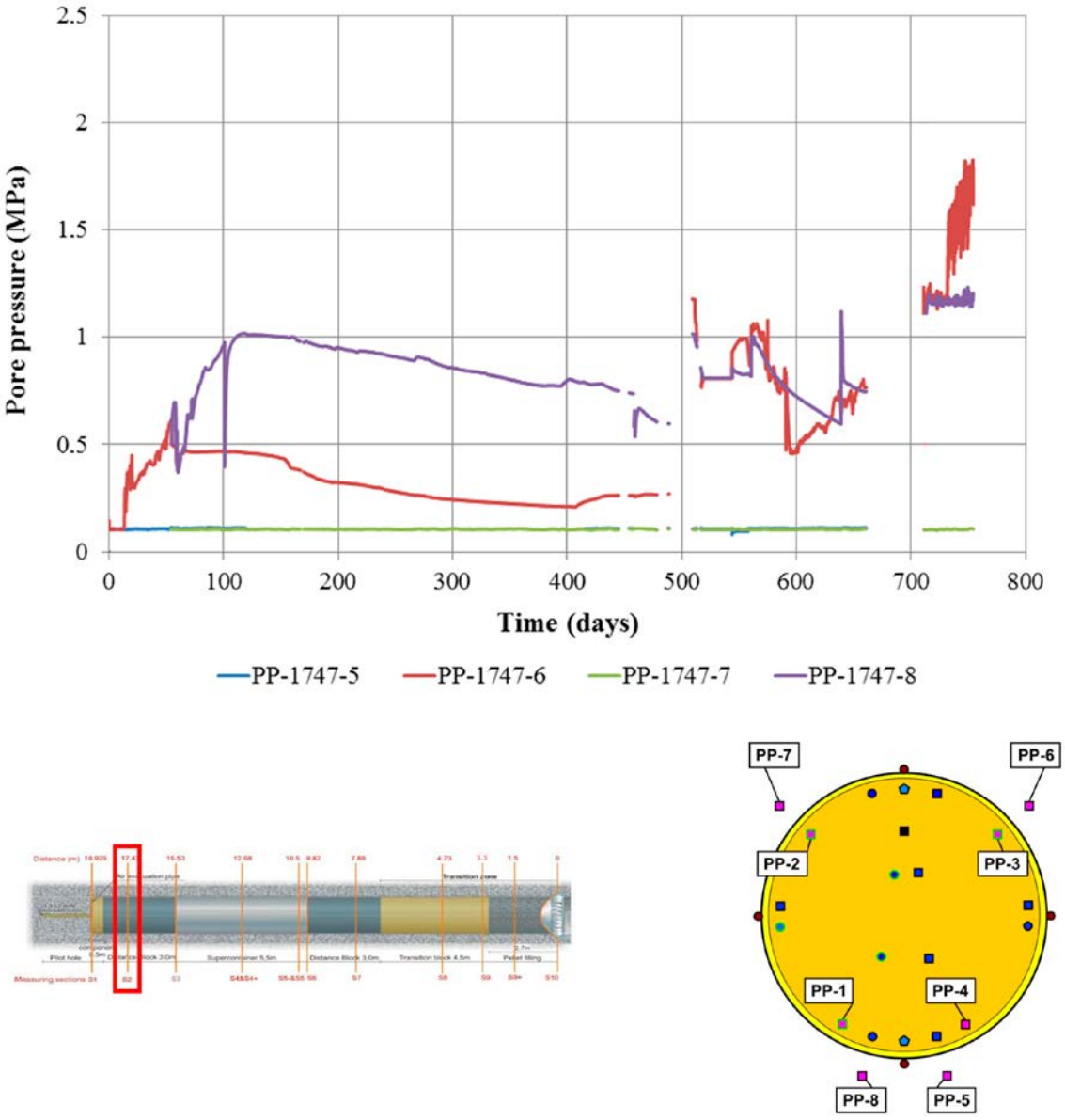

Figure 4-17. *Response of outer pore pressure sensors (PP-5 to PP-8) in drift section S-2.*

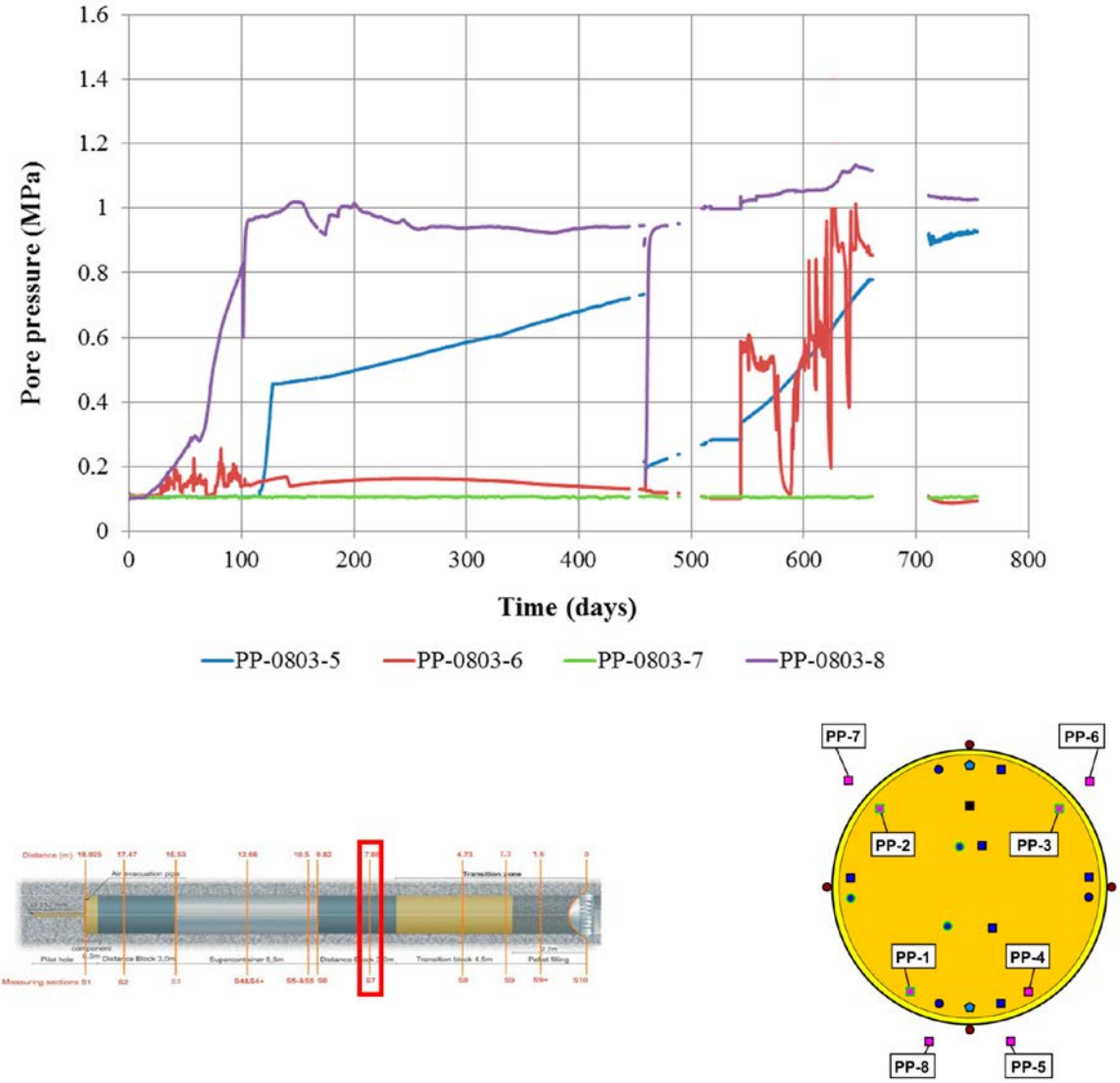

Figure 4-18. *Response of outer pore pressure sensors (PP-5 to PP-8) in drift section S-7.*

5 Transition zone

5.1 Inner sensor positions

The location of the inner sensors and other information is presented in Tables 5-1 (drift section 8), 5-2 (drift section 9) and 5-3 (drift section 10). The relevant drift sections are identified in Figure 3-1.

Table 5-1. Numbering and position of inner transition zone sensors in drift section 8 (transition blocks).

	Coordinate system ÄSPÖ 96							
Point No.	Easting [m]	Northing [m]	Point Elevation [m]	Drawing label	Sensor code in SICADA	Sensor code in SCADA	Assembly tag label	Manufacturer
1	1 919.068	7 252.991	−217.082	WP4	PXK146WP4	WP-0480-4	WP0480-4	Wescor
2	1 919.069	7 253.198	−217.054	WF2	PXK146WF2	WF-0480-2	WF0480-2	Delta-T
3	1 919.068	7 253.406	−217.081	WC6	PXK146WC6	WC-0480-6	WC0480-6	Aitemin
4	1 919.062	7 253.062	−217.346	WP1	PXK146WP1	WP-0480-1	WP0480-1	Wescor
5	1 919.062	7 253.336	−217.346	WC3	PXK146WC3	WC-0480-3	WC0480-3	Aitemin
6	1 919.052	7 252.400	−217.803	WP5	PXK146WP5	WP-0480-5	WP0480-5	Wescor
7	1 919.050	7 252.400	−217.903	WC7	PXK146WC7	WC-0480-7	WC 0480-7	Aitemin
8	1 919.050	7 253.198	−217.853	WC1	PXK146WC1	WC-0480-1	WC0480-1	Aitemin
9	1 919.040	7 253.082	−218.287	WP2	PXK146WP2	WP-0480-2	WP0480-2	Wescor
10	1 919.039	7 253.315	−218.287	WC2	PXK146WC2	WC-0480-2	WC0480-2	Aitemin
11	1 919.032	7 252.991	−218.626	WP6	PXK146WP6	WP-0480-6	WP0480-6	Wescor
12	1 919.031	7 253.198	−218.652	WF1	PXK146WF1	WF-0480-1	WF0480-1	Delta-T
13	1 919.031	7 253.406	−218.626	WC4	PXK146WC4	WC-0480-4	WC0480-4	Aitemin
14	1 919.050	7 253.997	−217.803	WP3	PXK146WP3	WP-0480-3	WP0480-3	Wescor
15	1 919.047	7 253.997	−217.903	WC5	PXK146WC5	WC-0480-5	WC0480-5	Aitemin
16	1 918.860	7 253.861	−217.794	WSUS8	Transmitter	WSU-S8	Wireless	Aitemin

Table 5-2. Numbering and position of inner transition zone sensors in drift section 9 (transition blocks).

	Coordinate system ÄSPÖ 96							
Point No.	Easting [m]	Northing [m]	Point Elevation [m]	Drawing label	Sensor code in SICADA	Sensor code in SCADA	Assembly tag label	Manufacturer
1	1 920.398	7 253.200	−217.360	IB2	PXK159IB2	IB-0286-2	IB0311-2	Measurement specialities
2	1 920.499	7 253.264	−218.148	WC1	PXK160WC1	WC-0286-1	Wireless	Aitemin
3	1 920.372	7 253.200	−218.450	IB1	PXK159IB1	IB-0286-1	Wireless	Measurement specialities
4	1 920.739	7 253.201	−217.921	TP1	PXK163TP1	TP-0292-3	DRIFT	Geokon
5	1 920.524	7 253.200	−217.112	WF2	PXK160WF2	WF-0286-2	WF0286-2	Delta-T
6	1 920.486	7 253.408	−218.681	WC3	PXK160WC3	WC-0286-3	WC0286-3	Aitemin
7	1 920.523	7 252.993	−217.137	WP4	PXK160WP4	WP-0286-4	WP0286-4	Wescor
8	1 920.523	7 253.408	−217.136	WC5	PXK160WC5	WC-0286-5	WC0286-5	Aitemin
9	1 920.507	7 252.402	−217.858	WP5	PXK160WP5	WP-0286-5	WP0286-5	Wescor
10	1 920.505	7 252.402	−217.958	WC6	PXK160WC6	WC-0286-6	WC0286-6	Aitemin
11	1 920.511	7 253.136	−217.668	WP1	PXK160WP1	WP-0286-1	WP0286-1	Wescor
12	1 920.510	7 253.265	−217.669	WC2	PXK160WC2	WC-0286-2	Wireless	Aitemin
13	1 920.505	7 253.999	−217.858	WP3	PXK160WP3	WP-0286-3	WP0286-3	Wescor
14	1 920.502	7 253.999	−217.958	WC4	PXK160WC4	WC-0286-4	Wireless	Aitemin
15	1 920.315	7 253.863	−217.849	WSUS9	Transmitter	WSU-S9	Wireless	Aitemin
16	1 920.742	7 252.746	−217.651	DB2	PXK163DB2	DB-0286-2	Wireless	RDP
17	1 920.723	7 253.655	−218.176	DB1	PXK163DB1	DB-0286-1	Wireless	RDP
18	1 920.499	7 253.136	−218.146	WP2	PXK160WP2	WP-0286-2	WP0286-2	Wescor
19	1 920.487	7 252.993	−218.681	WP6	PXK160WP6	WP-0286-6	WP0286-6	Wescor
20	1 920.486	7 253.200	−218.707	WF1	PXK160WF1	WF-0286-1	WF0286-1	Delta-T

Table 5-3. Numbering and position of inner transition zone sensors in drift section 10 (pellet-filling zone/plug interface).

	Coordinate system ÄSPÖ 96							
Point No.	Easting [m]	Northing [m]	Point Elevation [m]	Drawing label	Sensor code in SICADA	Sensor code in SCADA	Assembly tag label	Manufacturer
1	1922.700	7252.311	−217.995	PP5	PXK182PP5	PP-0029- 5	PP-0000-5	Measurement specialities
2	1922.697	7254.097	−217.995	PP4	PXK182PP4	PP-0029-4	PP-0000-4	Measurement specialities
3	1922.698	7253.204	−217.995	TP1	PXK182TP1	TP-0029-1	Wireless	Geokon/ÅF
4	1922.698	7253.205	−217.925	PP1	PXK182PP1	PP-0029-1	Wireless	Measurement specialities
5	1922.935	7253.205	−217.347	PP3	PXK185PP3	PP-0029-3	Wireless	Measurement specialities
6	1922.903	7253.205	−218.667	PP2	PXK185PP2	PP-0029-2	Wireless	Measurement specialities
7	1922.719	7253.250	−217.099	GP1	PXK182GP1	GP-0029	GP-0000-1	Keller
8	1922.719	7253.158	−217.099	PP6	PXK182PP6	PP-0029-6	PP-0000-6	Measurement specialities
9	1922.642	7253.467	−217.934	WSUS10	Transmitter	WSU-S10	Wireless	Aitemin
10	1923.892	7253.207	−217.531	DC1	PXK200DC1	DC-100-1	Aitemin	RDP
11	1923.875	7253.207	−218.031	DC2	PXK200DC2	DC-100-2	Aitemin	RDP
12	1923.867	7253.207	−218.531	DC3	PXK200DC3	DC-100-3	Aitemin	RDP
13	1922.849	7253.205	−218.569	TP-2	PXK182TP2	TP-0029-2	Close to PP2	Geokon/ÅF
14	1922.902	7253.205	−217.404	TP-3	PXK182TP3	TP-0029-3	Close to PP3	Geokon/ÅF

5.2 Inner sensor results and comments

5.2.1 Relative humidity

The relative humidity sensors (WC-4, WC-6 and WC-7) in the peripheral positions of the transition block in section S-8 measured fast increases in the relative humidity reaching 100 % (saturation) within the first 300 days (see Figure 5-1). The process was slower at the top position (WC-6) as more time is required for water to reach this location. The signal from the sensor further inside the block (WC-2) showed a gradually increasing trend to below 85 % RH at the end of the period.

There are no data available from the wireless sensors as signals from WC-1 and WC-5 were lost a few hours after starting the test and that from sensor WC-3 was lost at close to 60 days.

The relative humidity sensors (WC-3 to WC-6) in the peripheral positions of the transition block in section S-9 have measured fast increases in relative humidity (Figure 5-2). Sensors WC-3 and WC-6 showed 100 % RH within 229 days. Sensor WC-5 recorded more gradual increases in RH, the signal was still increasing at day 543 when it was lost after reaching 97 % RH. These results are in keeping with the top positions saturating more slowly than the lower positions.

Very little data was received from the wireless sensors (WC-1, WC-2 and WC-4); signal was received from sensors WC-1 and WC-4 only from day 50 to 60 and no signal at all was received from sensor WC-2. After day 543 no signal was being received from any sensors in this location.

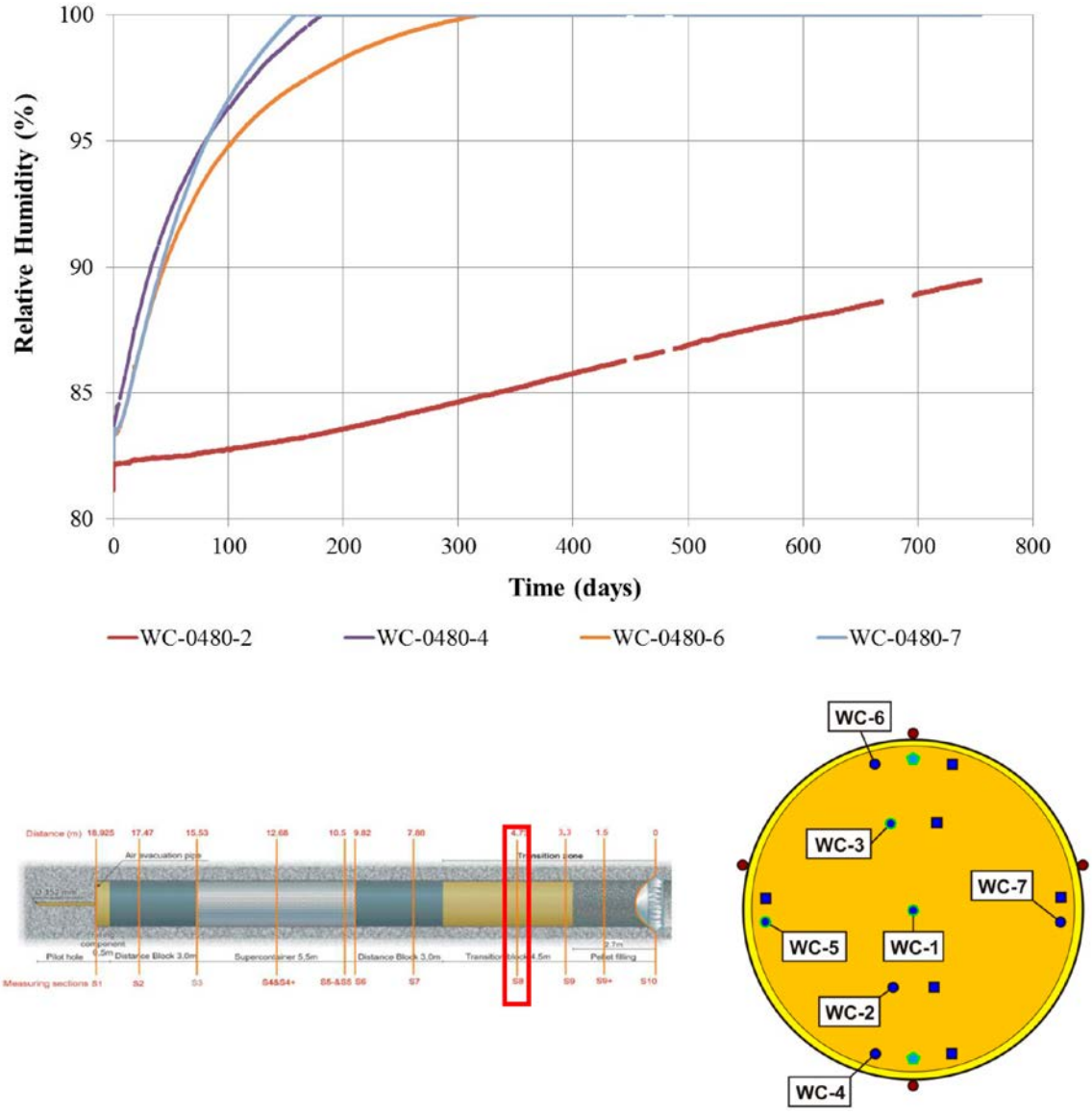

Figure 5-1. *Response of capacitive hygrometer sensors at inner transition zone positions in drift section S-8. A total of seven such sensors were installed in this section. The radial distance of sensor WC-2 to the rock wall is 400 mm and that of sensors WC-4 to WC-7 to the rock wall is 125 mm.*

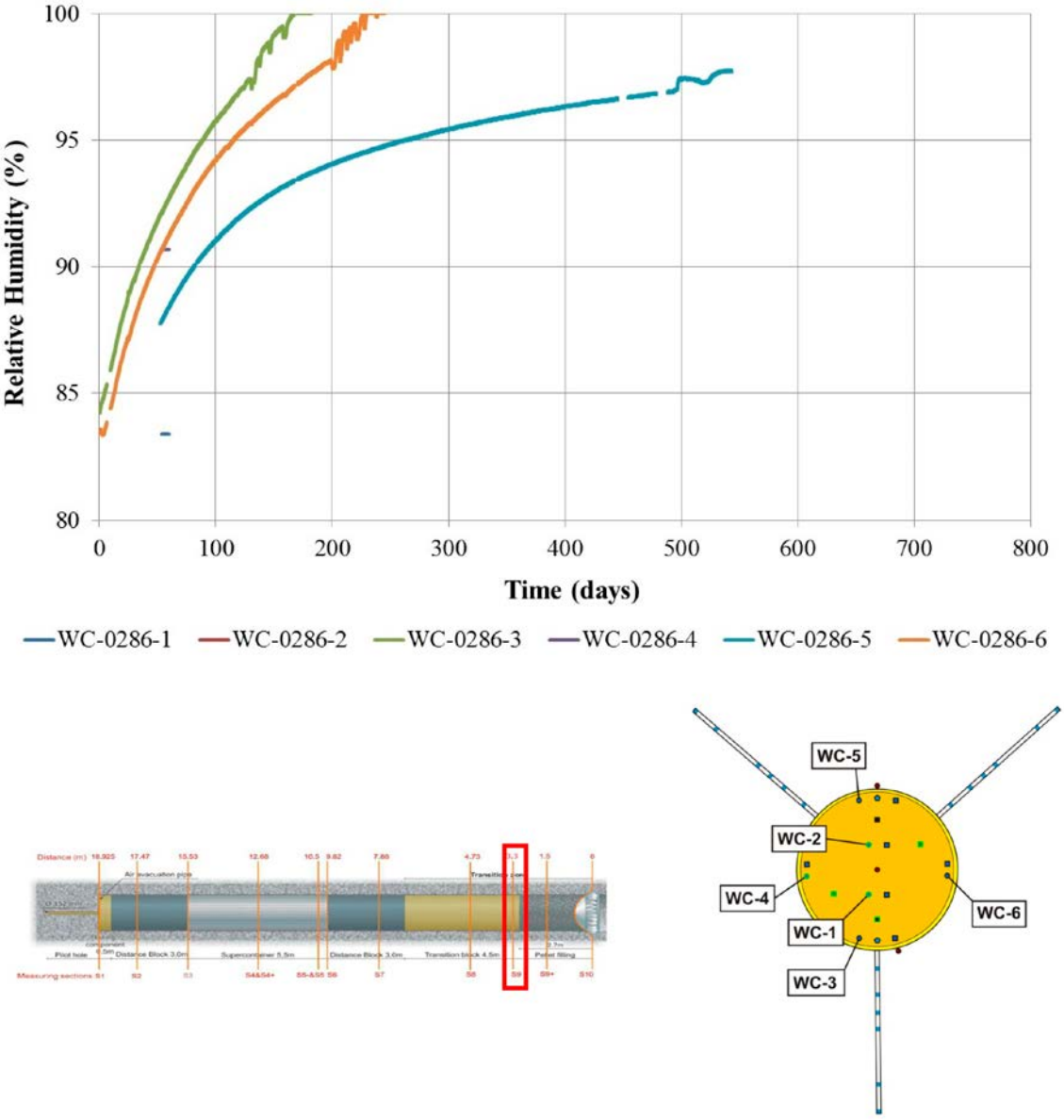

Figure 5-2. *Response of capacitive hygrometer sensors at inner transition zone positions in drift section S-9. A total of six such sensors were installed in this section. The radial distance of sensors WC-1 and WC-2 to the rock wall is 675 mm and that of sensors WC-3 to WC-6 to the rock wall is 125 mm.*

5.2.2 Suction

As indicated previously, in-range signals from the psychrometers correspond only to suction established at 95 % relative humidity. For temperatures between 5 °C and 15 °C, the suction at 95 % relative humidity should be between 6.6 and 6.8 MPa.

A total of six psychrometer sensors were installed in S-8 (see Figure 5-3). Sensors WP-3, WP-4, WP-5 and WP-6 in peripheral locations have reached in-range suction limits. All sensors came into range at more or less at the same time with that at the top being delayed in accord with the RH measurements (see Figure 5-1). The psychrometer sensors provide higher resolution concerning full saturation and, as can be observed, this condition was most closely reached only at the bottom of the drift while the remaining sensor positions show less saturation.

The signals for sensors closer to the center have not yet started to approach in-range limits. All signals were lost after day 551 and reestablished on day 767.

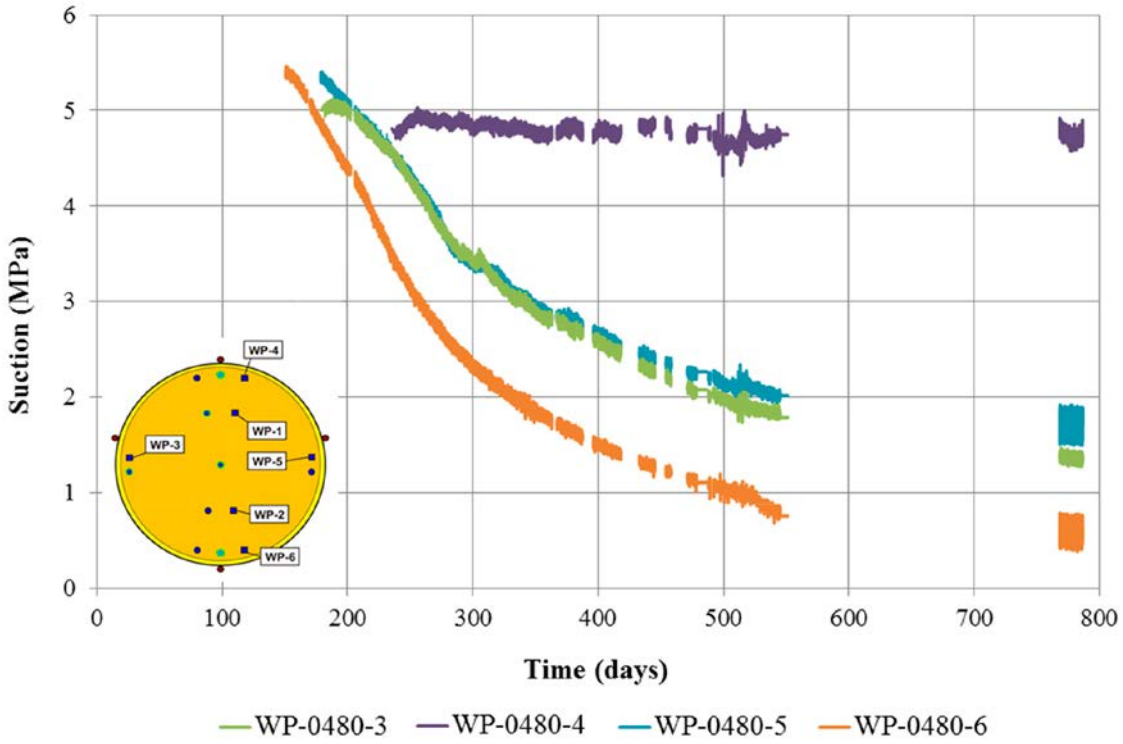

Figure 5-3. *Decay in psychrometer signal for sensors WP-3 to WP-6 in inner transition zone positions in drift section 8 after reaching in-range suction limits. The radial distance of sensors WP-1 and WP-2 to the rock wall is 675 mm and that of sensors WC-3 to WP-6 to the rock wall is 125 mm.*

A total of six psychrometer sensors were installed in S-9 as well (see Figure 5-4). The signals from all of these sensors are noisier than those in S-8.

Although the signals are noisy, it is evident that sensors WP-3, WP-4, WP-5 and WP-6 in peripheral locations have reached in-range suction limits. Sensor WP-6 developed such signal first, by day 150, while the others do so after day 300. Once again, it is the case that the top location is delayed relative to the other positions, in accord with the capacitive hygrometer data. The psychrometer sensors provide higher resolution concerning full saturation and, as can be observed, this condition (suction close to zero) was not reached at any location.

The signals for the sensors closer to the center of the block have not yet started to approach in-range limits. All signals were lost after day 551 and reestablished on day 767.

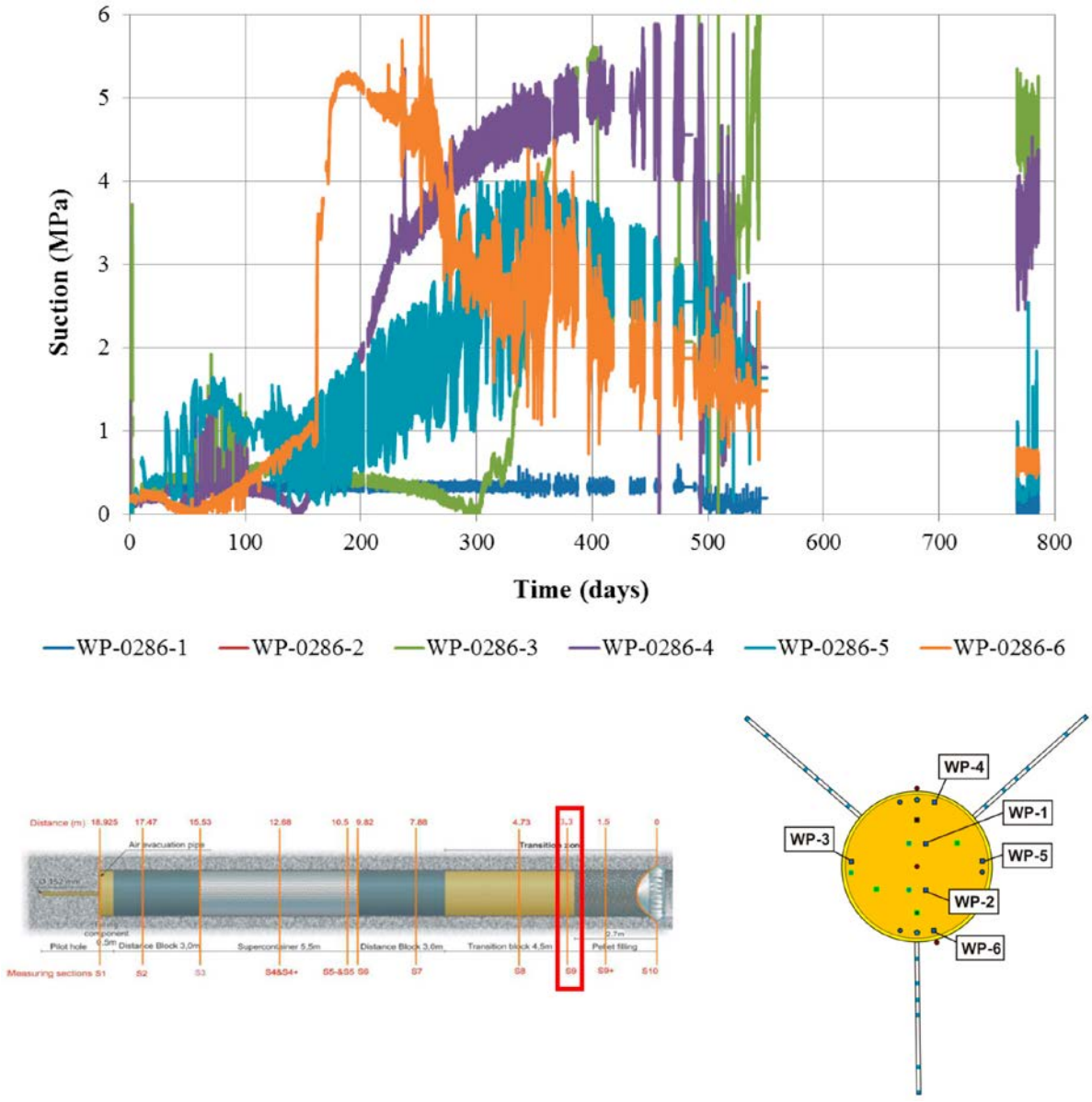

Figure 5-4. *Response of psychrometers at inner transition zone positions in drift section S-9. The radial distance of sensors WP-1 and WP-2 to the rock wall is 675 mm and that of sensors WC-3 to WP-6 to the rock wall is 125 mm.*

5.2.3 Pore pressure

Six pore pressure sensors were installed at the interface between the pellet-filling zone and the plug in drift section 10 (see Figure 5-5). Signal was not recorded from sensors PP-4, PP-5 and PP-6 until approximately day 50. No signal has been received from wireless sensors PP-1, PP-2 or PP-3 since 11.12.2013. Sensor PP-4 showed a sharp increase in pressure before day 100 to 0.8 MPa which decreased afterwards to values ranging between 0.5 and 0.6 MPa. This signal then jumped to above 0.6 MPa and remained steady until the end of the measurement period. After day 255, the signal from sensor PP-6 started increasing and reached values above 0.5 MPa by the end of the measurement period. Sensor PP-5 remained slightly above 0.1 MPa during the entire period.

A gas pressure sensor was also installed at the interface between the pellet-filling zone and the plug in drift section 10 (see Figure 5-6). The sensor range was 250 kPa and it was installed for the purposes of measuring the gas pressure during saturation if the DAWE procedure was not followed. As DAWE was followed, the sensor was flooded quickly, in less than 10 days, and essentially measured water pressure. This sensor was changed to a higher range (3 MPa) pore pressure sensor at day 389. An abrupt signal peak was registered at day 466 to nearly 1.2 MPa which then fell to 0.47 MPa and continues to slowly increase.

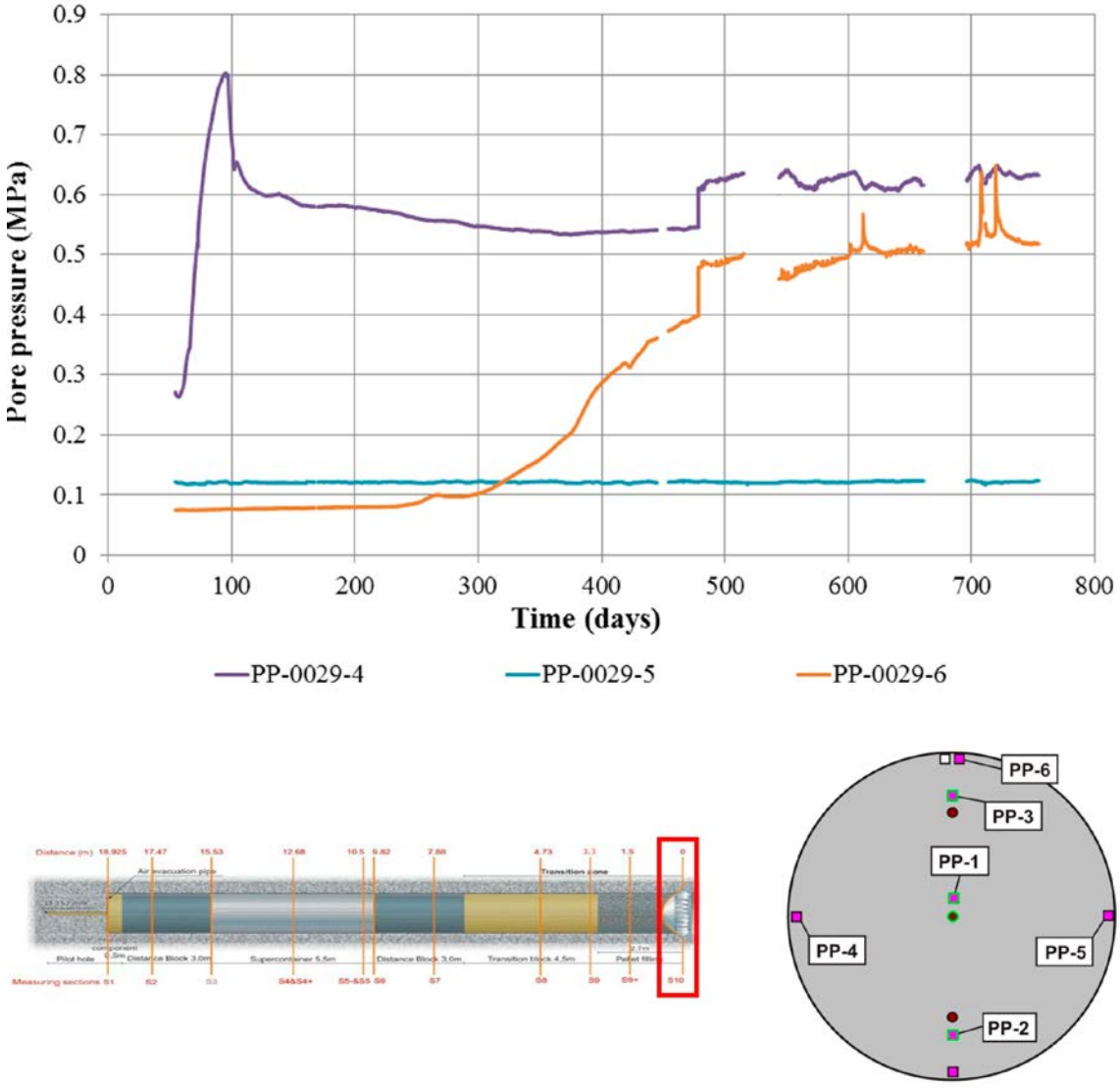

Figure 5-5. *Response of pore pressure sensors at inner transition zone positions at the interface between the pellet-filling zone and the plug in drift section 10.*

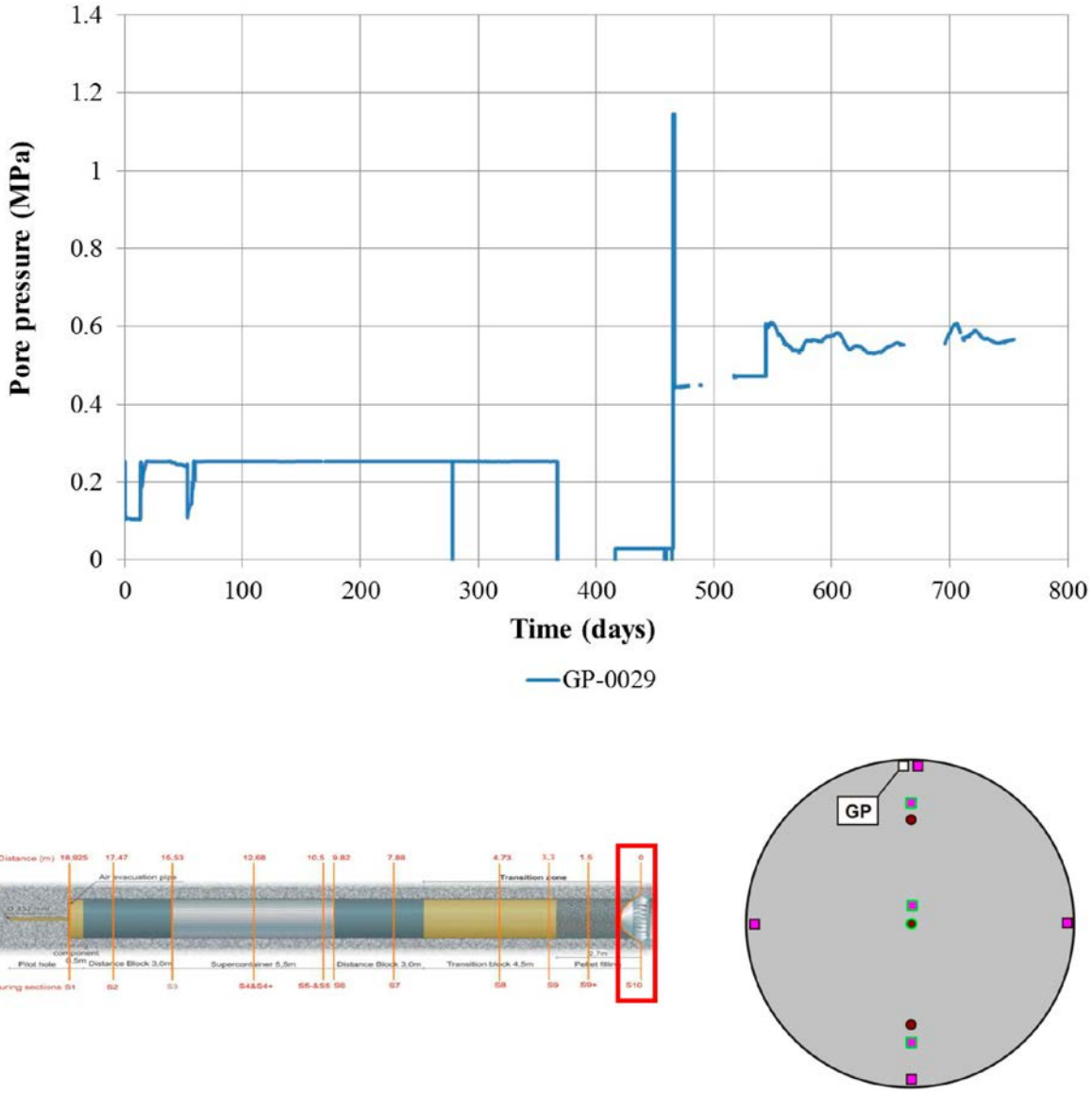

Figure 5-6. *Response of gas pressure sensor at inner transition zone position at the top of the interface between the pellet-filling zone and the plug in drift section 10.*

5.2.4 Water content

In S-9, two soil moisture sensors (WF-1 and WF-2) were installed (see Figure 5-7). After day 50 the signal from sensor WF-1 showed a steady increase to volumetric water content values around 0.36 m^3/m^3 to over 400 days whereas that from sensor WF-2 only slowly increased to 0.10 m^3/m^3 over the same time period. Signals from both sensors abruptly fell at around day 480 and soon after became extremely noisy.

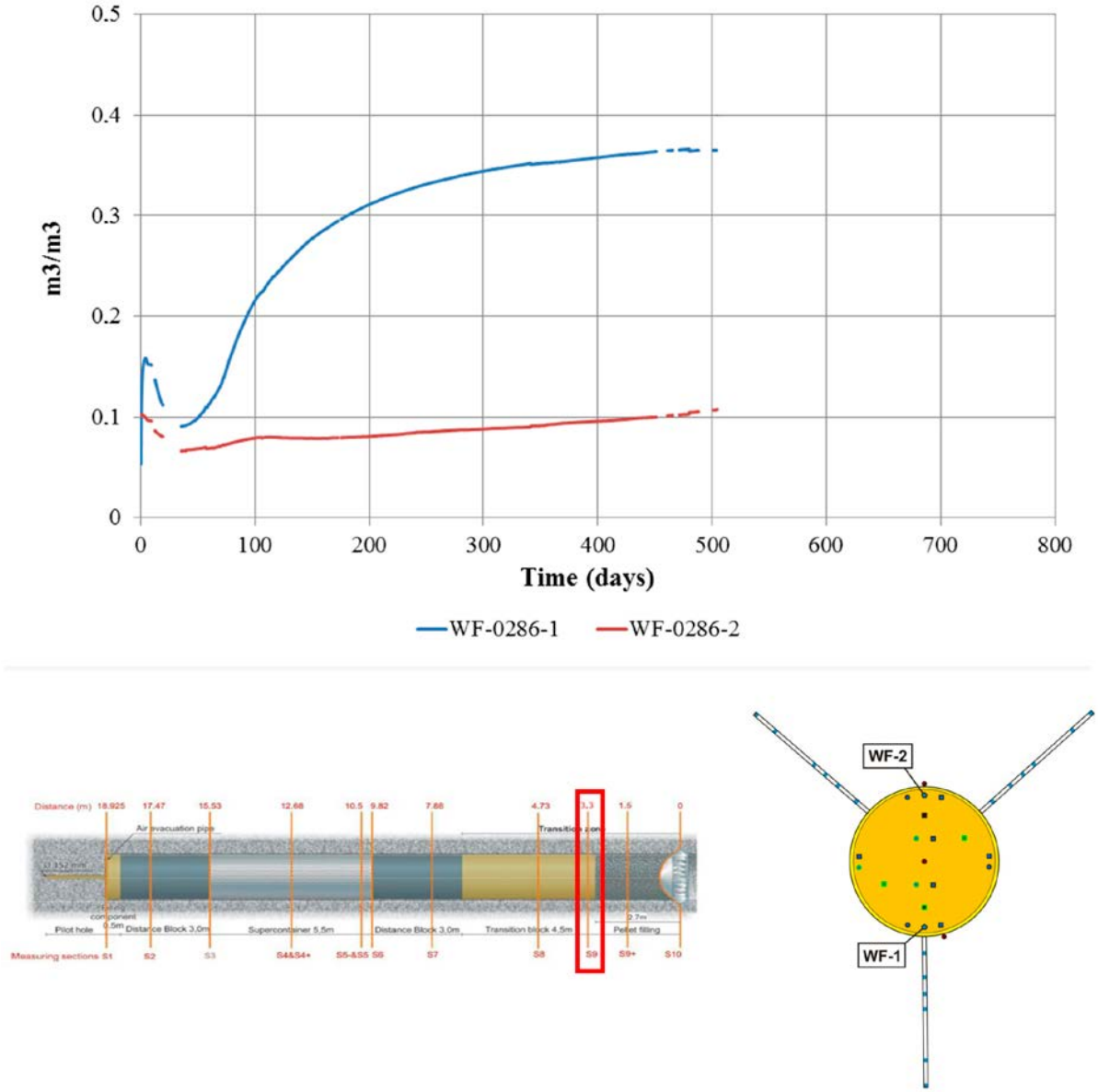

Figure 5-7. *Response of soil moisture sensors at inner transition zone positions in drift section S-9. The distance of the sensors to the rock wall is 125 mm.*

5.2.5 Inclination

Results from the inclinometer sensors installed in S-9 are presented in Figure 5-8. A total of two such sensors were installed in this section (IB-0286-1 and IB-0286-2). Sensor IB-1 is a wireless sensor and no signal has been received from it. Only inclination, relative to that after emplacement, along the x-axis from sensor IB-2 was measured. A sudden change in inclination was registered after the first 3 days to a relatively constant value above 1.5° suggesting a sudden rotation of the block towards the pilot borehole. At day 489 a slight, sudden drop in signal was observed.

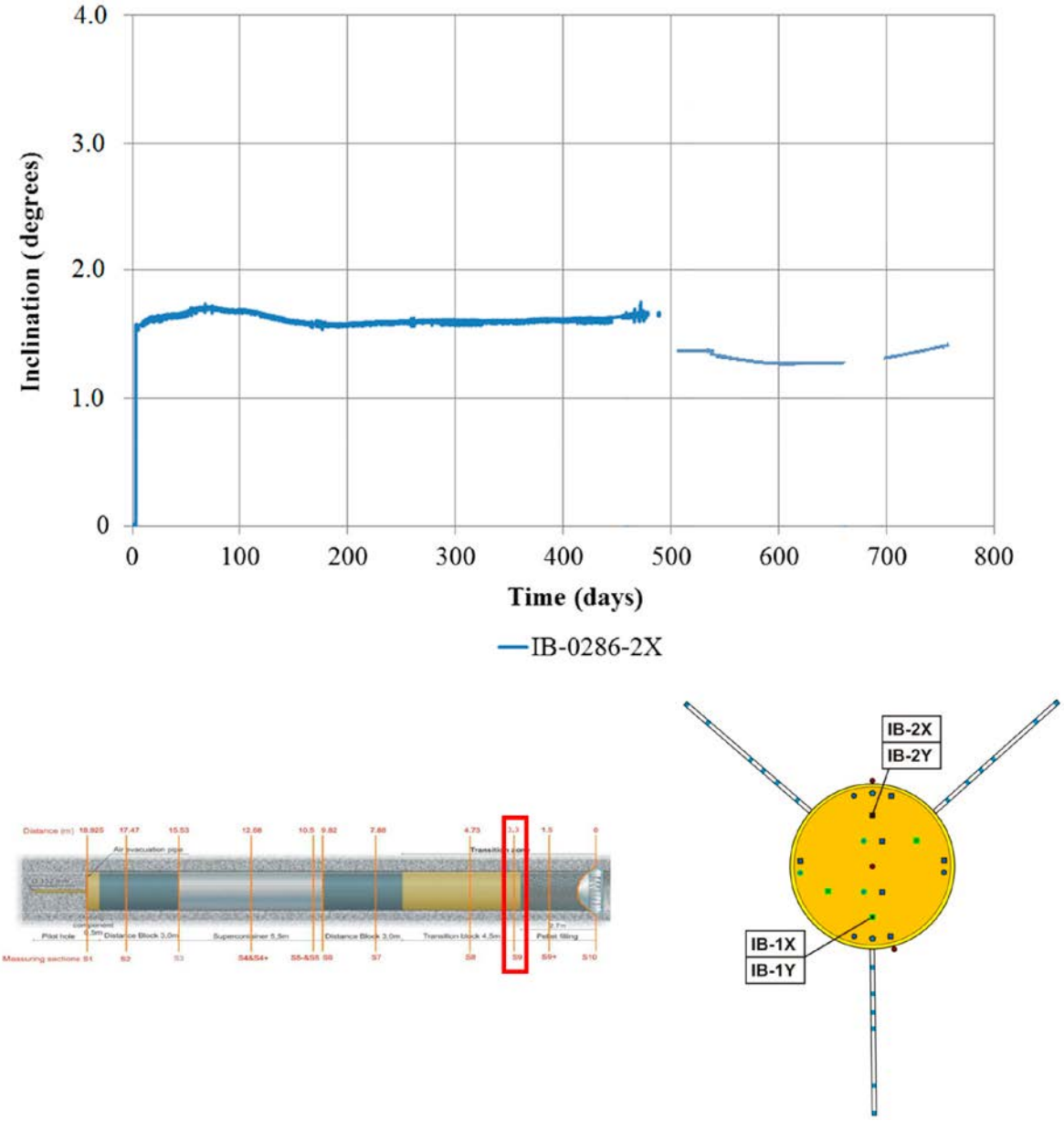

Figure 5-8. *Response of the inclinometer sensors at inner transition zone positions in drift section S-9.*

5.2.6 Displacement

Two wireless displacement sensors (DB-0286-1 and DB-0286-2) were installed in drift section 9. Signal was received from these sensors only between 29 January to 5 February 2013.

5.2.7 Total pressure

Total pressure sensors were installed at the pellet-filled zone/plug interface (Figure 5-9). The pressure is measured orthogonal to the plug. A total of three such sensors were installed in this section (TP-0029-1, TP-0029-2 and TP-0286-3). Sensor TP-1 is a wireless sensor and no signal has been received from it. No pressure was detected by either sensor TP-2 or TP-3 until day 200 when they both showed increasing but noisy signals. After day 478, at which maximum peak values below 2.5 MPa were measured, signals were lost from both sensors.

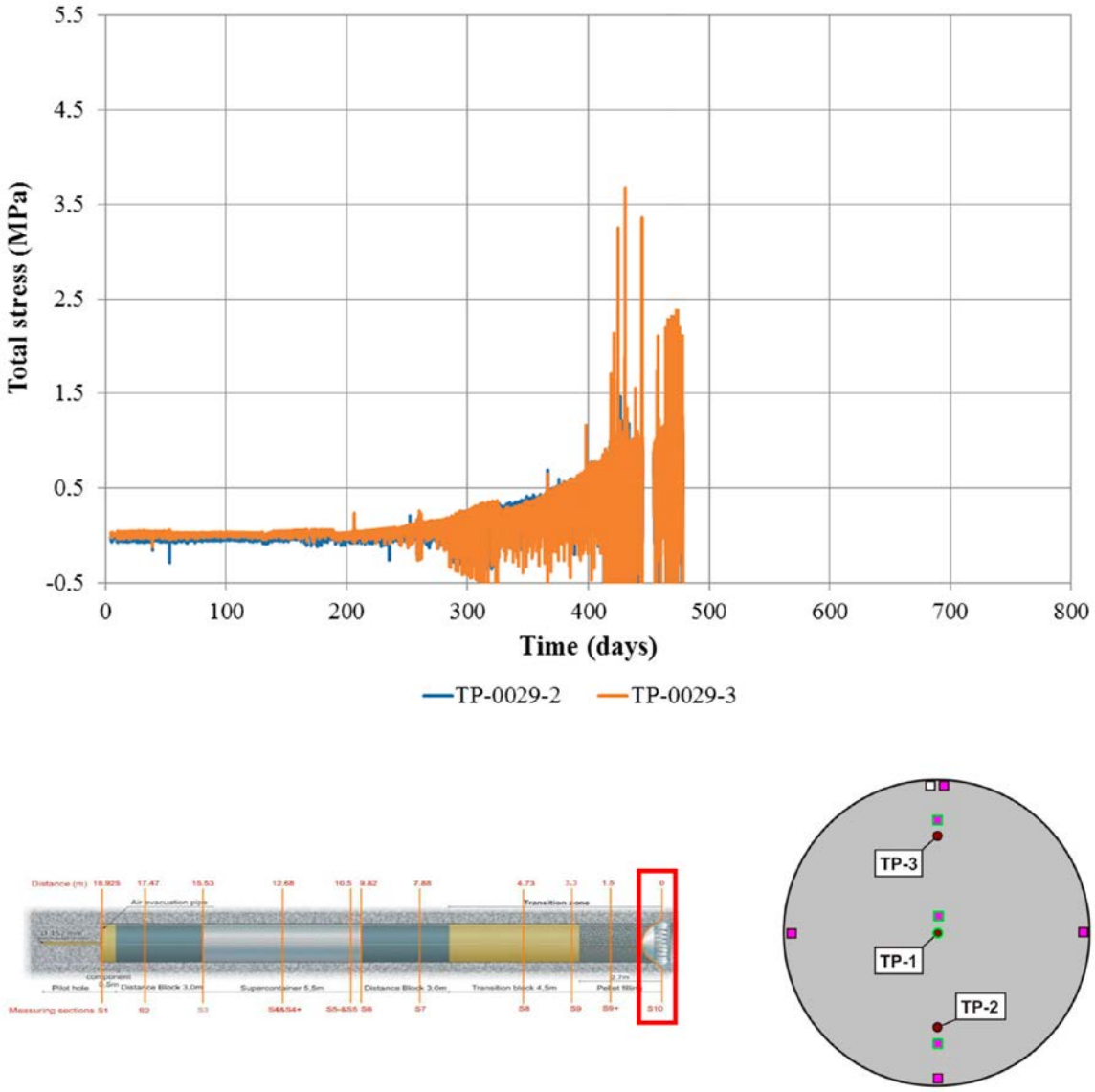

Figure 5-9. *Response of total pressure sensors at the pellet-filled zone/plug interface in drift section S-10.*

5.3 Outer sensor positions

The location of the outer sensors and other information is presented in Tables 5-4 and 5-5 (drift sections 8 and 9) and 5-6 (drift section 9+). This section also contains information regarding the strain gauges on the plug face (Table 5-7).

Table 5-4. Numbering and position of outer transition zone sensors in drift section 8.

Point No.	Easting [m]	Northing [m]	Point Elevation [m]	Drawing label	Sensor code in SICADA	Sensor code in SCADA	Assembly tag label	Manufacturer
25	1918.782	7253.204	−216.928	TP-3	PXK143TP3	TP-0449-3	TP-0449-3	Geokon
26	1918.778	7252.300	−217.620	TP-2	PXK143TP2	TP-0449-2	TP-0449-2	Geokon
27	1918.774	7253.203	−218.771	TP-1	PXK143TP1	TP-0449-1	TP-0449-1	Geokon
28	1918.774	7254.085	−217.615	TP-4	PXK143TP4	TP-0449-4	TP-0449-4	Geokon

Table 5-5. Numbering and position of outer transition zone sensors in drift section 9.

Point No.	Easting [m]	Northing [m]	Point Elevation [m]	Drawing label	Sensor code in SICADA	Sensor code in SCADA	Assembly tag label	Manufacturer
29	1 920.494	7 252.961	−218.804	TP-2	PXK161TP2	TP-0277-2	TP-0277-2	Geokon
30	1 920.498	7 253.212	−216.991	TP-1	PXK161TP1	TP-0277-1	TP-0277-1	Geokon

Table 5-6. Numbering and position of outer transition zone sensors in drift section 9+.

Point No.	Easting [m]	Northing [m]	Point Elevation [m]	Drawing label	Sensor code in SICADA	Sensor code in SCADA	Assembly tag label	Manufacturer
31	1 922.365	7 253.203	−217.058	TP-4	PXK178TP4	TP-0000-4	TP-0000-4	Geokon
32	1 922.316	7 252.301	−217.739	TP-1	PXK178TP1	TP-0150-1	TP-0150-1	Geokon
33	1 922.314	7 252.303	−218.227	TP-3	PXK178TP3	TP-0000-3	TP-0000-3	Geokon
34	1 922.302	7 253.192	−218.901	TP-2	PXK178TP2	TP-0000-2	TP-0000-2	Geokon
35	1 922.324	7 254.082	−218.233	TP-5	PXK178TP5	TP-0000-5	TP-0000-5	Geokon
36	1 922.363	7 254.081	−217.739	TP-2	PXK179TP2	TP-0150-2	TP-0150-2	Geokon

Table 5-7. Numbering and position of sensors in rock wall in drift section 9.

	Coordinate system ÄSPÖ 96							
Point No.	Easting [m]	Northing [m]	Point Elevation [m]	Drawing label	Sensor code in SICADA	Sensor code in SCADA	Assembly tag label	Manufacturer
1	1 920.505	7 251.669	−217.045	PP-2	PXK16PP2	PP-0292-2	PP-0292-2	Keller
2	1 920.547	7 250.325	−216.256	PP-5	PXK16PP5	PP-0292-5	PP-0292-5	Keller
3	1 920.572	7 249.549	−215.800	PP-8	PXK16PP8	PP-0292-8	PP-0292-8	Keller
4	1 920.600	7 248.635	−215.264	PP-11	PXK16PP11	PP-0292-11	PP-0292-11	Keller
5	1 920.625	7 247.851	−214.803	PP-14	PXK16PP14	PP-0292-14	PP-0292-14	Keller
6	1 920.742	7 244.135	−212.622	PP-17	PXK16PP17	PP-0292-17	PP-0292-17	Keller
7	1 920.448	7 253.208	−219.700	PP-1	PXK16PP1	PP-0292-1	PP-0292-1	Keller
8	1 920.384	7 253.206	−221.259	PP-4	PXK16PP4	PP-0292-4	PP-0292-4	Keller
9	1 920.347	7 253.205	−222.158	PP-7	PXK16PP7	PP-0292-7	PP-0292-7	Keller
10	1 920.262	7 253.202	−224.226	PP-10	PXK16PP10	PP-0292-10	PP-0292-10	Keller
11	1 920.226	7 253.201	−225.125	PP-13	PXK16PP13	PP-0292-13	PP-0292-13	Keller
12	1 920.090	7 253.196	−228.433	PP-16	PXK16PP16	PP-0292-16	PP-0292-16	Keller
13	1 920.523	7 254.695	−217.053	PP-3	PXK16PP3	PP-0292-3	PP-0292-3	Keller
14	1 920.557	7 255.607	−216.515	PP-6	PXK16PP6	PP-0292-6	PP-0292-6	Keller
15	1 920.586	7 256.382	−216.058	PP-9	PXK16PP9	PP-0292-9	PP-0292-9	Keller
16	1 920.643	7 257.906	−215.159	PP-12	PXK16PP12	PP-0292-12	PP-0292-12	Keller
17	1 920.672	7 258.680	−214.701	PP-15	PXK16PP15	PP-0292-15	PP-0292-15	Keller
18	1 920.815	7 262.476	−212.461	PP-18	PXK16PP18	PP-0292-18	PP-0292-18	Keller

5.4 Outer sensor results and comments

5.4.1 Total pressure

Total pressure measurements are presented in Figures 5-10 to 5-12.

In S-8, four total pressure sensors were installed at the rock wall around the transition zone block (Figure 5-10). The signal responses were similar to those observed in S-7, i.e. all of the sensors measured increasing pressures up to day 106 to values around 0.8 MPa which then decreased to 0.65 MPa. The signals from sensors TP-2 and TP-4 (located at the sides) continued increasing over the measurement period steadily to pressures of 1.2 MPa. The signal from sensor TP-1 (at the bottom) decreased to pressures of 0.55 MPa by day 300 and then continued increasing over the measurement period steadily to pressures of 0.8 MPa. The signal from sensor TP-3 (at the top) decreased to pressures of 0.5 MPa by day 400 after which it increased briefly and then continued decreasing over the measurement period steadily to pressures of 0.4 MPa.

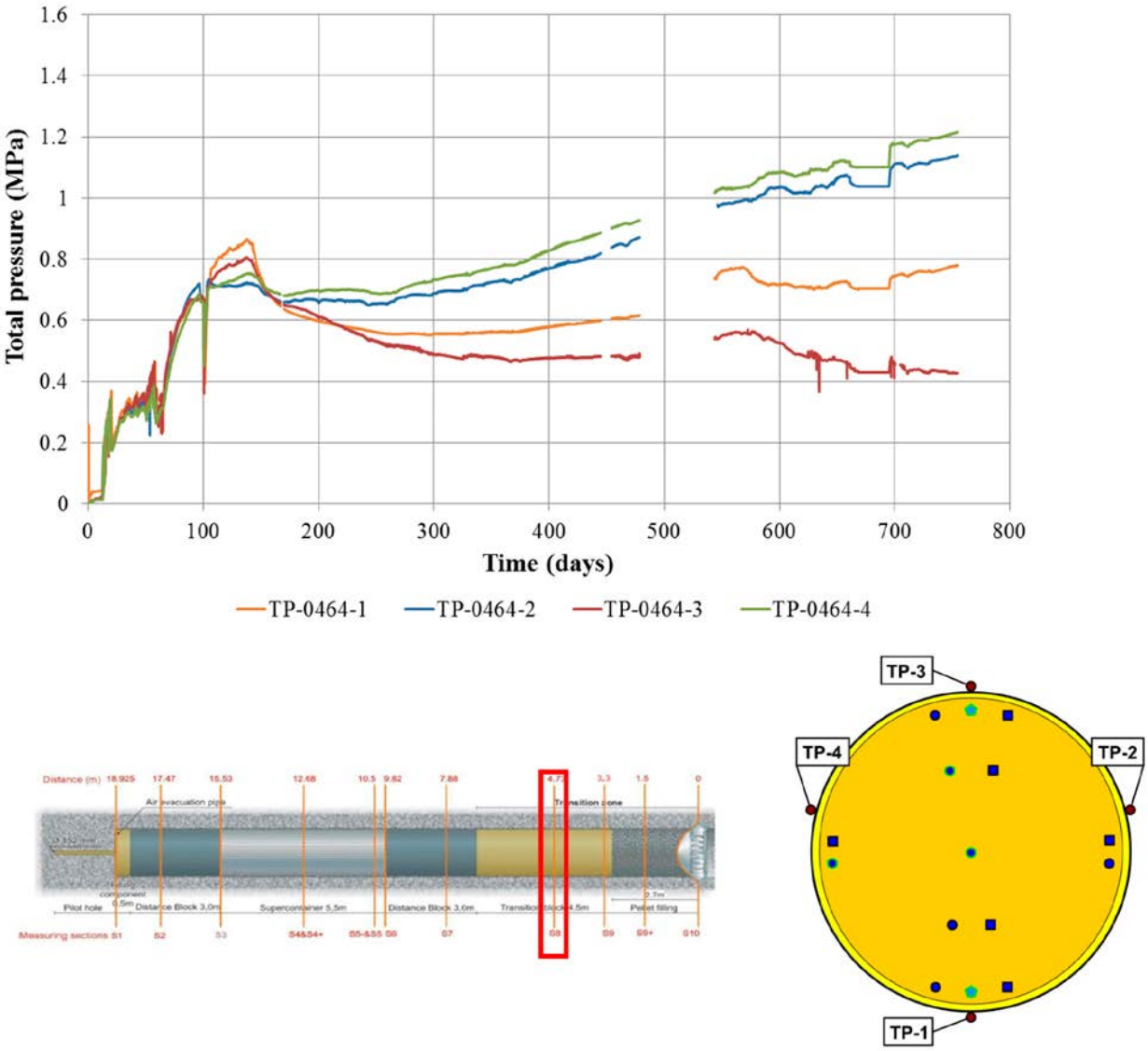

Figure 5-10. *Response of total pressure sensors at outer transition zone positions (at the rock wall surface) in drift section 8.*

Two total pressure sensors were installed at the rock wall at the top and bottom of the drift in section S-9 (see Figure 5-11). TP-1 corresponds to a sensor installed in the buffer block but this sensor is not functioning properly. Similar to the total pressure sensors in drift section 8 (see Figure 5-10), sensor TP-2 (at the top) shows increasing pressure to 0.5 MPa at day 100 which then slowly decrease to 0.4 MPa by day 480. The signal from sensor TP-2 then showed a sudden jump to 1 MPa where it more or less remained through the measurement period.

Sensor TP-3 (at the bottom) measured steadily increasing pressures up to over 3.5 MPa by the end of the measurement period. The signal from this sensor is exceptionally high taking into account that this section resides in the dry part of the drift (see Figure 1-4). The presence of pellet filling close to this section could be providing some influence.

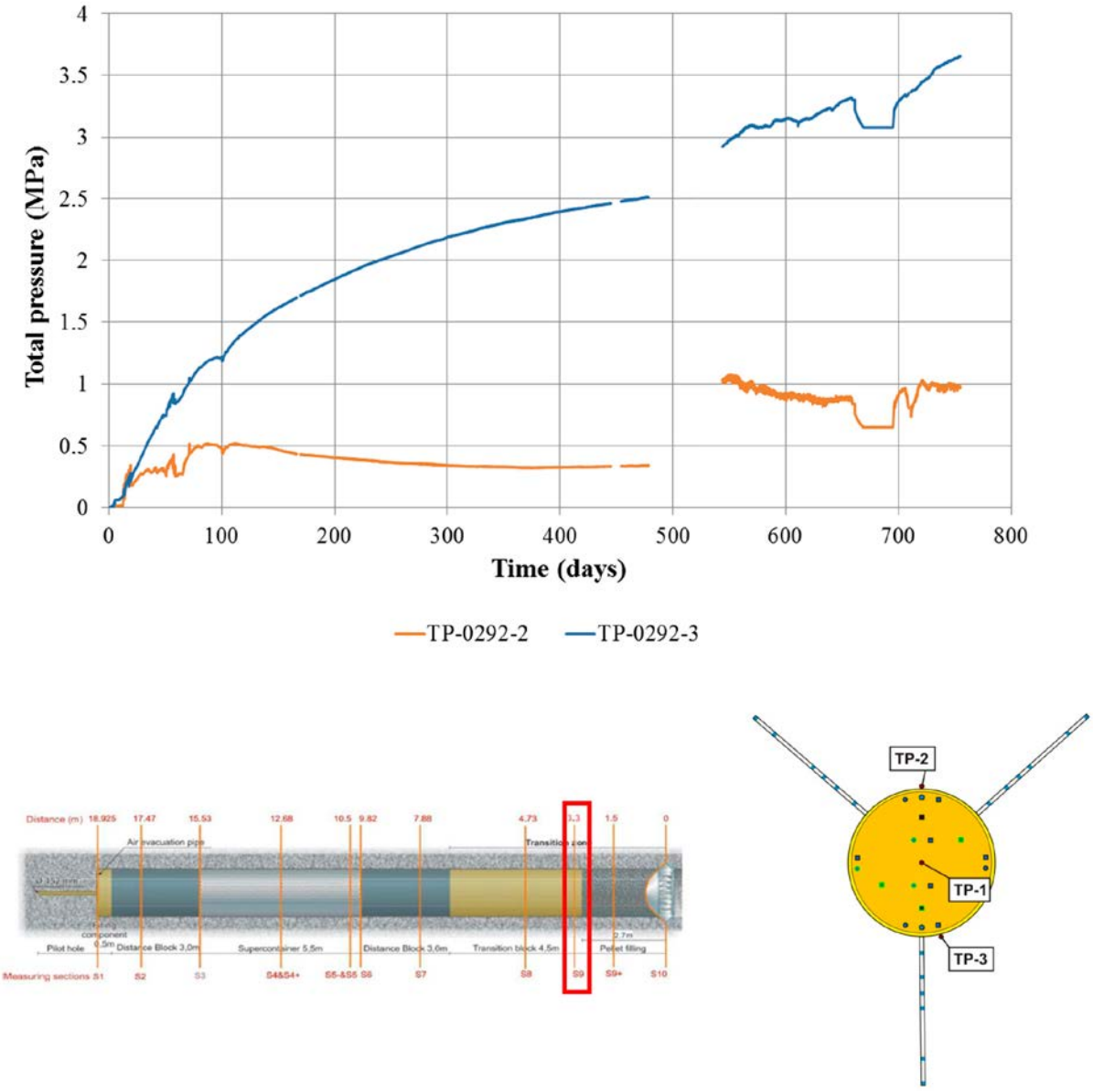

Figure 5-11. *Response of total pressure sensors at outer transition zone positions (at the rock wall surface) in drift section 9.*

Six total pressure sensors were installed in the pellet-filled zone in S-9+ (see Figure 5-12). The sensors all measure similar behavior of rapidly increasing pressures up to day 100 followed by shallow drops and then slow increases over the course of the measurement period. Final, relatively constant, pressures of 0.85, 0.65, 0.65, 0.6, 0.6 and 0.3 MPa were measured for sensors TP-4, TP-2, TP-5, TP-3, TP-6 and TP-1, respectively. Given that these pressures are higher than those expected on the basis of swelling pressure from the pellet filling alone (100–200 kPa), much of the measured pressure is likely due to water pressure.

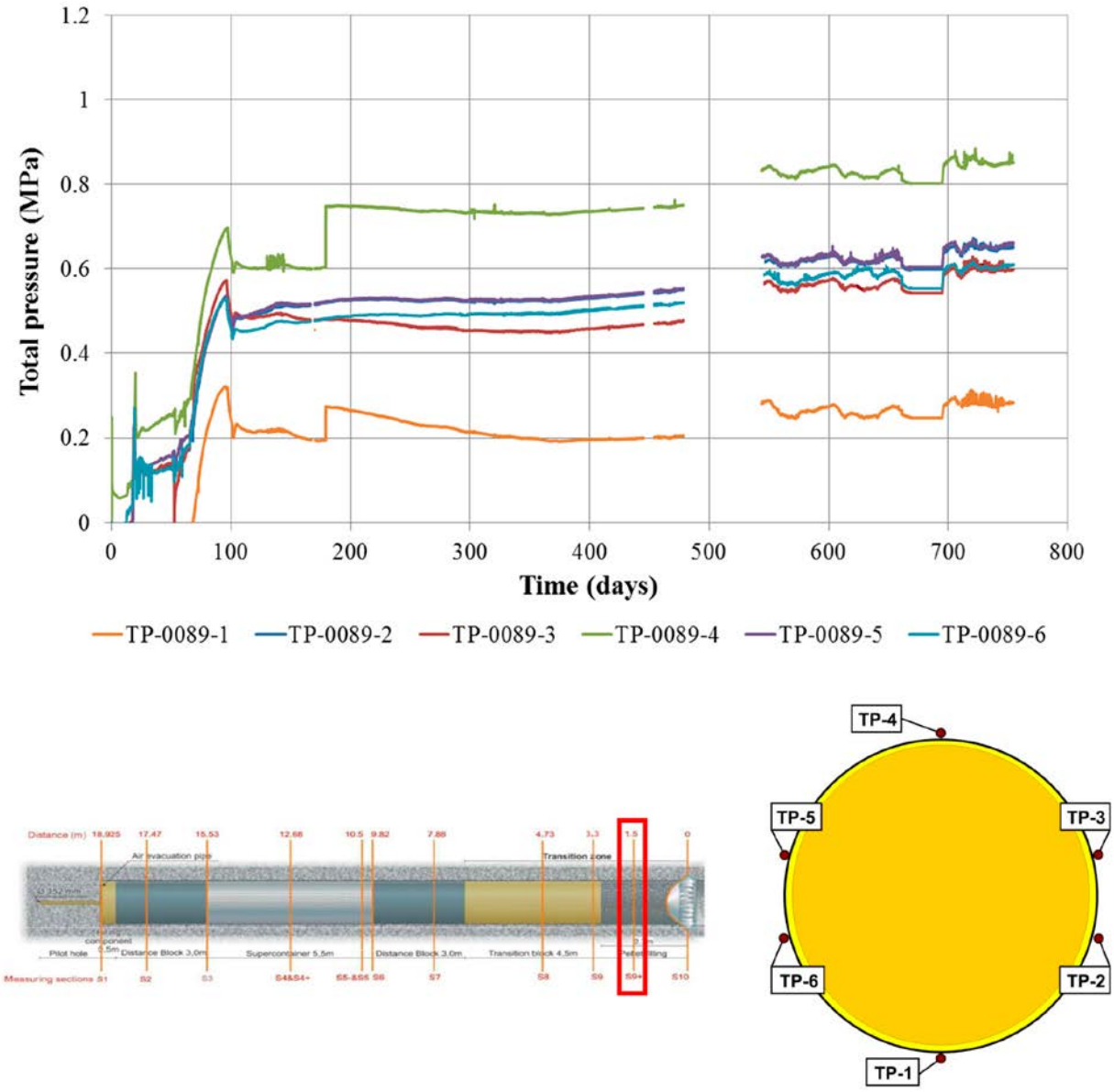

Figure 5-12. *Response of total pressure sensors at outer transition zone positions (at the rock wall surface) in drift section 9+.*

5.4.2 Pore pressure

Pore pressure measurements in the three boreholes drilled into the rock wall in drift section 9 are presented in Figures 5-13 to 5-15. The packer system generated peak pressures on December 10 and 27, 2013. These peaks were registered by the total pressure sensors.

Six pore pressure sensors were installed in the bottom borehole (see Figure 5-13). After installation the measured signals leveled off to different values relative to their position in the borehole with higher values corresponding to longer distances from the drift. Up to day 500, sensor PP-1 (near sensor) was reading 0.5 MPa while sensor PP-16 (far sensor) showed 1.2 MPa. After day 500 the signal from sensor PP-1 jumped to 1 MPa in line with sensors PP-4 and PP-7.

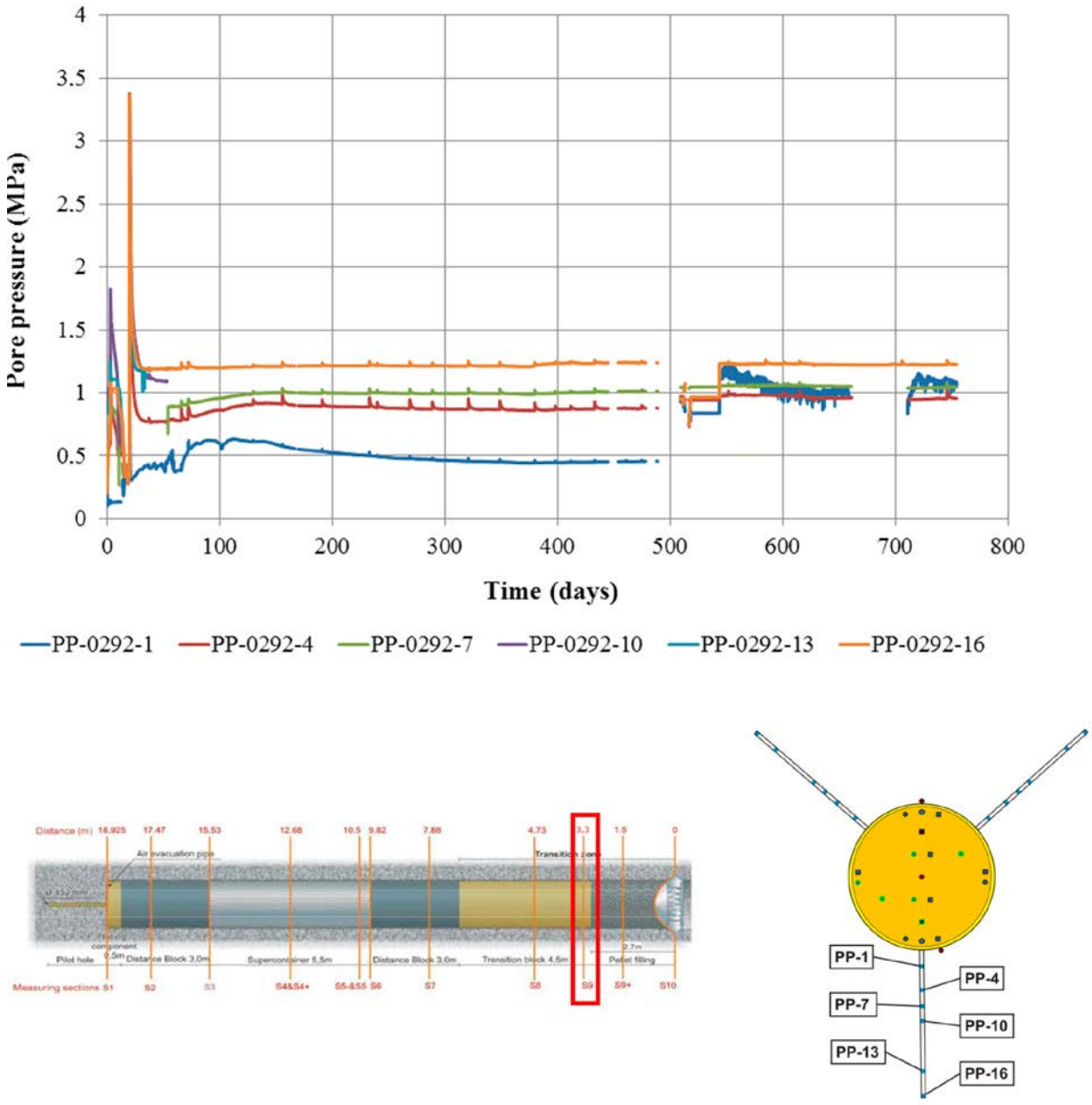

Figure 5-13. *Response of pore pressure sensors at outer transition zone positions in borehole 1 (KA1619A04 in Äspö reference) in drift section 9.*

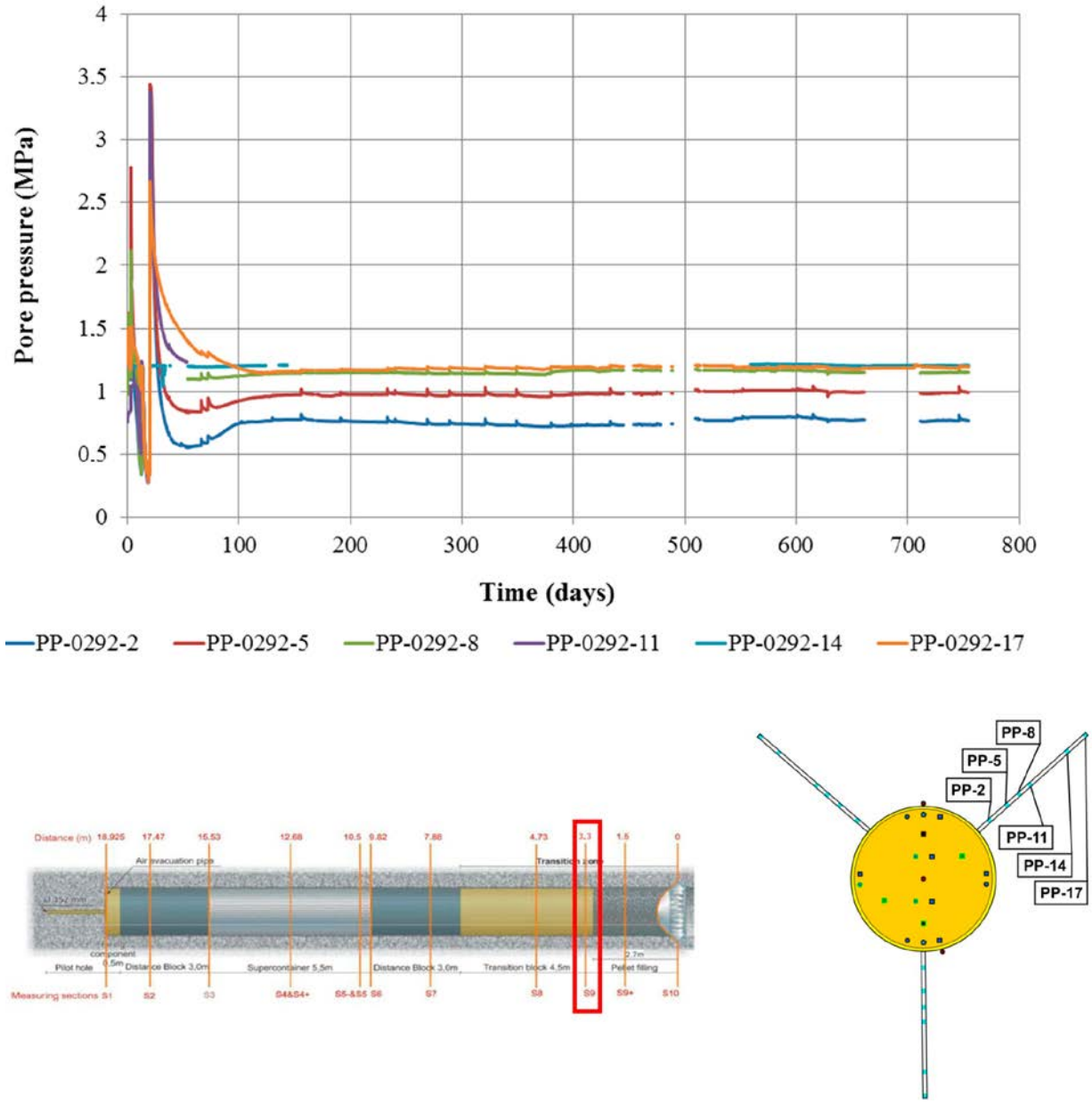

Figure 5-14. *Response of pore pressure sensors at outer transition zone positions in borehole 2 (KA1619A03 in Äspö reference) in drift section 9.*

Six pore pressure sensors were installed in the upper right borehole (see Figure 5-14). Again, after installation the measured signals leveled off to different values relative to their position in the borehole with higher values corresponding to longer distances from the drift. At the end of the measurement period sensors PP-17, PP-14 and PP-8 showed pressures of 1.2 MPa, sensor PP-5 showed a pressure of 1 MPa and sensor PP-2 showed a pressure of 0.76 MPa.

Six pore pressure sensors were installed in the upper-left borehole (see Figure 5-15). After installation the measured signals for all of the sensors leveled off to the same value of 1.24 MPa suggesting that the six sections along this borehole are hydraulically connected.

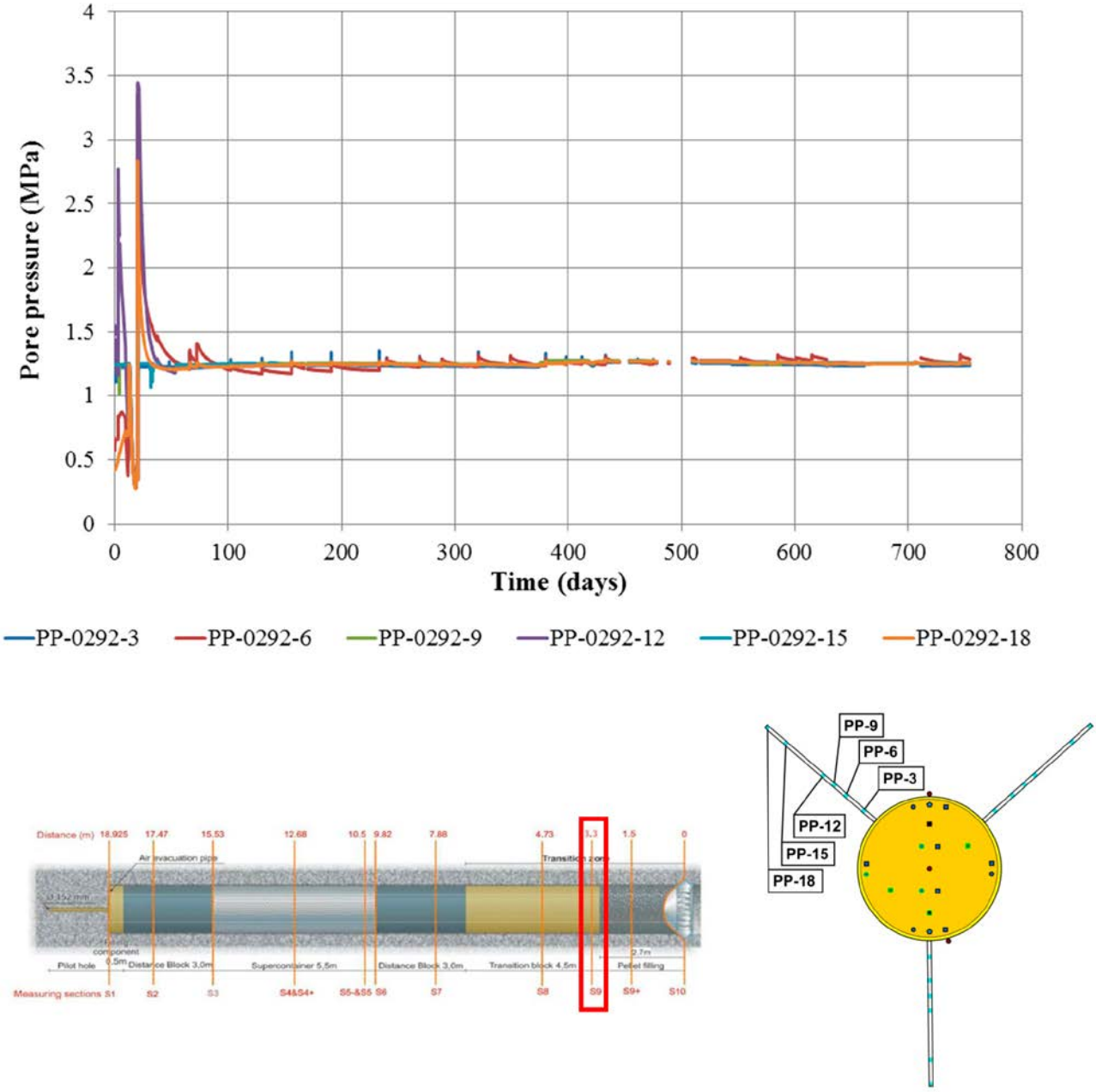

Figure 5-15. *Response of pore pressure sensors at outer transition zone positions in borehole 3 (KA1620A01 in Äspö reference) in drift section 9.*

5.4.3 Plug displacements

Signals from the three installed displacement sensors on the plug face are presented in Figure 5-16. Overall the measured displacements are quite small and near the limit of detection of the sensors. The linearity of the sensors is 0.1 % FS and the range is 25 mm, corresponding to a measurement uncertainty of ±25 µm. No significant movement (1–2 mm) was recorded during nearly the first 300 days of the test. The signal drops after 291 days were caused by intentional movements of the sensors. These movements were performed in order to check sensor functionality. The signal from sensor DC-1 became somewhat noisy after day 700.

5.4.4 Plug strains

Signals from strain gauge measurements on the plug face are presented in Figures 5-17 to 5-19.

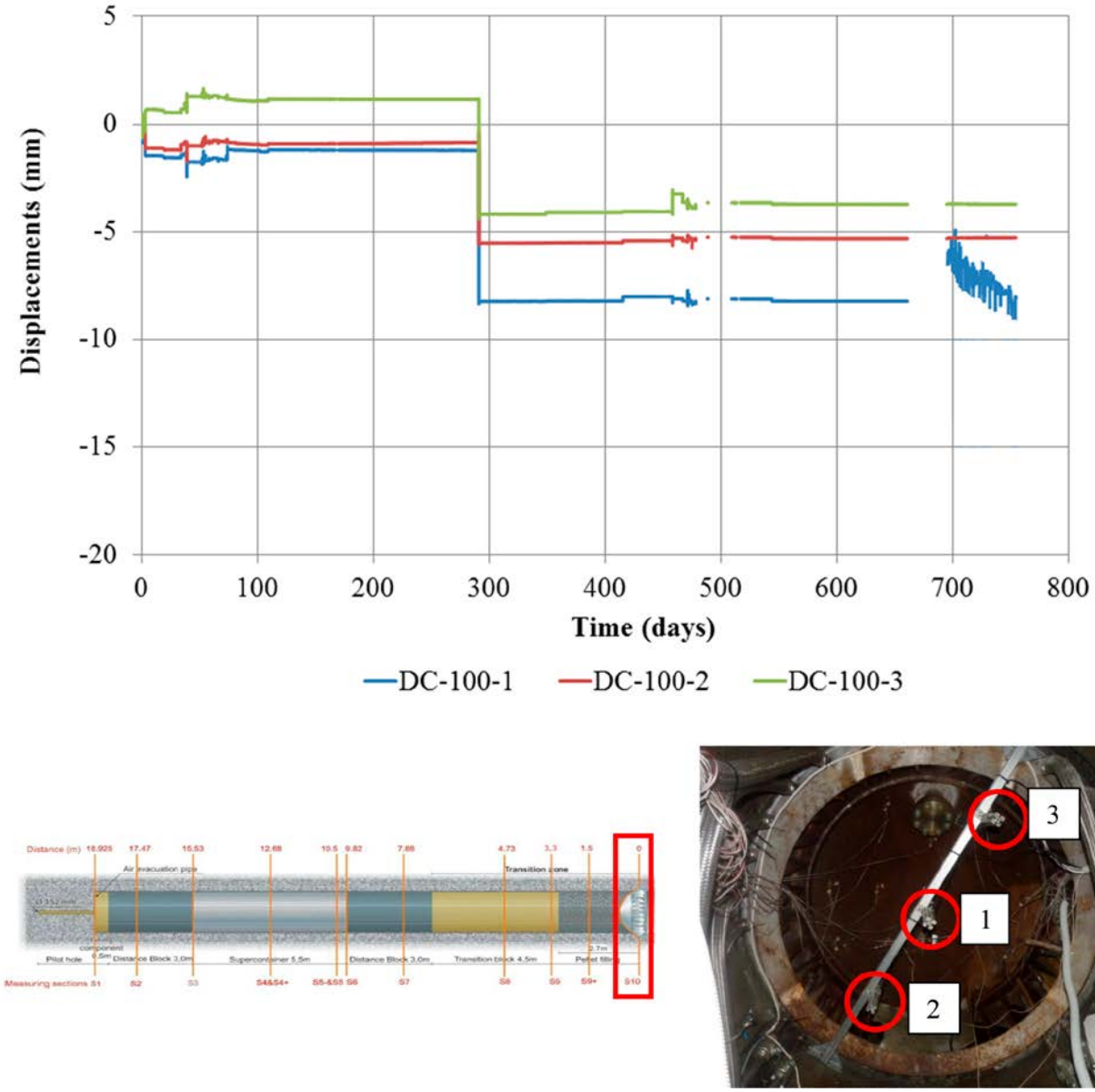

Figure 5-16. *Response of displacement sensors on the outer face of the plug in drift section 10.*

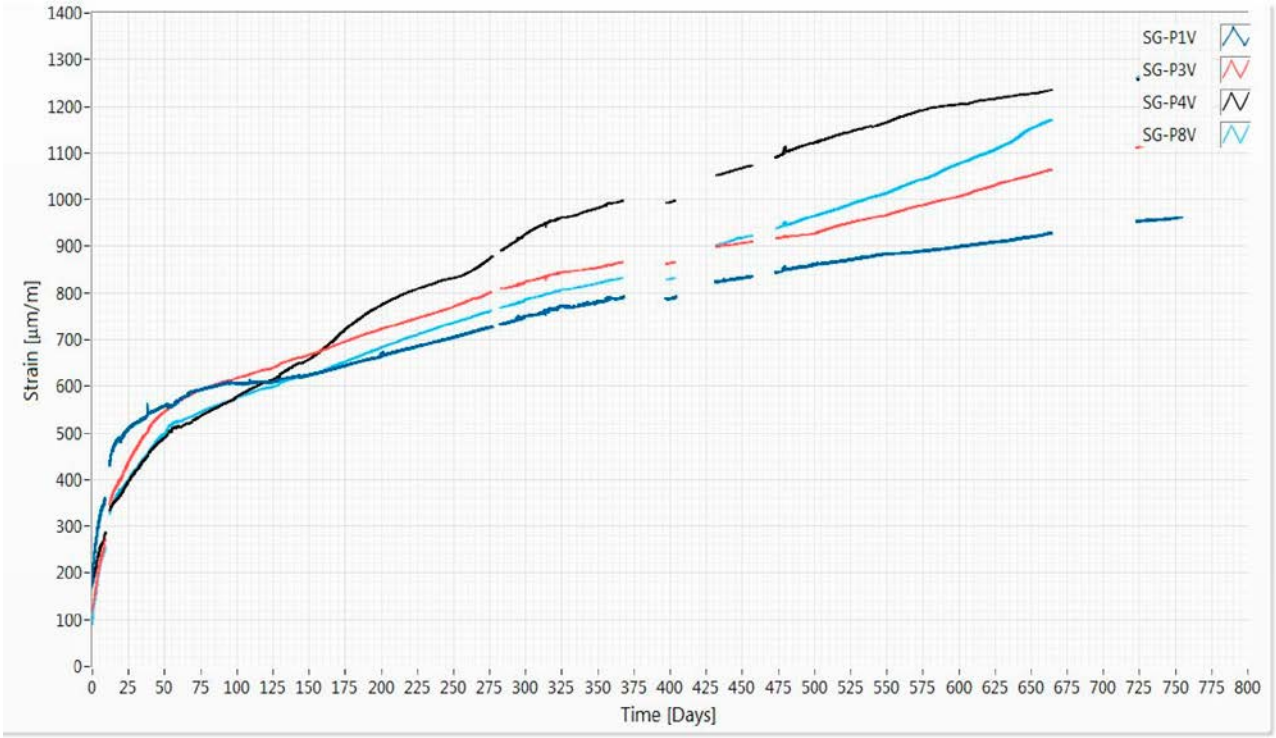

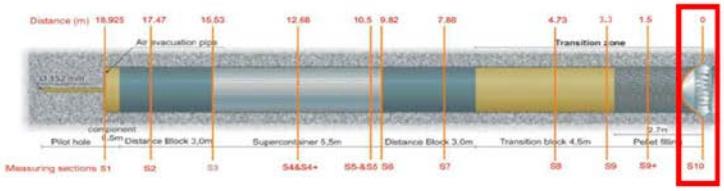

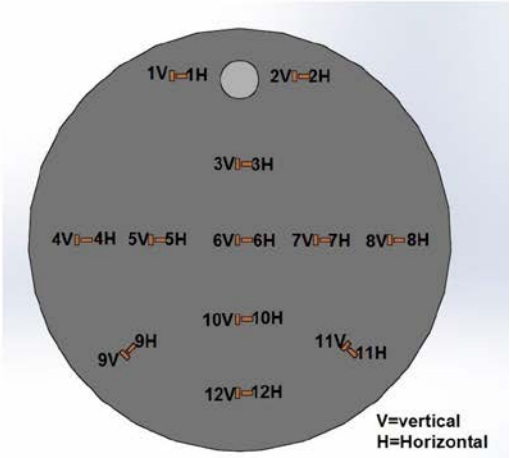

Figure 5-17. *Response of vertical strain gauges on the outer face of the plug in drift section 10. The data in this plot pertain to those vertical strain gauges which were functioning properly over the course of the measurement period. Increasing strains are observed over the course of the test indicating the development of pressure behind the plug.*

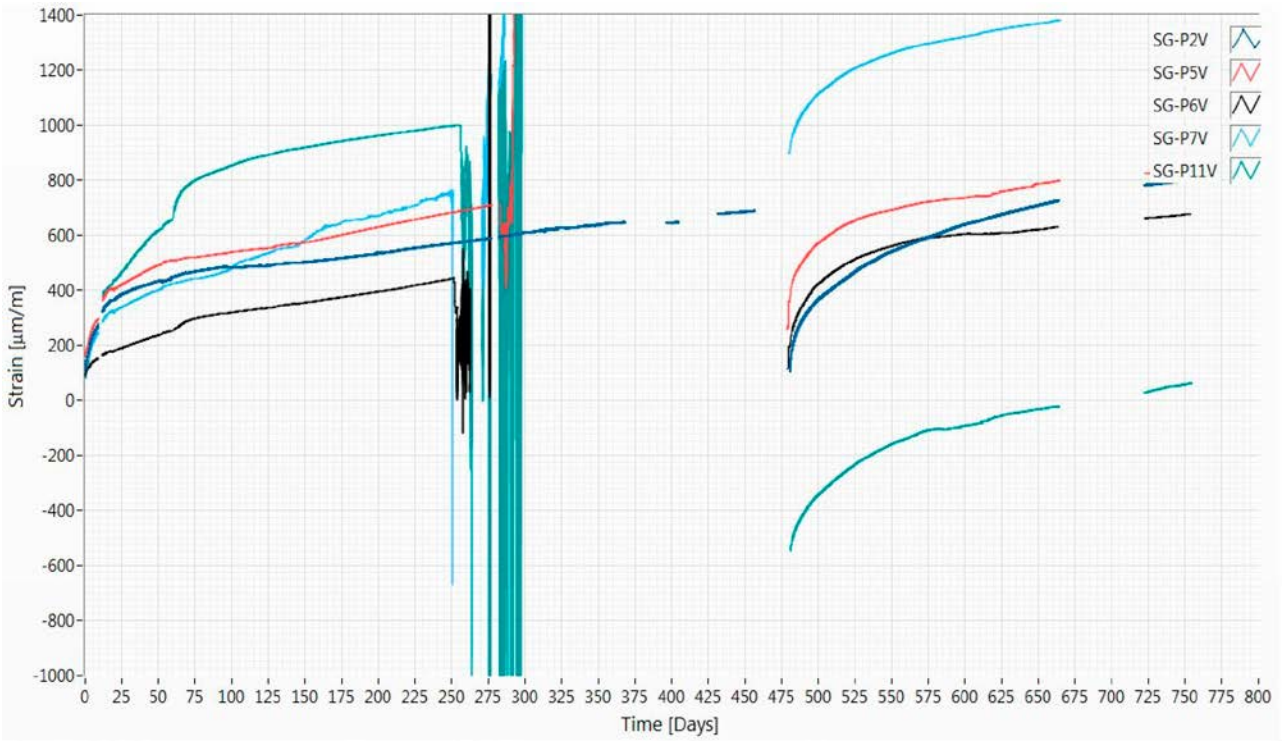

Figure 5-18. *Response of vertical strain gauges on the outer face of the plug in drift section 10. The data in this plot pertain to those vertical strain gauges which were replaced after 476 days. Increasing strains are observed indicating the development of pressure behind the plug.*

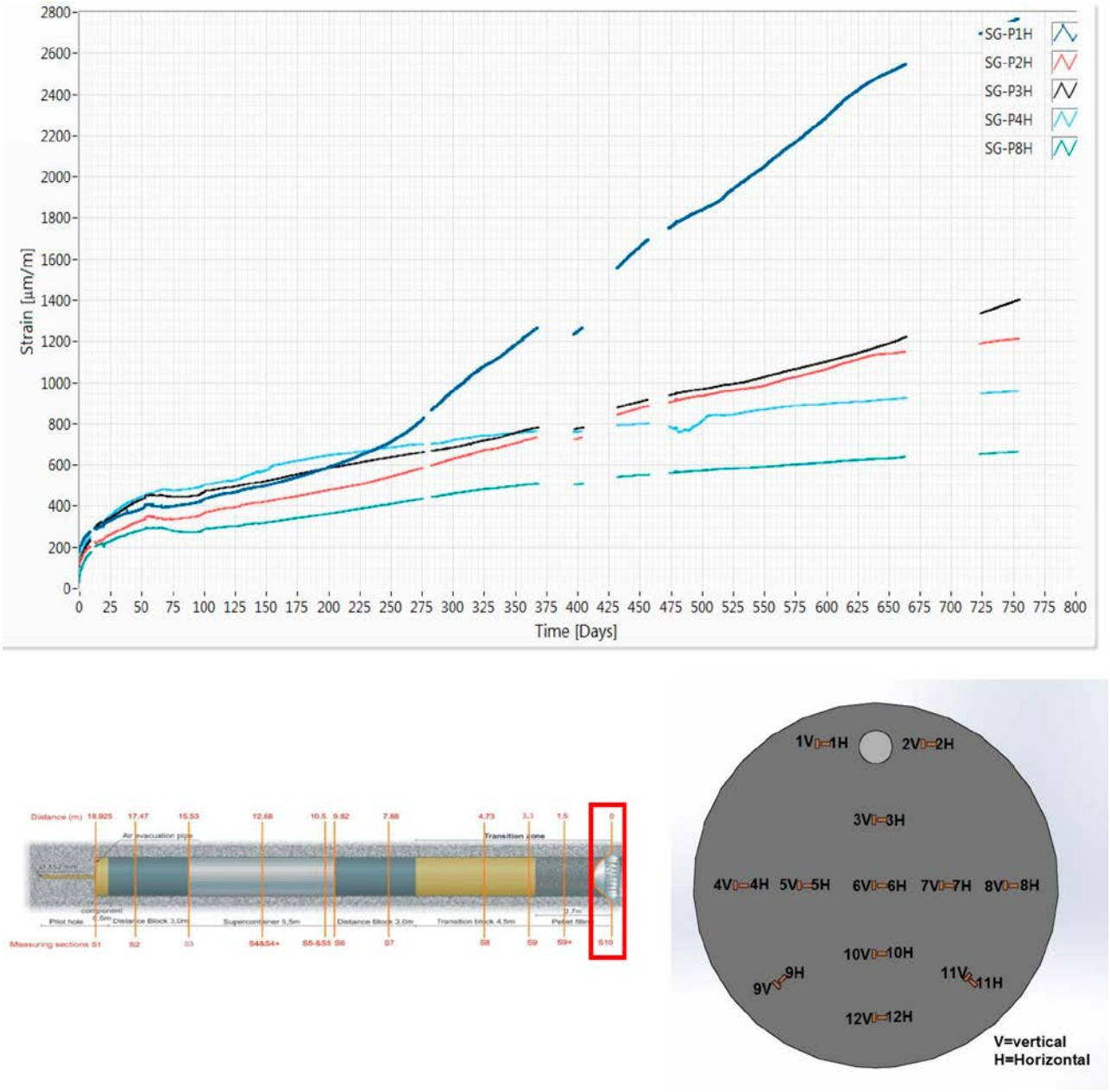

Figure 5-19. *Response of horizontal strain gauges on the outer face of the plug in drift section 10. The data in this plot pertain to those strain gauges which were functioning properly over the course of the measurement period. Increasing strains are observed over the course of the test indicating the development of pressure behind the plug.*

6 Supercontainer

6.1 Inner sensor positions

The location of the inner sensors and other information is presented in Tables 6-1 (drift section 4), 6-2 (drift section 4), 6-3 (drift section 5) and 6-4 (drift section 5).

Table 6-1. Numbering and position of inner Supercontainer sensors in drift section 4.

	Coordinate system ÄSPÖ 96							
Point No.	Easting [m]	Northing [m]	Point Elevation [m]	Drawing label	Sensor code in SICADA	Sensor code in SCADA	Assembly tag label	Manufacturer
1	1910.864	7252.987	−216.798	WP2	PXK061WP2	WP-1299-2	WP-1293-2	Wescor
2	1910.861	7252.599	−216.954	PP3	PXK061PP3	PP-1299-3	PP-1293-3	Measurement specialities
3	1910.848	7252.418	−217.491	WP3	PXK061WP3	WP-1299-3	WP-1293-3	Wescor
4	1910.846	7252.419	−217.591	WC4	PXK061WC4	WC-1299-4	WC-1293-4	Aitemin
5	1910.833	7252.599	−218.128	PP4	PXK061PP4	PP-1299-4	PP-1293-4	Measurement specialities
6	1910.828	7252.987	−218.284	WP4	PXK061WP4	WP-1299-4	WP-1293-4	Wescor
7	1910.827	7253.386	−218.284	WC1	PXK061WC1	WC-1299-1	WC-1293-1	Aitemin
8	1910.831	7253.773	−218.128	PP1	PXK061PP1	PP-1299-1	PP-1293-1	Measurement specialities
9	1910.843	7253.955	−217.591	WC2	PXK061WC2	WC-1299-2	WC-1293-2	Aitemin
10	1910.846	7253.955	−217.491	WP1	PXK061WP1	WP-1299-1	WP-1293-1	Wescor
11	1910.859	7253.186	−217.006	TP2	PXK061TP2	TP-1299-2	TP-1299-2	Geokon/ÅF
12	1910.864	7253.186	−216.771	WF2	PXK061WF2	WF-1299-2	WF-1293-2	Delta-T
13	1910.867	7253.187	−216.678	TP4	PXK061TP4	TP-1244-4	TP-1299-4	Geokon/ÅF
14	1910.845	7253.722	−217.541	TP1	PXK061TP1	TP-1299-1	TP-1299-1	Geokon/ÅF
15	1910.827	7.253.186	−218.311	WF1	PXK061WF1	WF-1299-1	WF-1293-1	Delta-T
16	1910.847	7252.651	−217.541	TP3	PXK061TP3	TP-1299-3	TP-1299-3	Geokon/ÅF
17	1910.863	7253.386	−216.798	WC3	PXK061WC3	WC-1299-3	WC-1293-3	Aitemin
18	1910.859	7253.774	−216.954	PP2	PXK061PP2	PP-1299-2	PP-1293-2	Measurement specialities

Table 6-2. Numbering and position of inner Supercontainer displacement and inclinometer sensors in drift section 4.

	Coordinate system ÄSPÖ 96							
Point No.	Easting [m]	Northing [m]	Point Elevation [m]	Drawing label	Sensor code in SICADA	Sensor code in SCADA	Assembly tag label	Manufacturer
1	1911.329	7253.187	−217.007	IS2	PXK072IS2	IS-1252-2	No data	Measurement specialities
2	1911.060	7253.187	−218.433	DS1	PXK069DS1	DS-1275-1	DS-1492-1	RDP
3	1911.079	7254.069	−217.554	DS2	PXK069DS2	DS-1275-2	DS-1492-2	RDP
4	1911.082	7252.305	−217.553	DS4	PXK069DS4	DS-1275-4	DS-1492-4	RDP
5	1911.295	7253.187	−218.407	IS1	PXK072IS1	IS-1252-1	No data	Measurement specialities
6	1911.102	7253.187	−216.671	DS3	PXK069DS3	DS-1275-3	DS-1492-3	RDP

Table 6-3. Numbering and position of inner Supercontainer sensors in drift section 5.

	Coordinate system ÄSPÖ 96							
Point No.	Easting [m]	Northing [m]	Point Elevation [m]	Drawing label	Sensor code in SICADA	Sensor code in SCADA	Assembly tag label	Manufacturer
1	1913.289	7252.991	−216.889	WP2	PXK0087WP2	WP-1008-2	WP 1008-2	Wescor
2	1913.289	7253.190	−216.863	WF2	PXK0087WF2	WF-1008-2	WF 1008-2	Delta-T
3	1913.288	7253.390	−216.890	WC4	PXK0087WC4	WC-1008-4	Wireless	Aitemin
4	1913.291	7253.190	−216.804	PP4	PXK0087PP4	PP-1008-4	Wireless	Measurement specialities
5	1913.272	7252.361	−217.633	PP5	PXK0087PP5	PP-1008-5	PP 1008-5	Measurement specialities
6	1913.273	7252.422	−217.583	WP3	PXK0087WP3	WP-1008-3	WP 1008-3	Wescor
7	1913.271	7252.422	−217.683	WC5	PXK0087WC5	WC-1008-5	WC 1008-5	Aitemin
8	1913.253	7252.991	−218.376	WP4	PXK0087WP4	WP-1008-4	WP1008-4	Wescor
9	1913.251	7253.190	−218.462	PP2	PXK0087PP2	PP-1008-2	PP 1008-2	Measurement specialities
10	1913.252	7253.190	−218.403	WF1	PXK0087WF1	WF-1008-1	WF 1008-1	Delta-T
11	1913.252	7253.389	−218.376	WC2	PXK0087WC2	WC-1008-2	WC 1008-2	Aitemin
12	1913.271	7253.959	−217.583	WP1	PXK0087WP1	WP-1008-1	WP 1008-1	Wescor
13	1913.269	7254.020	−217.633	PP3	PXK0087PP3	PP-1008-3	Wireless	Measurement specialities
14	1913.268	7253.959	−217.683	WC3	PXK0087WC3	WC-1008-3	Wireless	Aitemin
15	1913.272	7253.190	−217.583	PP1	PXK0087PP1	PP-1008-1	Wireless	Measurement specialities
16	1913.270	7253.190	−217.683	WC1	PXK0087WC1	WC-1008-1	Wireless	Aitemin
17	1913.040	7253.190	−217.377	TP3	PXK085TP3	TP-1033-3	TP 1033-3	Geokon/ÅF
18	1913.034	7252.940	−217.627	TP2	PXK085TP2	TP-1033-2	TP 1033-2	Geokon/ÅF
19	1913.028	7253.190	−217.877	TP1	PXK085TP1	TP-1033-1	TP 1033-1	Geokon/ÅF
20	1913.033	7253.440	−217.627	TP4	PXK085TP4	TP-1033-4	TP 1033-4	Geokon/ÅF
21	1913.081	7253.853	−217.573	WSU	Transmitter	WSU-S4	Wireless	Aitemin

Table 6-4. Numbering and position of inner Supercontainer displacement sensors in drift section 5.

	Coordinate system ÄSPÖ 96							
Point No.	Easting [m]	Northing [m]	Point Elevation [m]	Drawing label	Sensor code in SICADA	Sensor code in SCADA	Assembly tag label	Manufacturer
1	1912.546	7252.813	−217.233	DS3	PXK081DS3	DS-1082-3	DS-0977-3	RDP
2	1912.544	7253.565	−217.233	DS2	PXK081DS2	DS-1082-2	DS-0977-2	RDP
3	1912.526	7253.565	−217.985	DS4	PXK081DS4	DS-1082-4	DS-0977-4	RDP
4	1912.527	7252.806	−217.992	DS1	PXK081DS1	DS-1082-1	DS-0977-1	RDP

6.2 Inner sensor results and comments

6.2.1 Relative humidity

Signals from the relative humidity sensors are presented in Figures 6-1 and 6-2.

Three (WC-1, WC-2 & WC-4) of the four relative humidity sensors in peripheral positions of the bentonite block in section S-4 (see Figure 6-1) measured fast increases in the relative humidity, reaching 100 % after 700 days. The RH measured by WC-3 (top position) decreased to 30 % at the beginning of the test but then followed the same pattern of growth shown by the other sensors reaching

a level of 65 % RH at the end of the measurement period. The reasons for the initial decrease are unknown but may be related to block cracking/expansion. This behaviour matches with that registered in other sections (S-5 and S7), although in those cases the relative humidity increased suddenly to around 100 % followed by immediate drops. The bentonite blocks inside the Supercontainer are wetting more slowly than the transition zone or distance blocks.

Five relative humidity sensors were installed in S-5 (see Figure 6-2). Sensors WC-1, WC-2, WC-3 and WC-5 showed a spike in relative humidity during the DAWE phase of the test. Sensor WC-1 is located the furthest inside the Supercontainer. Sensor WC-2 measured full saturation after approximately 60 days. Signal was no longer available from sensor WC-5 after 5 days. Signal was no longer being received from the wireless sensors (WC-1, WC-3 and WC-4) after just over 100 days.

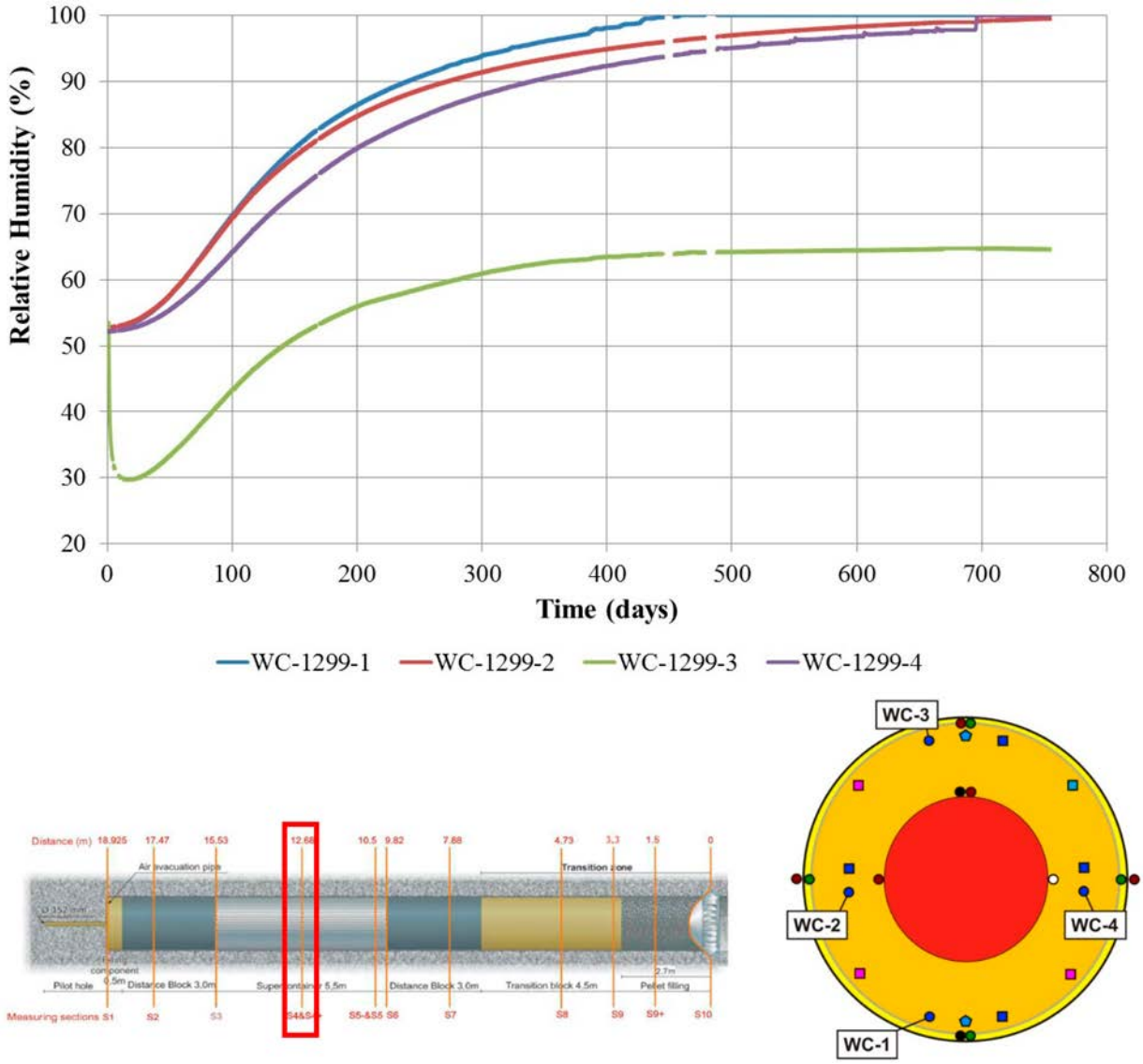

Figure 6-1. *Response of capacitive hygrometer sensors at inner Supercontainer positions (in the bentonite block) in drift section 4. The distance of the sensors to the rock wall is 155 mm.*

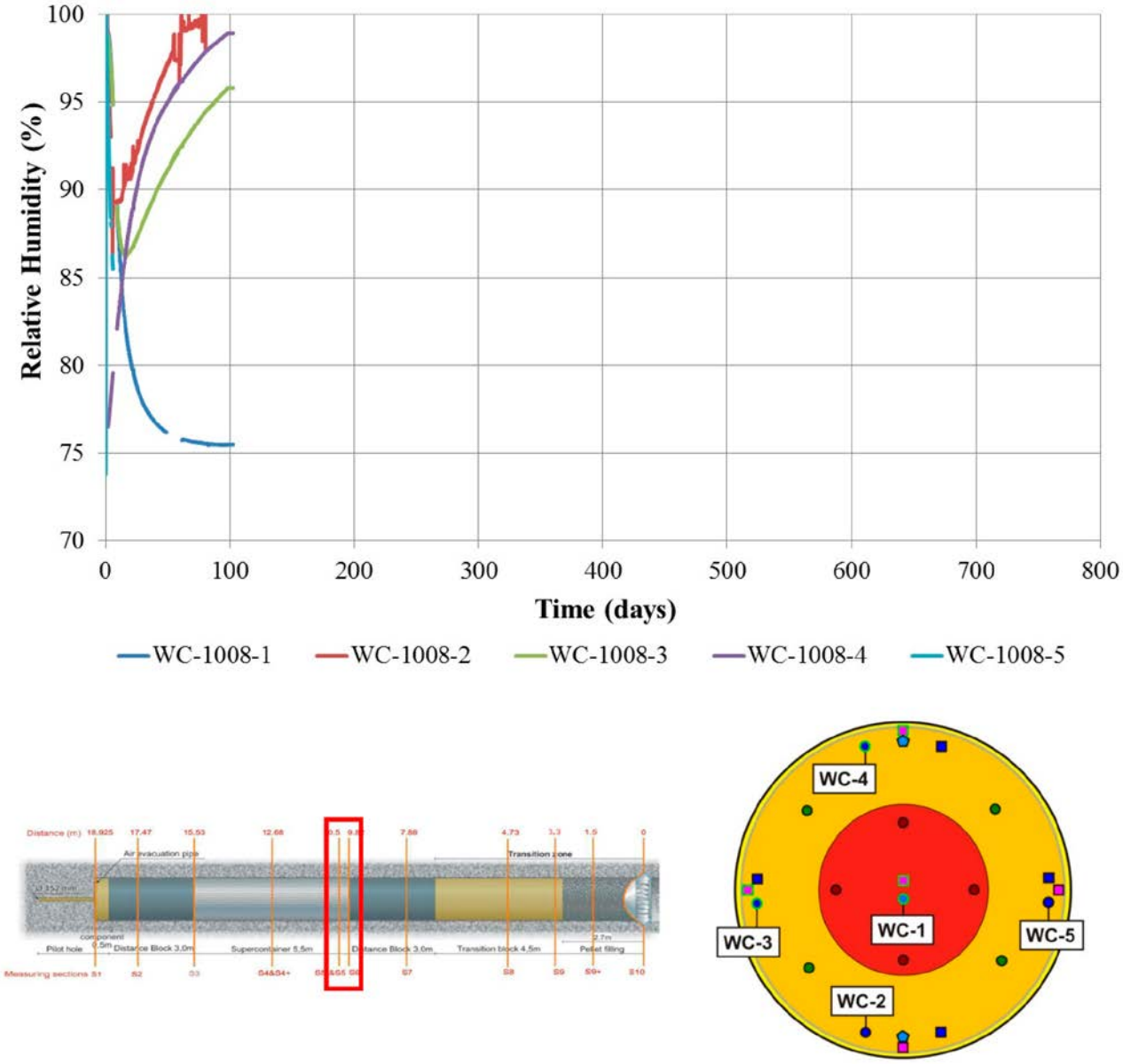

Figure 6-2. *Response of capacitive hygrometer sensors at inner Supercontainer positions in drift section 5. The distance of sensors WC-2 to WC-5 to the rock wall is 155 mm.*

6.2.2 Suction

In-range signals from the psychrometers correspond only to suction established at 95 % relative humidity. For temperatures between 5 °C and 15 °C, the suction at 95 % relative humidity should be between 6.6 and 6.8 MPa.

Four psychrometer sensors were installed in section S-4 (see Figure 6-3). The signals were lost after day 551, but they had not yet started to approach in-range limits before that time indicating that the block was not sufficiently saturated.

Four psychrometer sensors were installed in S-5 (see Figure 6-4). All of the sensors came into range at an early stage of the test, before 100 days. Measured suction was rather low for sensors WP-1, WP-3 and WP-4 by day 500. The signal from sensor WP-2 became rather noisy after day 200.

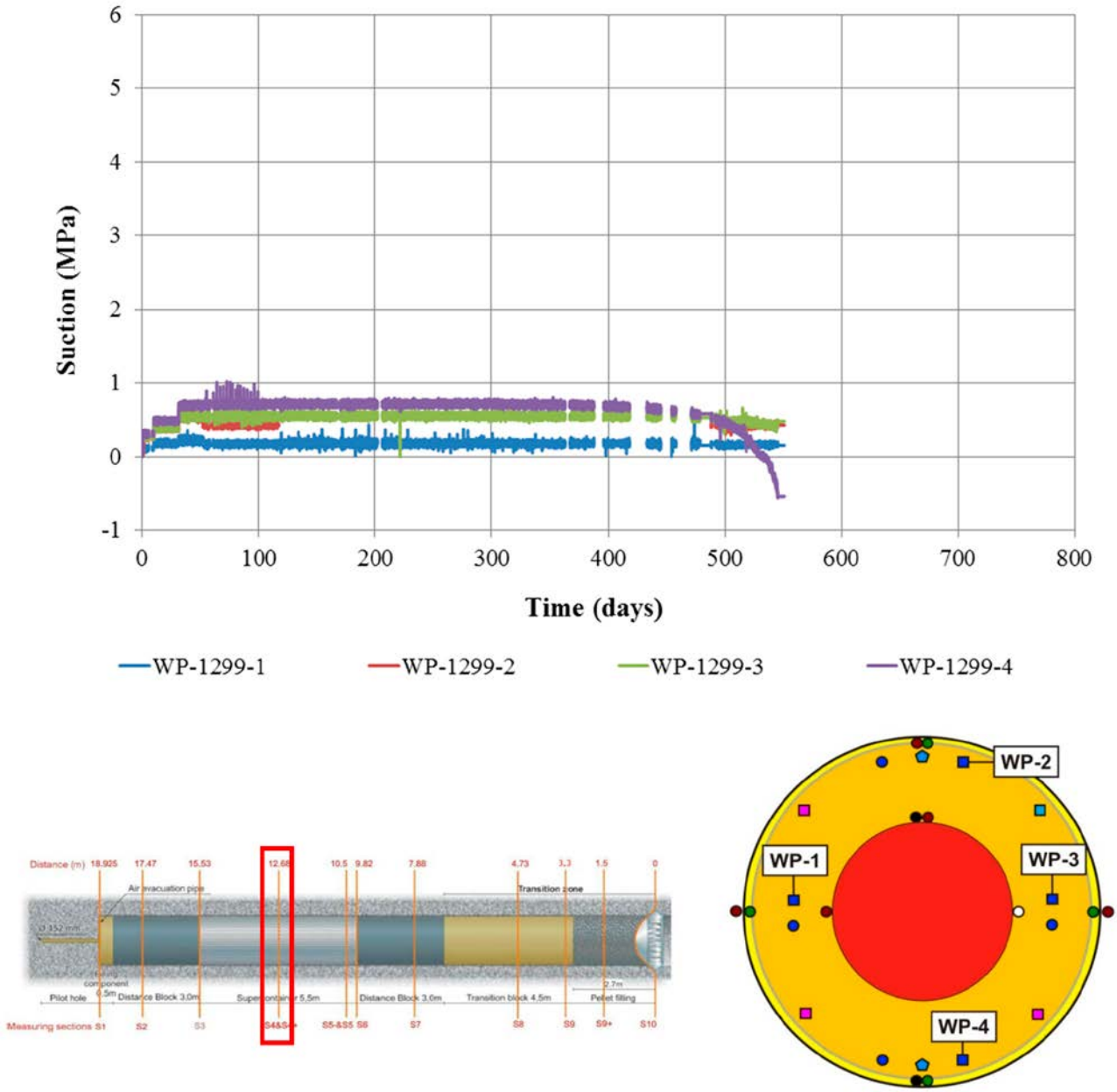

Figure 6-3. *Response of psychrometer sensors at inner Supercontainer positions (in the bentonite block) in drift section 4. The distance of the sensors to the rock wall is 155 mm.*

6.2.3 Pore pressure

Pore pressures in the Supercontainer blocks were measured with pore pressure sensors (Figures 6-5 and 6-6). The pressure in the gap between the supercontainer and the rock wall was measured with a gas pressure sensor (Figure 6-7).

Four pore pressure sensors were installed in section S-4, (see Figure 6-5). No signal was available from sensor PP-3 from the beginning of the test. Sensor PP-1 showed rapidly increasing pressure starting at day 77 to 1 MPa and then continued increasing more slowly to nearly 1.2 MPa before dropping to zero at day 400. Sensors PP-2 and PP-4 did not register any change in pore pressure until day 300 at which point the signals began to slowly rise to values of 0.3 and 0.1 MPa, respectively at the end of the measurement period. The signal pattern for sensor PP-2 is similar to that of sensor PP-4 in S-2 (see Figure 4-5).

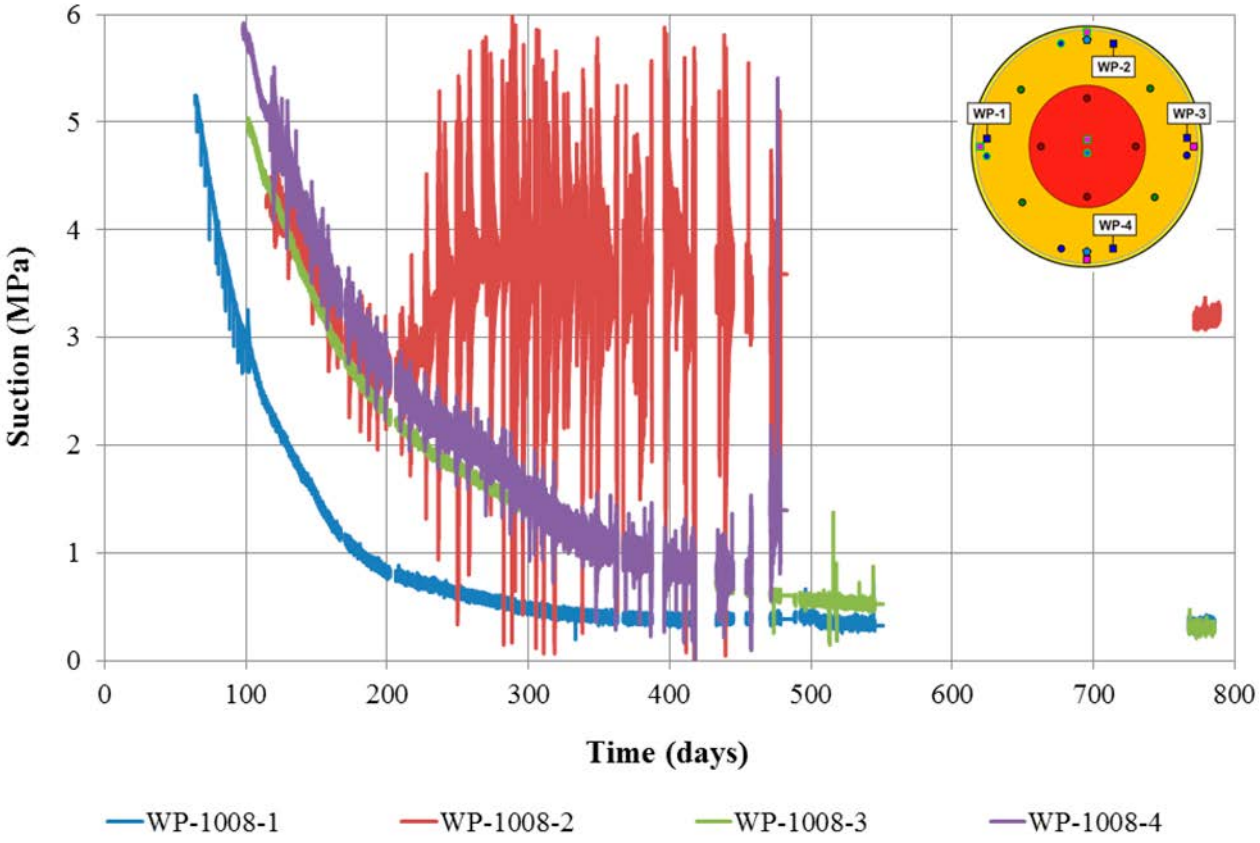

Figure 6-4. *Response of psychrometer signal for sensors WP-1, WP-2, WP-3 and WP-4 in inner Supercontainer positions in drift section 5 after reaching in-range suction limits. The distance of the sensors to the rock wall is 155 mm.*

Five pore pressure sensors were installed in S-5 (see Figure 6-6). Signals from the wireless sensors (PP-1, PP-3 and PP-4) were received only between day 70 to day 100. No signal was available from sensor PP-2. Sensor PP-5 showed rapidly increasing pressure starting at day 77 to 0.8 MPa and then continued increasing more slowly to 0.9 MPa by the end of the measurement period. This sensor is likely in contact with the (water-filled) gap between the supercontainer and the rock.

The gas sensor initially installed in S-6 had a range of 250 kPa and it was installed for the purposes of measuring the gas pressure if the DAWE procedure was not followed. As DAWE was followed, the sensor was flooded during the water filling and essentially measured water pressure. After approximately 20 days it reached its maximum capacity. This sensor was changed to a higher range pore pressure sensor at day 369. After a purge on day 466, the measured signal started to slowly rise from just over 0.4 MPa to nearly 0.6 MPa by the end of the measurement period.

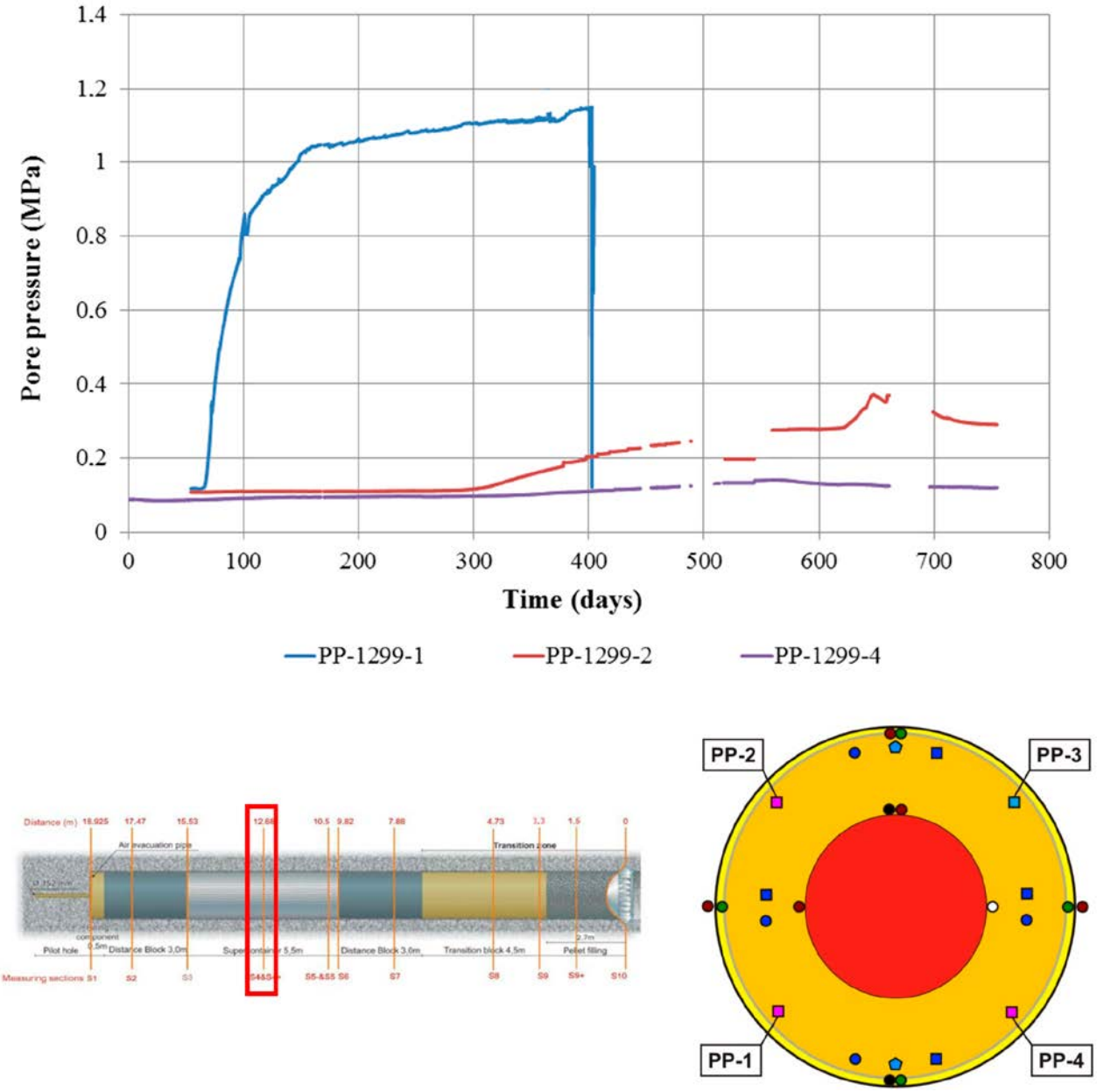

Figure 6-5. *Response of pore pressure sensors at inner Supercontainer positions (in the bentonite block) in drift section 4. The distance of the sensors to the rock wall is 95 mm.*

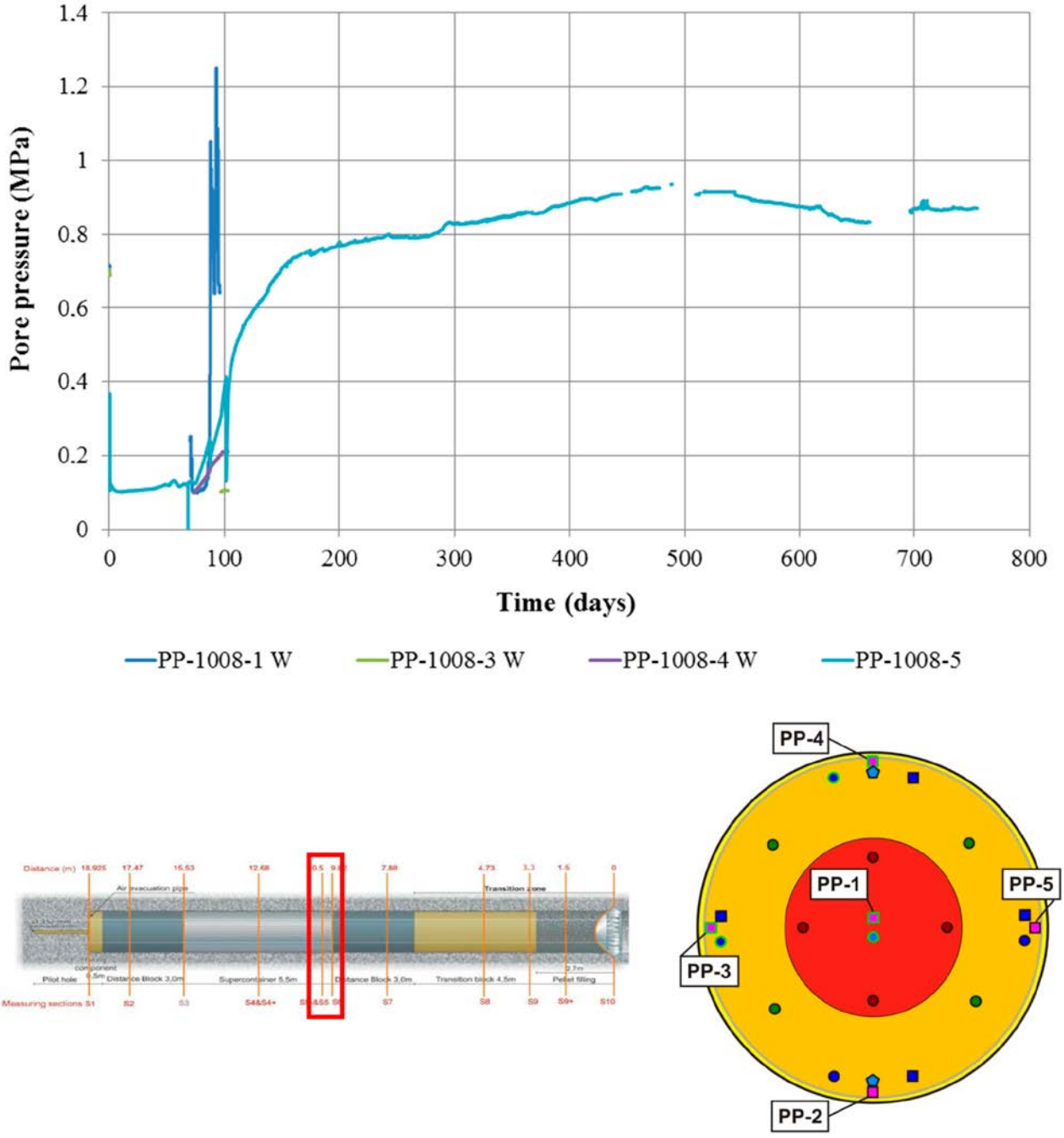

Figure 6-6. *Response of pore pressure sensors at inner Supercontainer positions (in the bentonite block) in drift section 5. The distance of the sensor PP-2 to PP-5 to the rock wall is 95 mm. PP-1 is at the axis drift and its distance to the rock wall is 925 mm.*

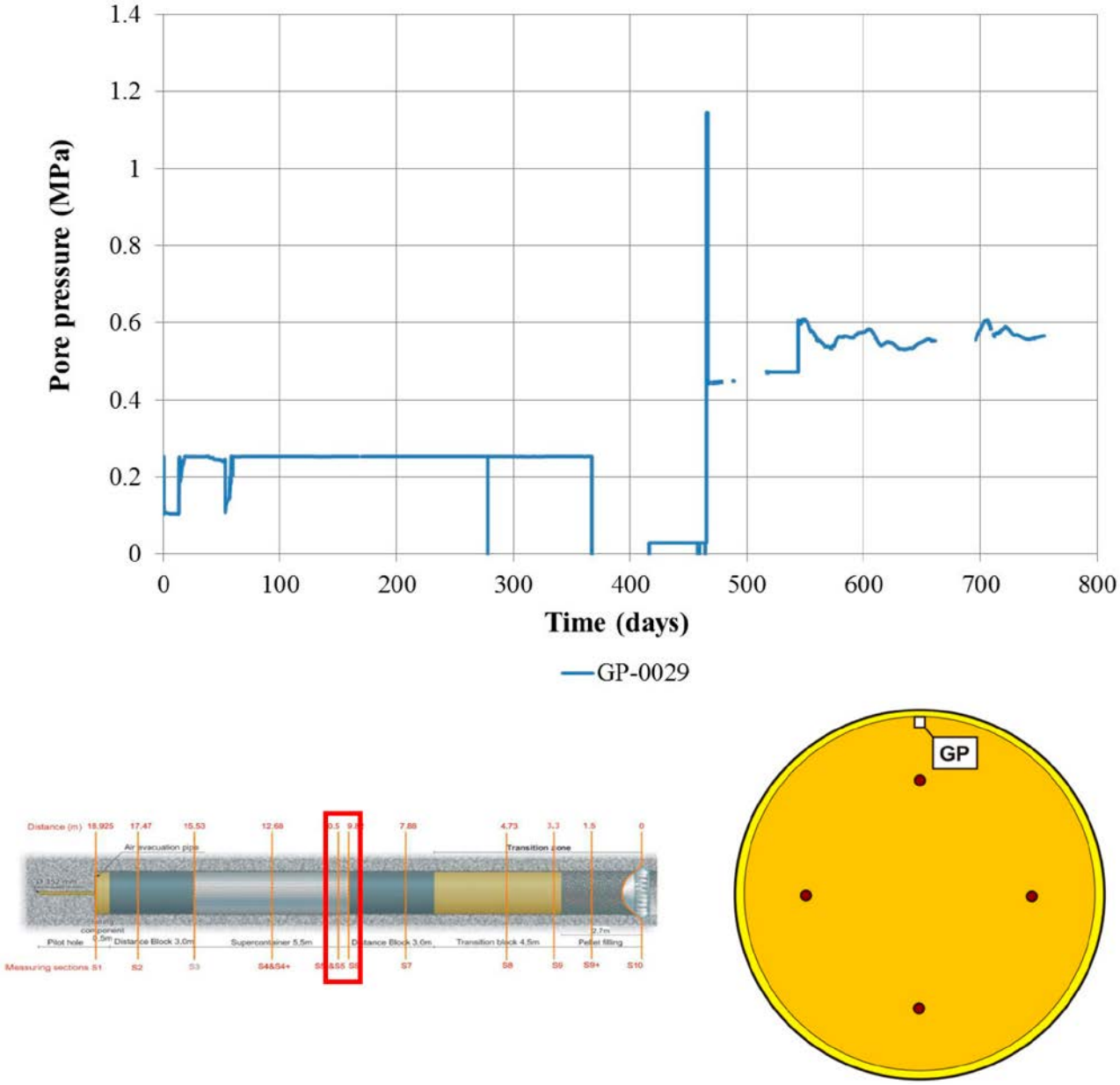

Figure 6-7. *Response of gas pressure sensor in drift section 6.*

6.2.4 Water content

Volumetric water content was measured with soil moisture sensors (Figures 6-8 and 6-9).

Two soil moisture sensors were installed in section S-4 (see Figure 6-9). Sensor WF-2 measured an increasing signal over the course of the test up to date 465 when it dropped suddenly and became extremely noisy. Sensor WF-1 (not presented) may have malfunctioned as it was displaying a constant signal until almost 60 days after which signal was no longer available.

Two soil moisture sensors were installed in S-5 (see Figure 6-9). After an initial drop, sensor WF-1 measured an increasing signal over most of the test. Similarly, sensor WF-2 showed increasing signal but at higher levels. Signals from both sensors dropped suddenly at day 489 and became rather noisy thereafter.

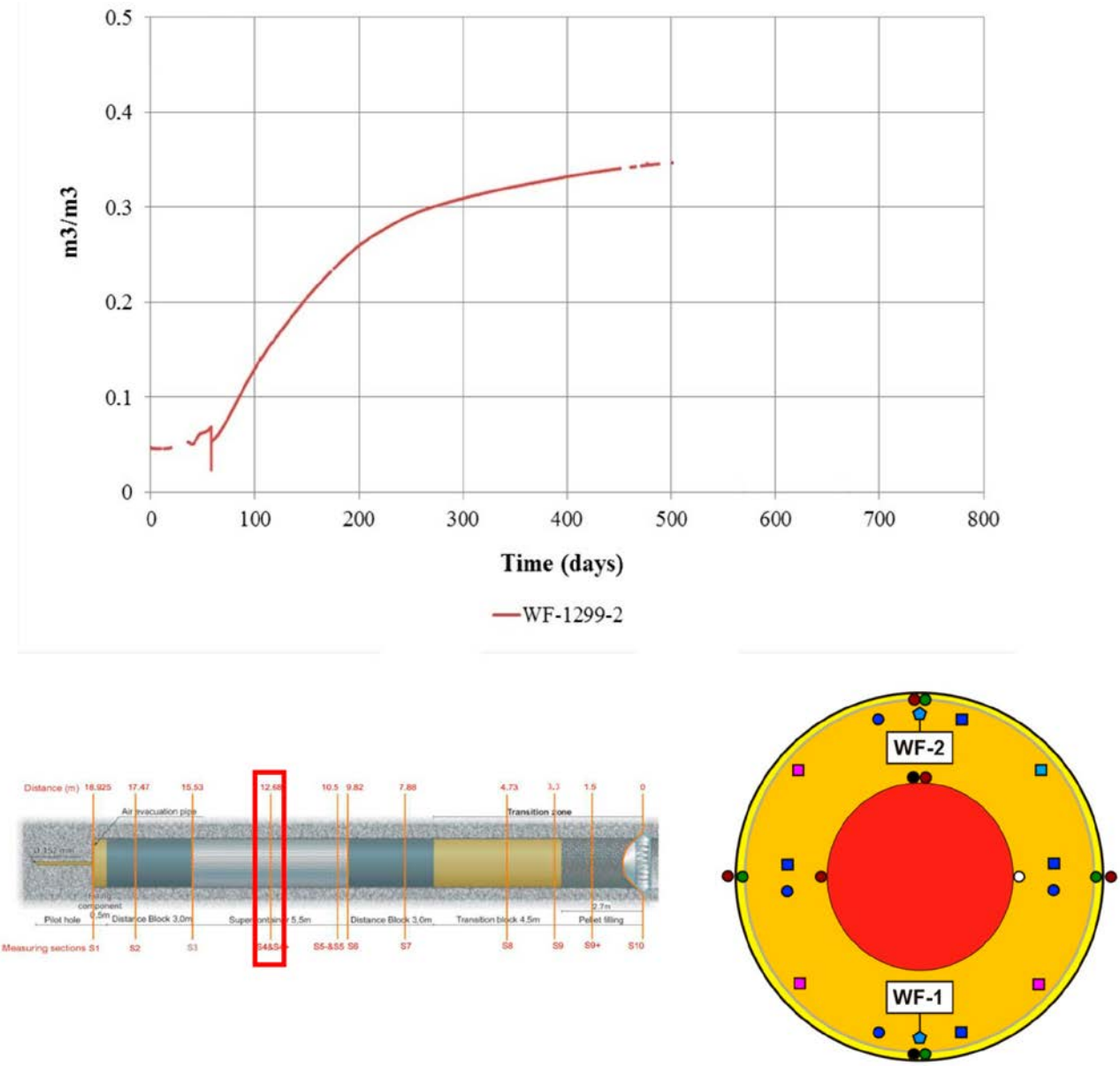

Figure 6-8. *Response of soil moisture sensors at inner Supercontainer positions (in the bentonite block) in drift section 4. The distance of the sensors to the rock wall is 155 mm.*

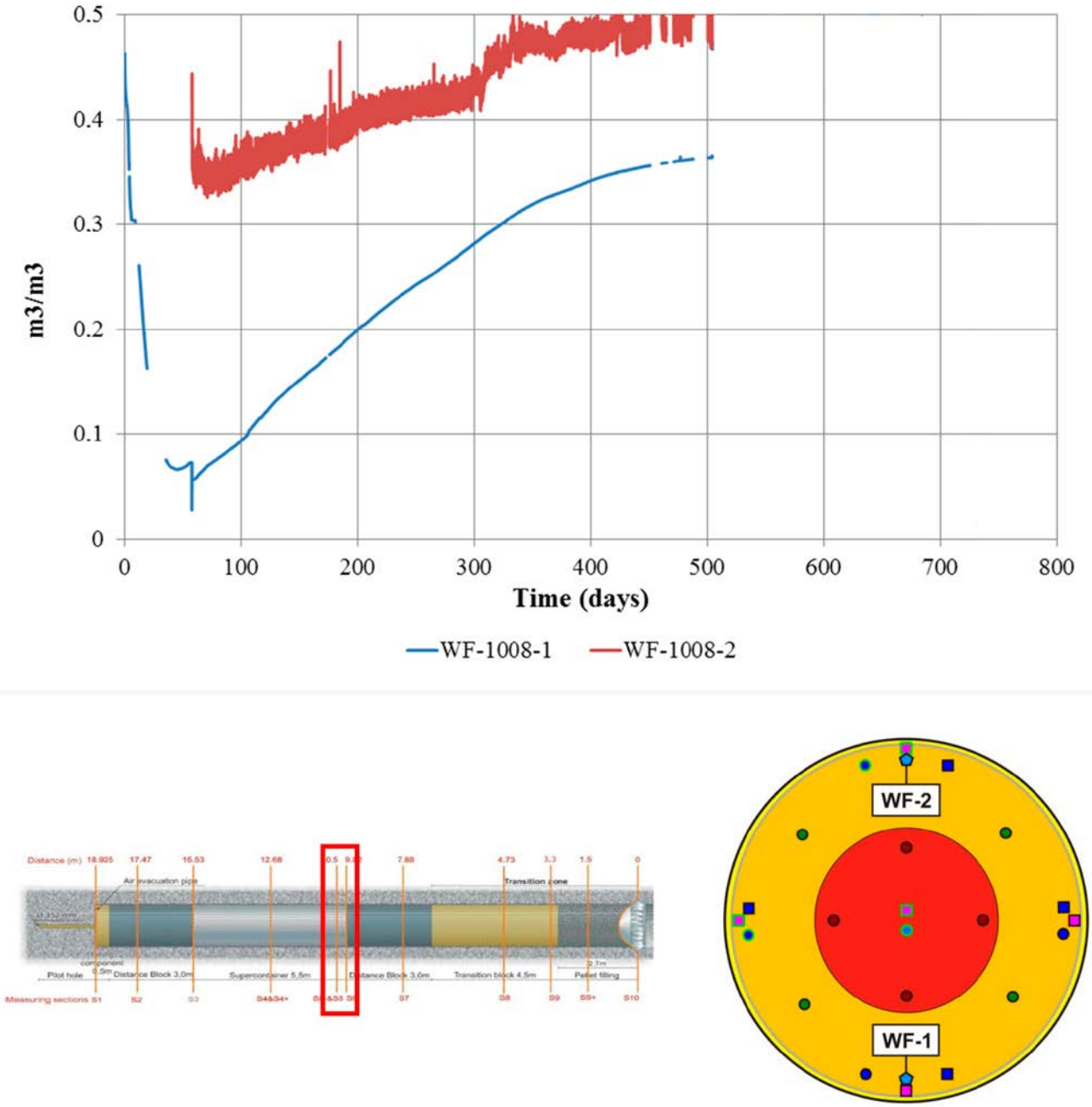

Figure 6-9. *Response of soil moisture sensors at inner Supercontainer positions (in the bentonite block) in drift section 5. The distance of the sensors to the rock wall is 155 mm.*

6.2.5 Inclination

Results from the inclinometer sensors are presented in Figure 6-10.

Two inclinometer sensors were installed in section S-4 (see Figure 6-10). Signal is being recorded only from sensor IS-1 along the x-axis. The sensor measurements suggest that the block showed first a sudden rotation to the left (counterclockwise) after 3 days which gradually reversed and further rotated to −1° where it remained to day 500. The signal then showed a drop to −1.2° and sudden rotation back to +1°. The signal then eventually increased to +2° at the end of the measurement period.

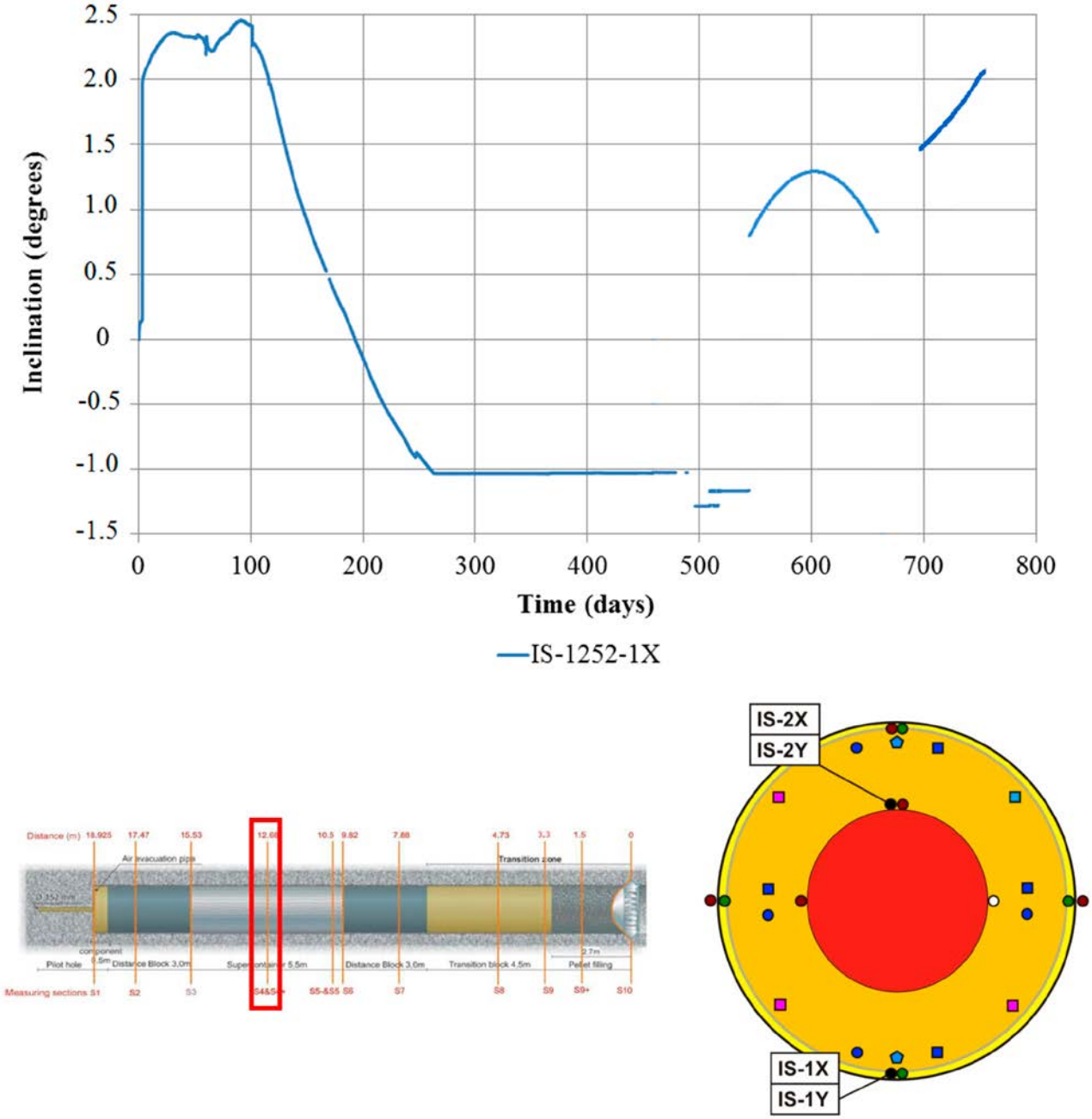

Figure 6-10. *Response of inclinometer sensor at inner Supercontainer positions (in the bentonite block) in drift section 4.*

6.2.6 Displacement

Results from the displacement sensors are presented in Figures 6-11 and 6-12.

Four displacement sensors were installed in section S-4 (see Figure 6-11). These sensors are fixed to the Supercontainer and measure displacement with respect to the rock wall.

Implausibly, sensors DS-2 and DS-4 both measured positive displacements, to 8.1 and 2.4 mm, respectively, from 30 to 50 days to day 418. At this point sensor DS-2 showed a sudden change in displacement to −11.6 mm possibly indicating that it was no longer attached to its original position. After day 500, the measured displacements for sensors DS-3 and DS-4 jumped to +5 mm and remained there, more or less, over the course of the measurement period. No signal was ever recorded from sensor DS-1.

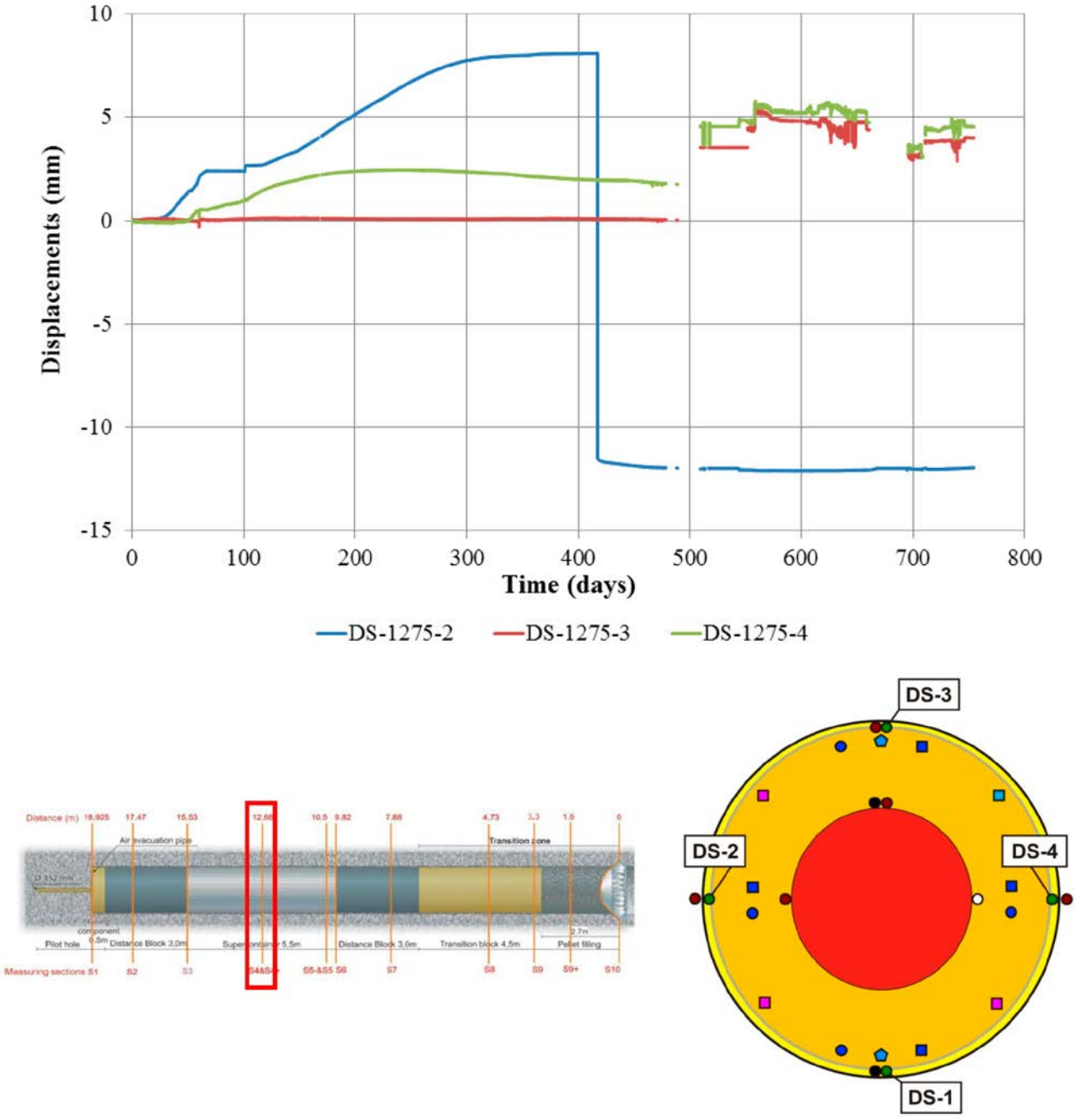

Figure 6-11. *Response of displacement sensors at inner Supercontainer positions in drift section 4.*

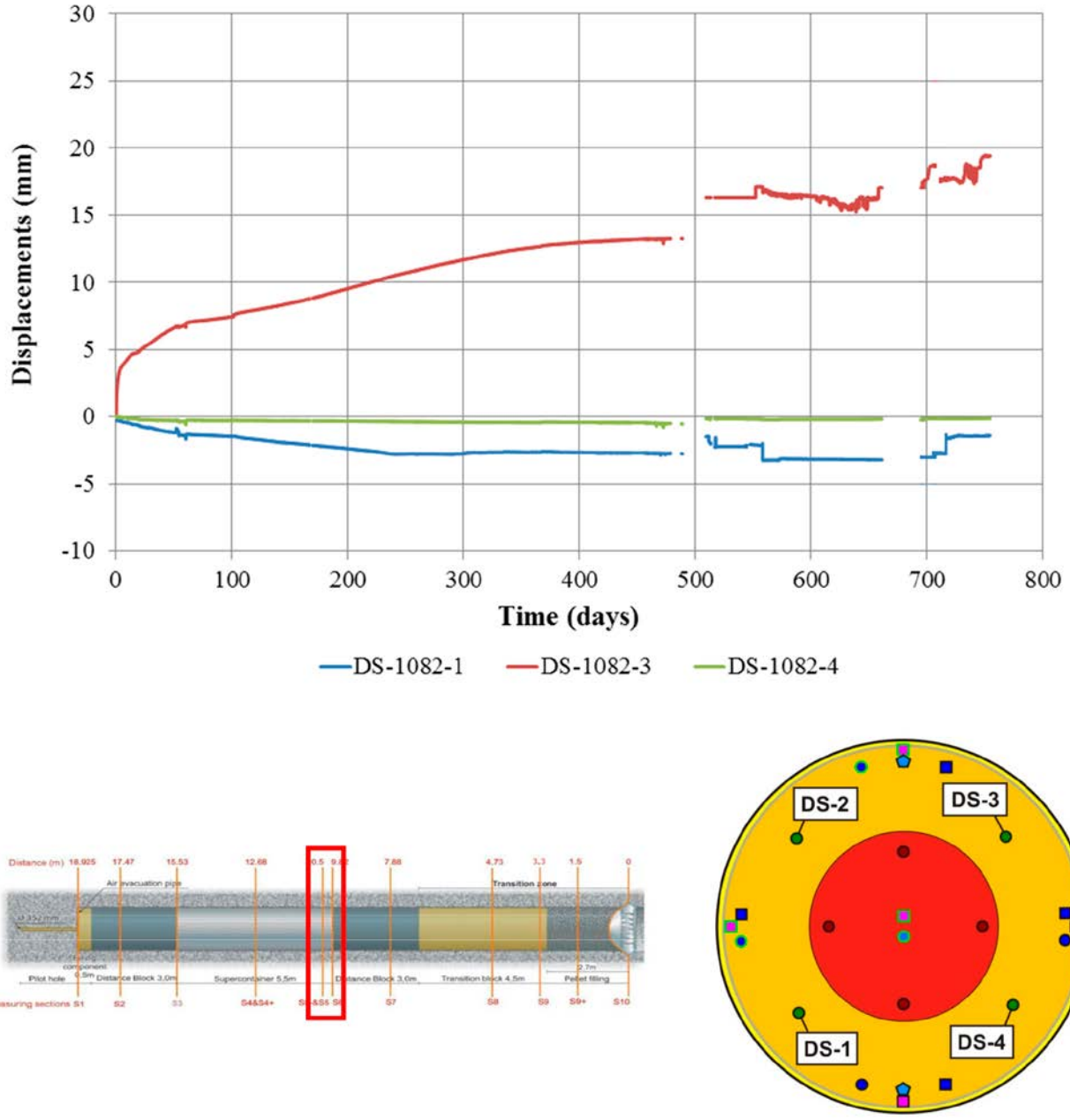

Figure 6-12. *Response of displacement sensors at inner Supercontainer positions in drift section 5.*

In S-5, the displacement sensors measure the radial displacement between the canister and the rock wall. Four sensors were installed (see Figure 6-12). Sensor DS-3 measured an increasing positive displacement (movement away from the rock wall) over the course of the test to reach almost 20 mm by the end of the measurement period. Incompatibly, sensor DS-1 showed a much smaller negative displacement (movement toward the rock wall) that reached almost −3.2 mm. Essentially, no change in displacement was observed with Sensor DS-4 and no signal was ever recorded from sensor DS-2. These signals are rather difficult to interpret, perhaps the block may be swelling more in the upper right area.

6.2.7 Total pressure

Results from the total pressure sensors are presented in Figures 6-13 to 6-15.

Four total pressure sensors were installed in section S-4 (see Figure 6-13). Only background noise was recorded by these sensors up to day 544, when they began to increase and reached 6 MPa by the end of the measurement period. The measurements after day 500 are of dubious accuracy.

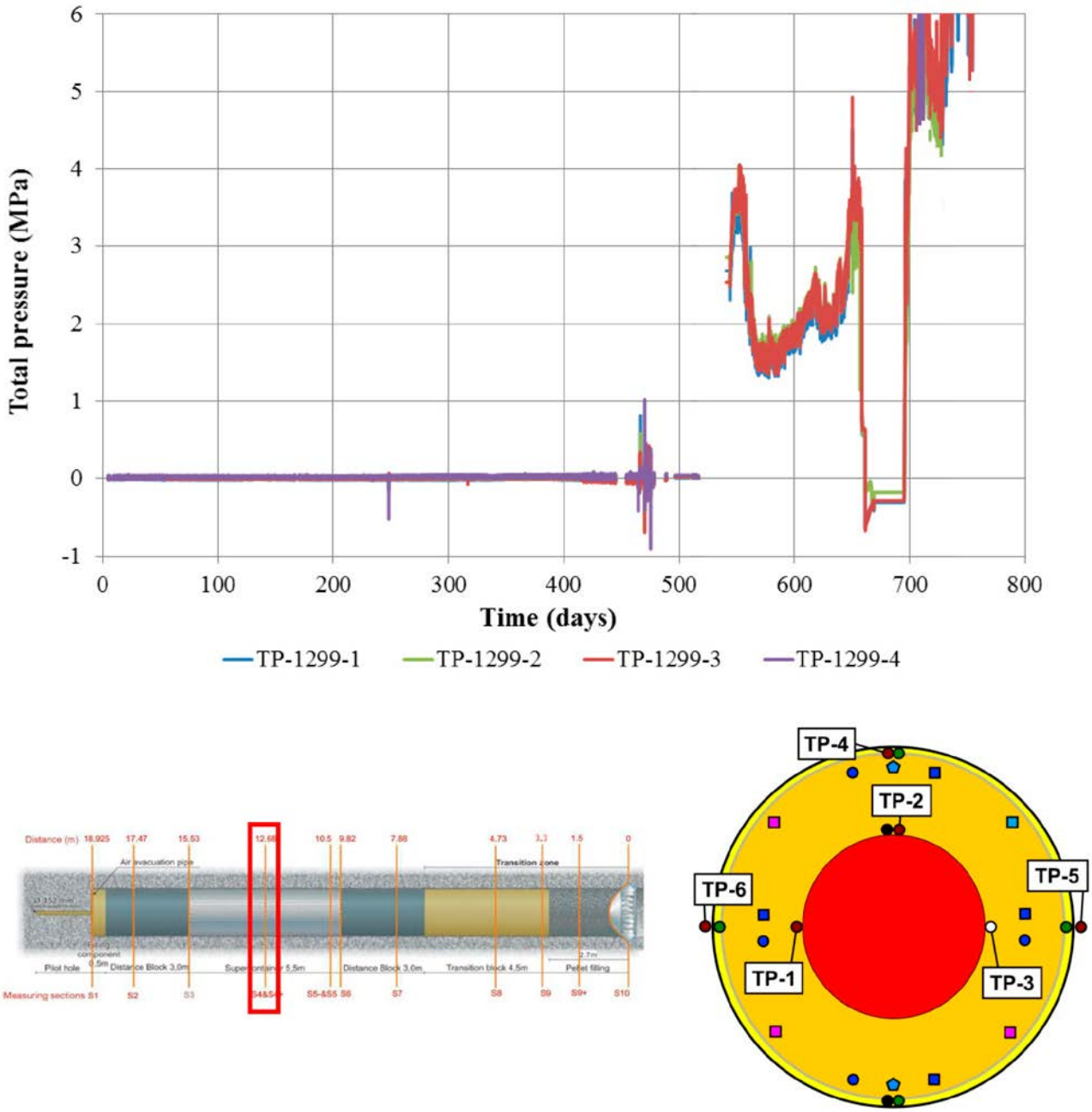

Figure 6-13. *Response of total pressure sensors at inner Supercontainer positions (in the bentonite block measuring at the ring block/canister interface and ring block/Supercontainer interface measuring radially to the drift axis) in drift section 4.*

In S-5, four total pressure sensors were installed (see Figure 6-14). Only background noise was recorded by these sensors up to day 513. The signals then dropped to negative pressures with increased noise levels.

Four total pressure sensors were installed in section S-6 (see Figure 6-15). These sensors showed responses very similar to those of the total pressure sensors in S-5.

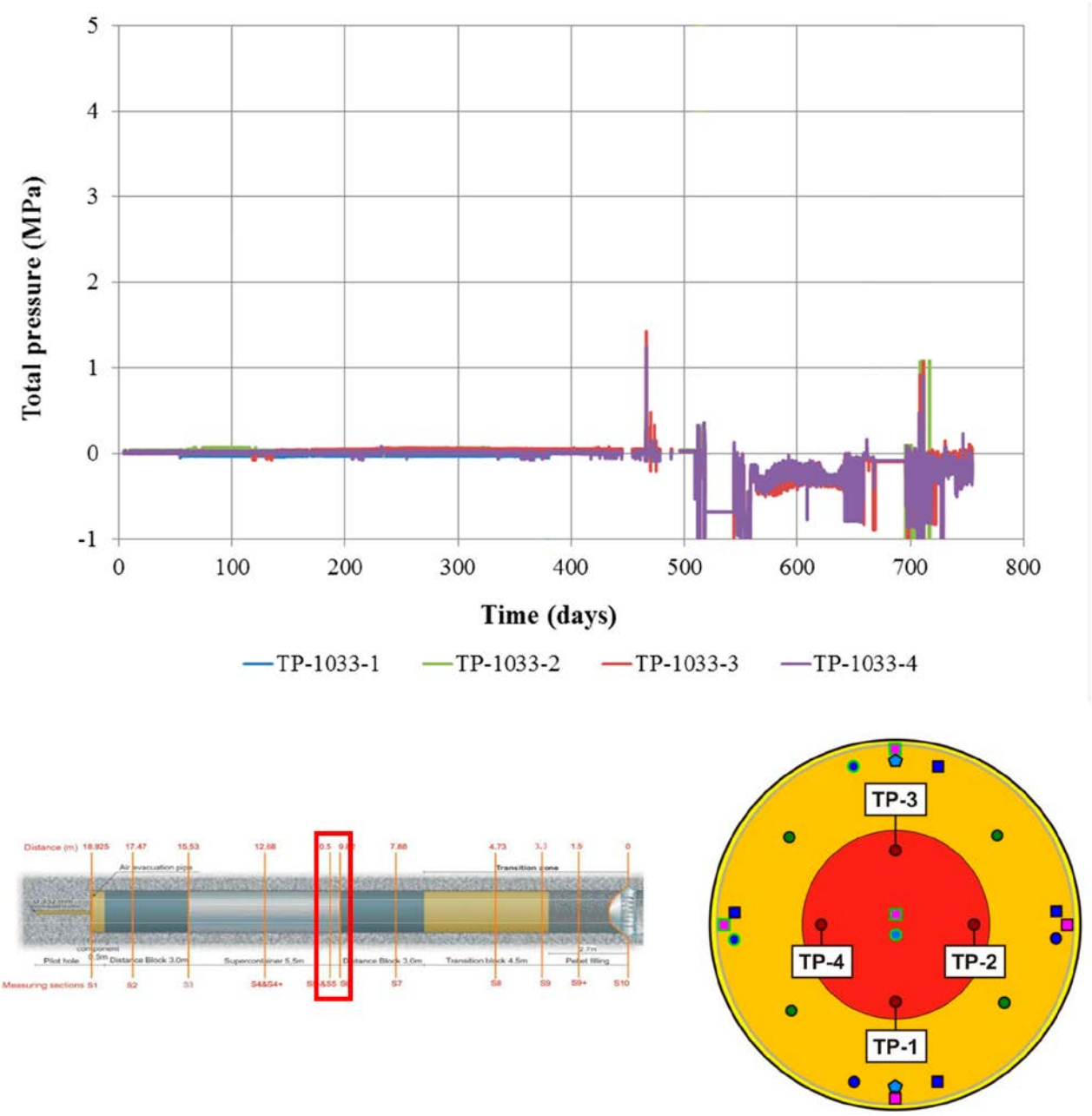

Figure 6-14. *Response of total pressure sensors at inner Supercontainer positions (in the bentonite block at the end block/canister interface measuring axially along the drift axis) in drift section 5.*

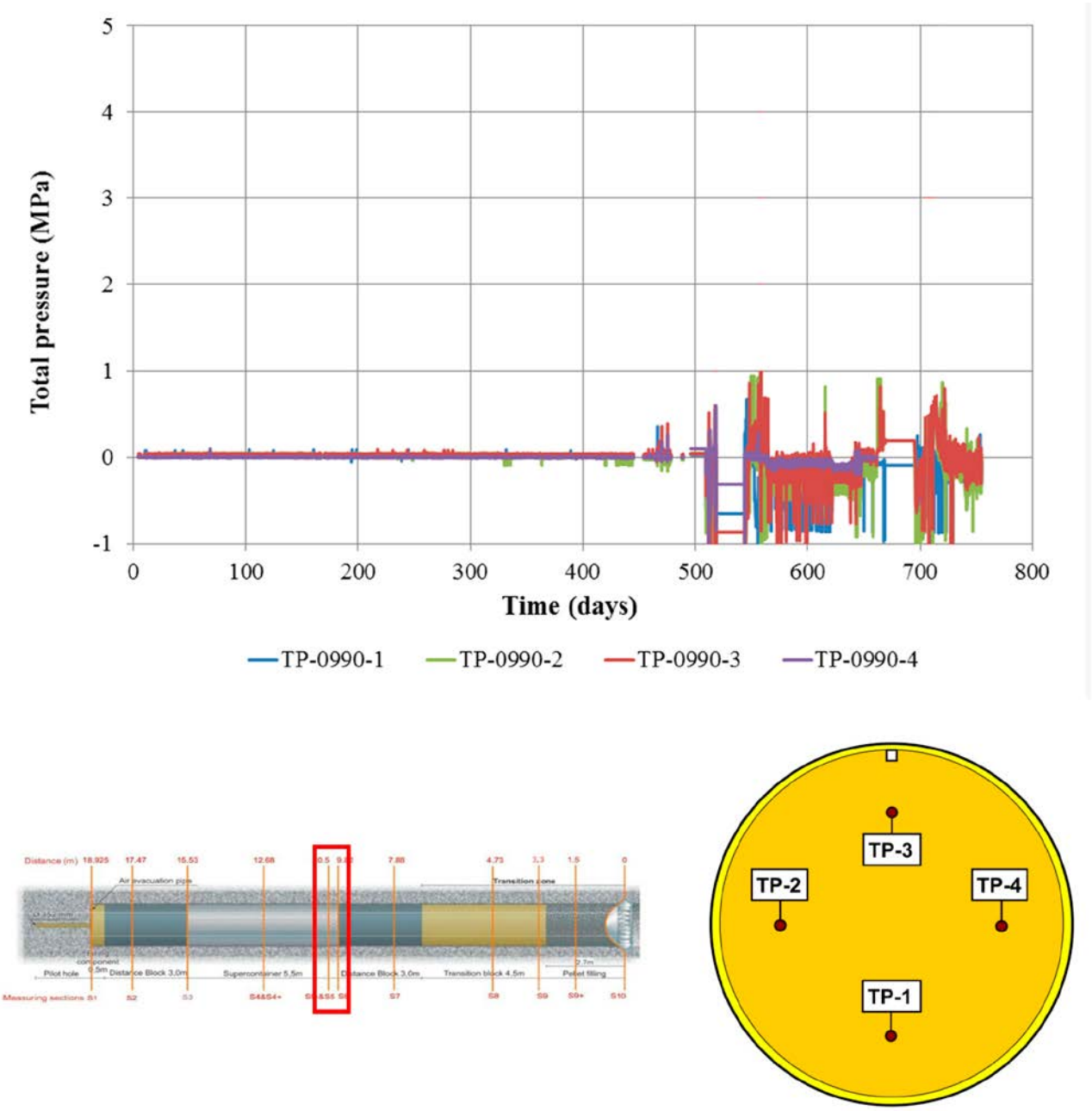

Figure 6-15. *Response of total pressure sensors at inner Supercontainer positions (in the bentonite block at the Supercontainer endplate/distance block interface measuring axially along the drift axis) in drift section 6.*

6.2.8 Strains

The results from the strain gauge measurements on the Supercontainer surface are presented in Figure 6-16. Six of the strain gauges failed a few days after the start of the test (Pintado et al. 2015). The remaining two strain gauges did not measure any significant strains up to nearly day 300 when they failed. The instability of the readings for SG-SP1after 250 days and for SG-SP2 after 190 days is probably due to failure of the strain gauges and not any actual Supercontainer damage. The strain gauges were applied without mechanical protection and it is possible that they were all damaged to some extent upon component installation in the drift.

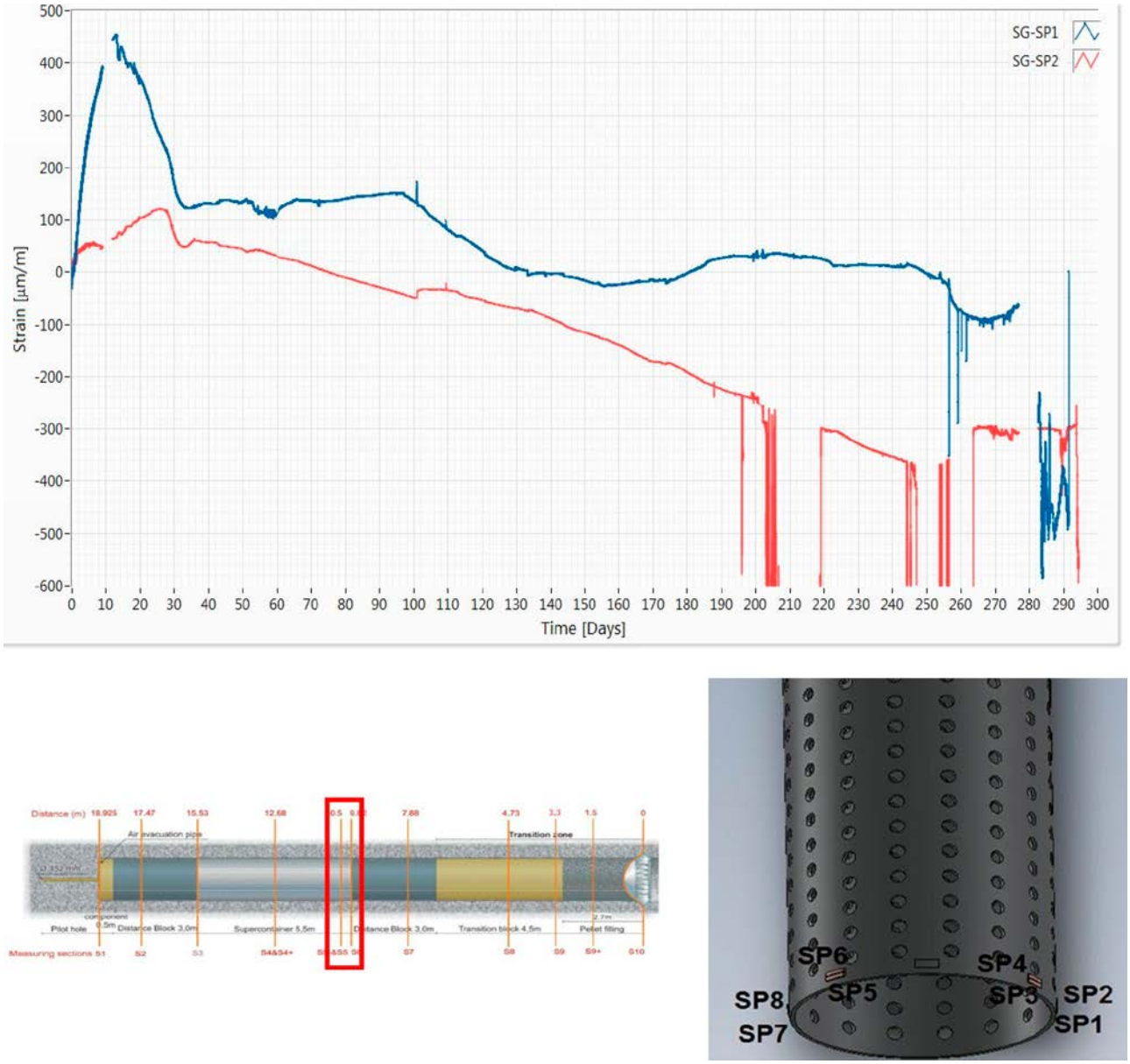

Figure 6-16. *Response of strain gauges to circumferential strains on the Supercontainer surface in drift section 6. Signal was recorded from only two of the strain gauges (SG-SP1 and SG-SP2) beyond a few days into the test.*

6.3 Outer sensor positions

The location of the sensors and other information is presented in Table 6-5.

Table 6-5. Numbering and position of outer Supercontainer sensors in drift section 4.

	Coordinate system ÄSPÖ 96							
Point No.	Easting [m]	Northing [m]	Point Elevation [m]	Drawing label	Sensor code in SICADA	Sensor code in SCADA	Assembly tag label	Manufacturer
15	1910.661	7254.110	-217.551	TP-8	PXK062TP8	TP-1259-8	TP-1259-8	Geokon
16	1910.670	7252.268	-217.547	TP-7	PXK062TP7	TP-1259-7	TP-1259-7	Geokon

6.4 Outer sensor results and comments

Only total pressure measurements are made in outer Supercontainer positions.

Two total pressure sensors were installed in section S-4 (see Figure 6-17). Both sensors showed increasing pressure from the beginning of the test leveling off after 100 days at values around 0.85 MPa. After day 200 the signals started to steadily increase reaching between 1.6 to 1.7 MPa by the end of the measurement period.

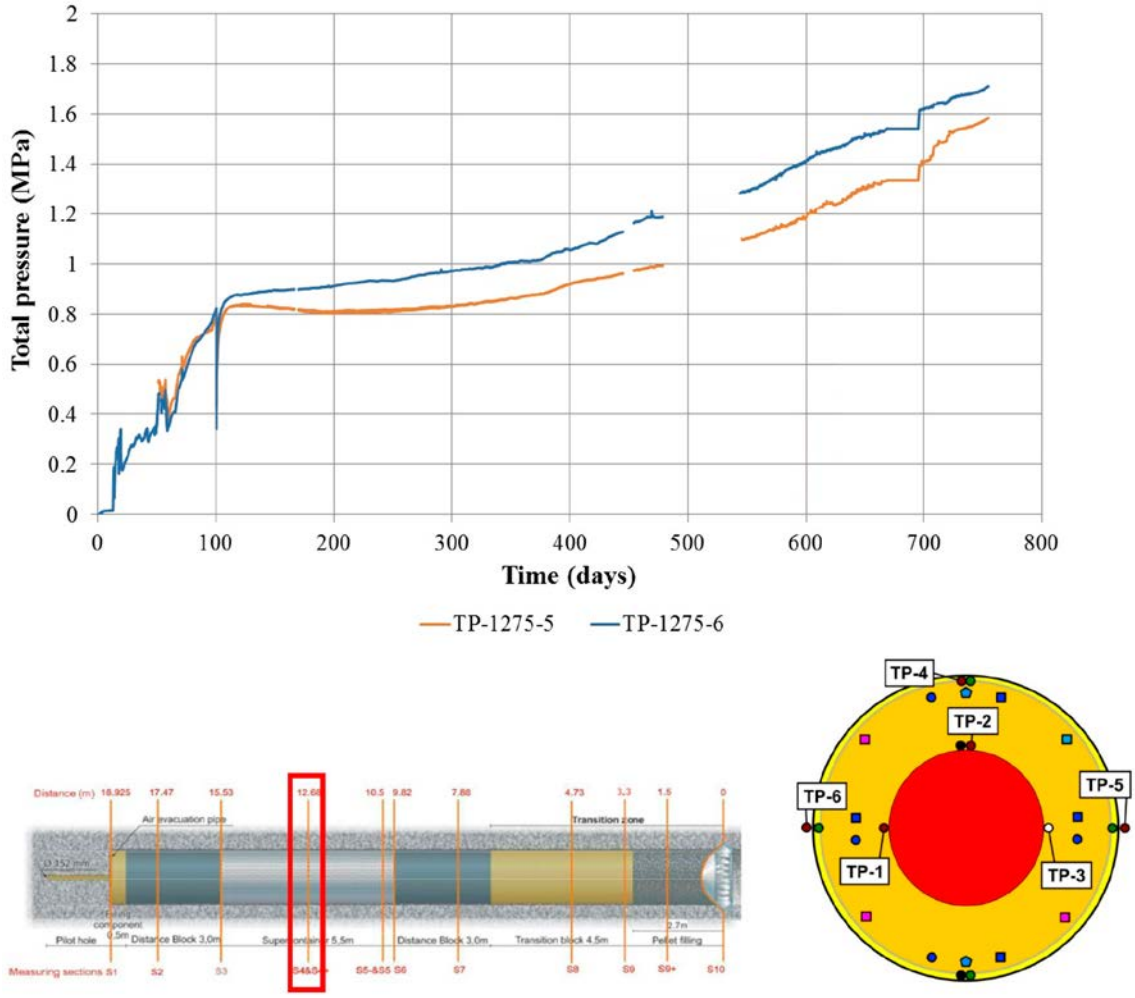

Figure 6-17. *Response of total pressure sensors at outer Supercontainer positions (at the rock wall surface) in drift section 4.*

7 Assessment of the state of the test

7.1 Total pressure

At the early stages of the test, the total pressures measured at the drift walls were similar to the pore pressures measured by some of the pore pressure sensors in the rock and by pore sensors located in the blocks at the gap between the drift component and the rock wall (see Figure 7-1). It was only in drift section 1 that higher pressures (possibly including some component of swelling pressure against the rock wall) were measured. This result is reasonable given that the bentonite block in this location is in close contact with the drift end sensors.

The total pressure sensors at the rock walls measured similar responses in the Supercontainer section and in the distance block sections on either side of the Supercontainer section. Somewhat odd measurements were observed in the transition zone section as sensors at the same section position but different circumferential locations on the rock wall gave quite different responses. The reasons for these anomalous readings are unknown.

In some cases, the measured total pressures were clearly higher than the pore pressures at the same drift locations (Figure 7-2).

The total pressures measured in the pellet-filling zone seem to be strongly correlated with pore pressure (see Figure 7-3). Considering that the swelling pressure expected in the pellet-filling zone should not be higher than 400 kPa based on density (Karnland et al. 2016, Martikainen and Schatz 2011, Kiviranta and Kumpulainen 2011, Kiviranta et al. 2016), it is likely the case that some contribution from water pressure is included in the total pressure response presented in Figure 7-3.

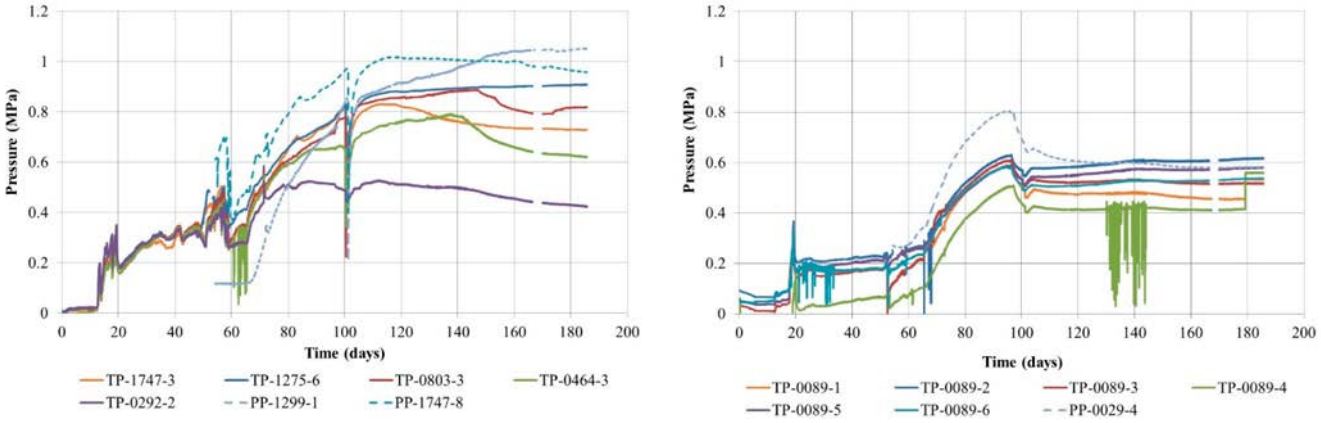

Figure 7-1. *Comparison of total pressures and pore pressures measured within the first 200 days of the test.*

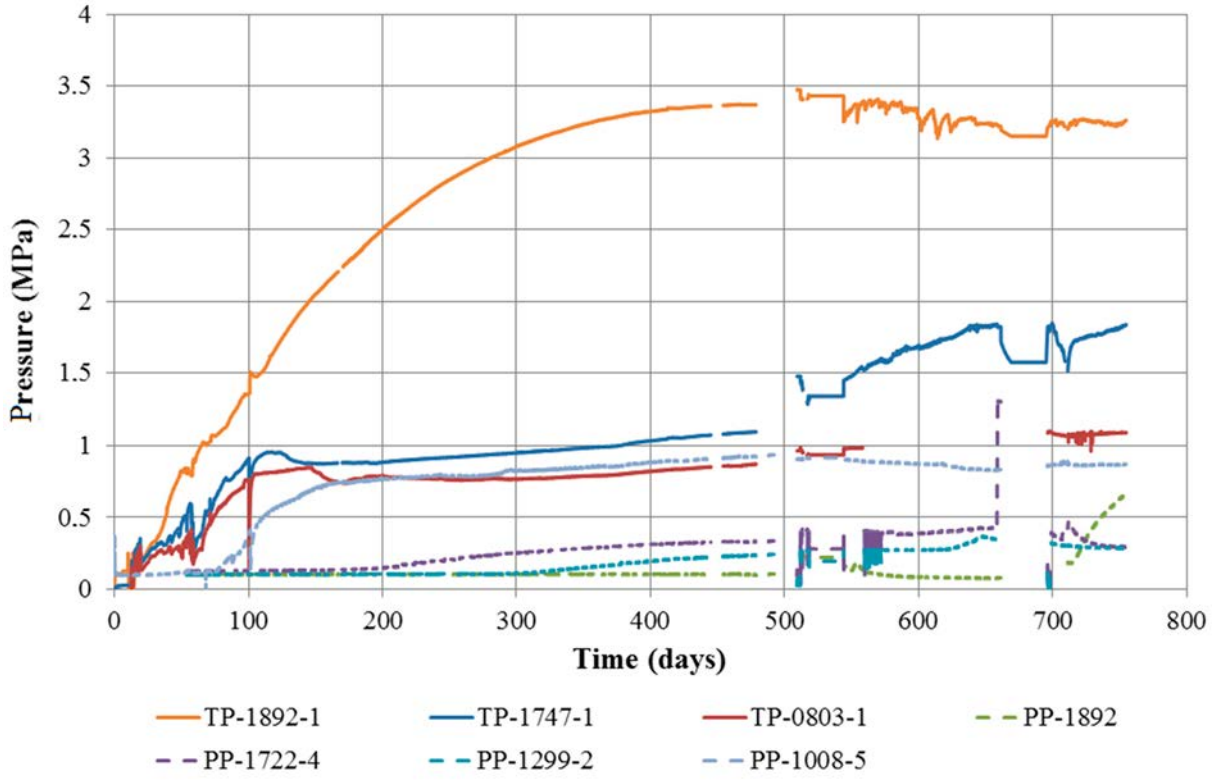

Figure 7-2. *Response of total pressure sensors at upper and bottom of the rock wall surface in the MPT drift (TP-1892-1 in S1, TP-1747-1 in S-2 and TP-0803-1 in S-7) in comparison with representative pore pressure sensor responses (PP-1892-1 in S1, PP-1722-4 in S2, PP-1299-2 in S4 and PP-1008-5 in S-5).*

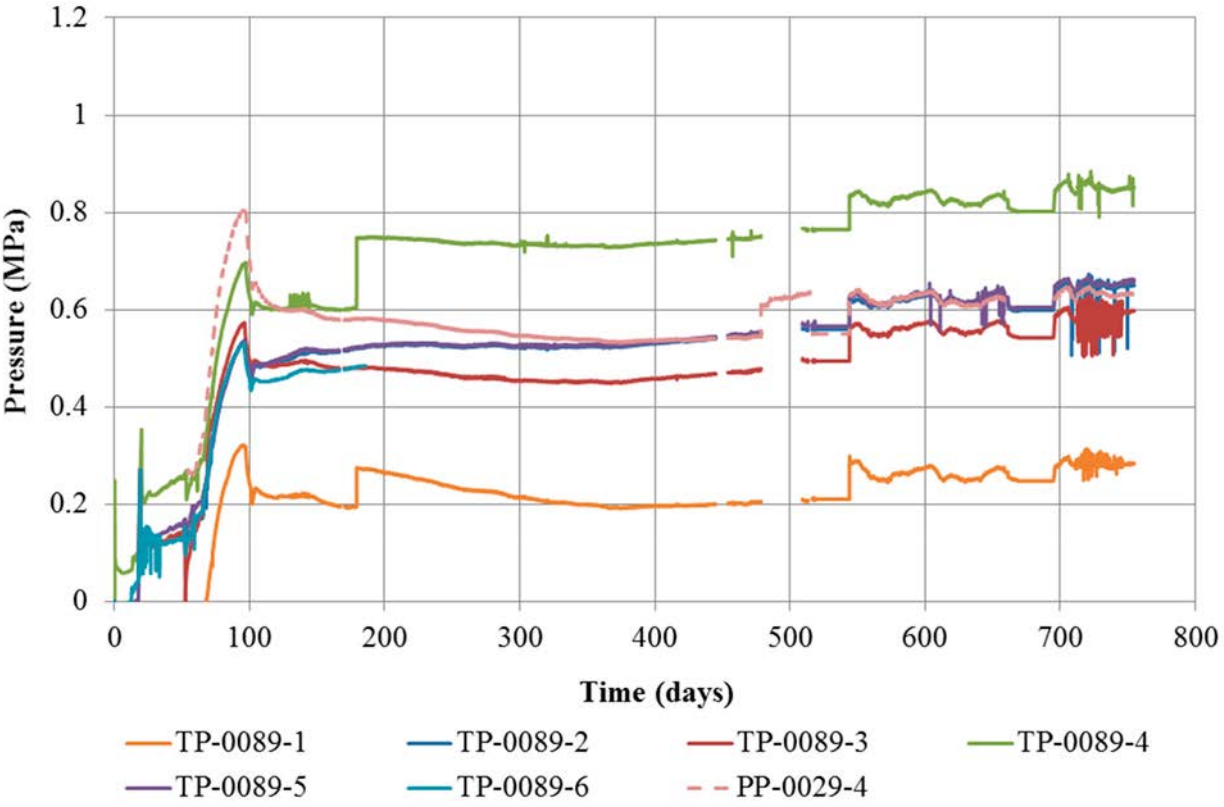

Figure 7-3. *Response of total pressure sensors in transition zone positions in the pellet-filling (S-9+) and the pore pressure measured in S-10 with sensor PP-0029-4. All of the sensors display similar evolution measuring pressures between approximately 300 to 900 kPa at the end of the measurement period.*

7.2 Borehole pore pressures

Pore pressure measurements were made in the three boreholes drilled into the rock wall in drift section 9 (see Figures 5-13 to 5-15) in small cavities separated by packers, see Appendix 1. Stable measurements were observed in all boreholes. Pore pressures after 185 and 474 days at different distances from the tunnel wall are presented in Figure 7-4.

The sensors in boreholes 1 and 2 displayed expected behavior with increasing pressures being measured at deeper distances into the rock. The measurements in borehole 3 indicate that the packers did not properly seal the sensor cavities from one another or that borehole 3 intersects other features which hydraulically connect the sensor cavities to each other.

In all cases, the pressures measured after 185 and 474 days are quite similar.

7.3 Saturation

The saturation process can be followed initially with the capacitive hygrometer sensors (Figures 7-5 and 7-6). These sensors are able to measure the full range of humidity from 0–100 %. However, above 95 % the level of uncertainty in the measured values increases and other methods are needed for accurate measurement. Psychrometer sensors were installed in order to allow coverage of the full range.

Figure 7-5 shows the evolution of the capacitive hygrometer sensors that first reached RH values close to 100 % in each section. It is apparent that the saturation process was faster close to the back end of the drift (S-2) and was slower when moving towards the plug (note that the data for WC-1299-1 corresponds to the block inside the Supercontainer in S-4). In general, the saturation was faster at the right hand side and at the bottom of the drift.

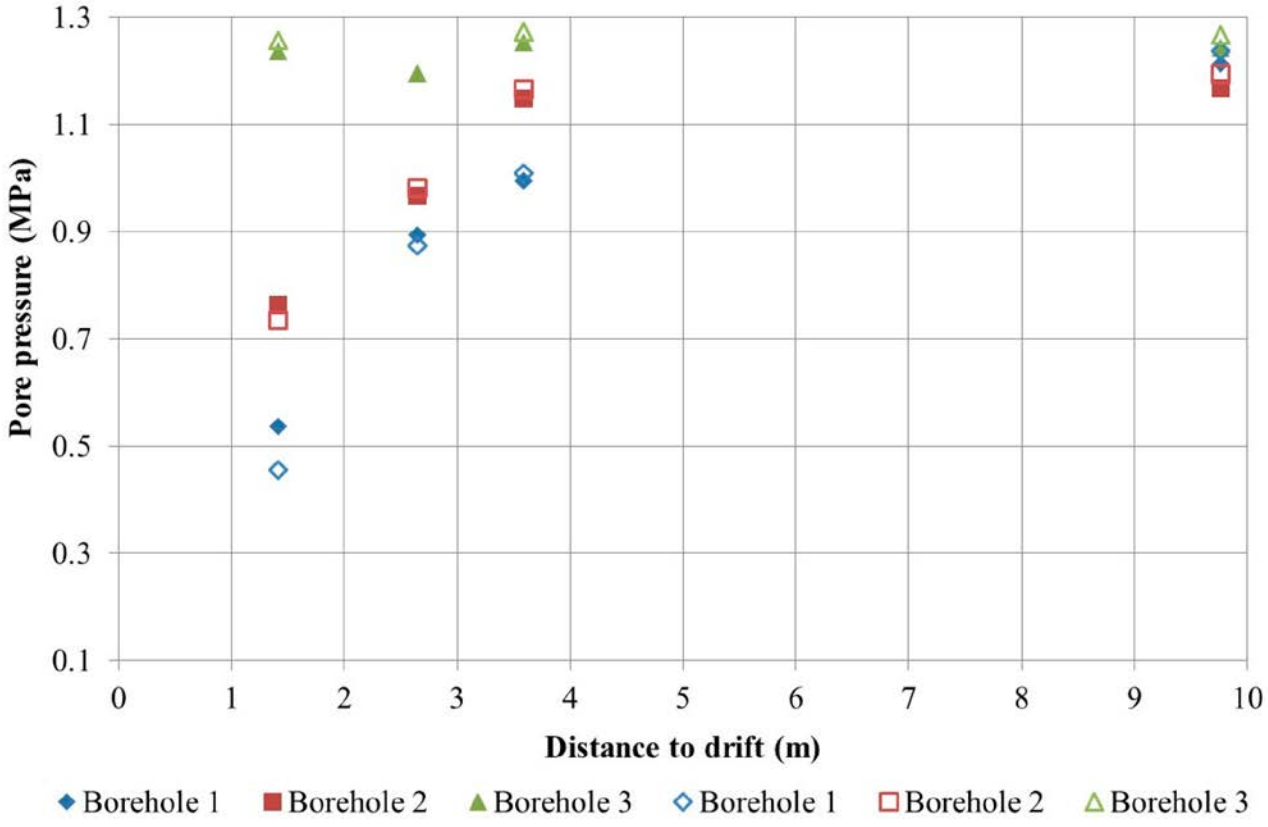

Figure 7-4. *Borehole pore pressures as a function of distance to drift after 185 days (filled symbols) and 474 days (open symbols).*

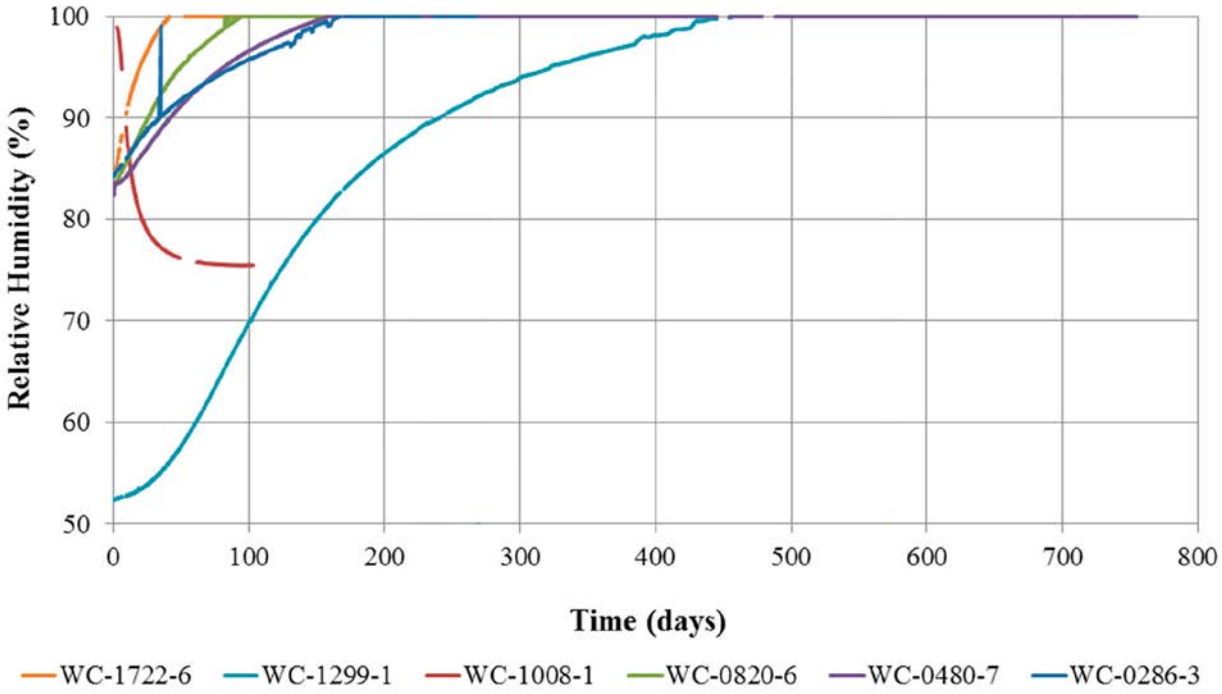

Figure 7-5. *Evolution of the relative humidity sensors that reached saturation first in different sections along the drift (1722-6 in S- 2, 1299-1 in S-4, 1008-1in S-5, 0820-6 in S-7, 0480-7in S-8 and 0286-3 in S- 9).*

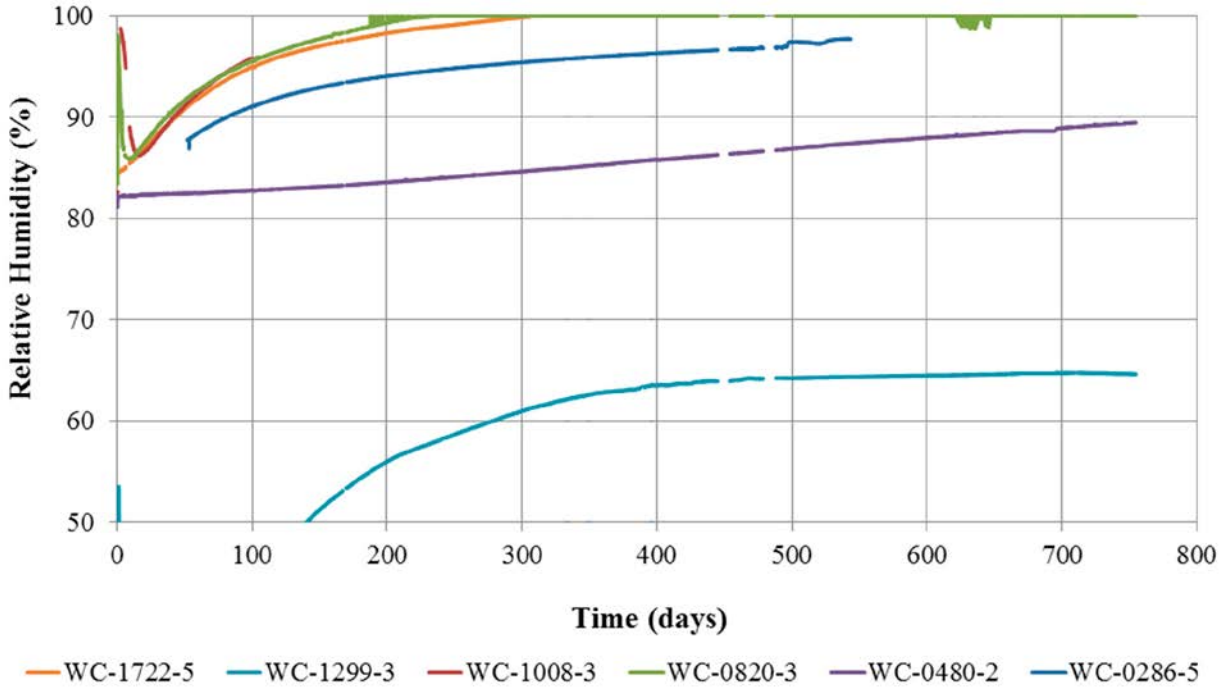

Figure 7-6. *Evolution of the relative humidity sensors that reached saturation last in different sections along the drift (1722-5 in S-2, 1299-3 in S-4, 1008-3 in S-5, 0820-3 in S-7, 0480-2in S-8 and 0286-5 in S-9).*

Figure 7-6 shows the evolution of the capacitive hygrometer sensors that took longer to reach values close to 100 % in each section. In general, the saturation was slower on top. Although the signal patterns are not as clear, it can be said that "saturation" from the point of view of the sensor measurements started to occur in a period not shorter that 300 days. It should be taken into account that, as has been emphasized previously, capacitive hygrometer measurements of relative humidity higher than 95 % have relatively large errors and these sensors are not valid for following the saturation process at low suction.

The initial relative humidity measurements depend on the initial water content of the blocks. Different types of blocks have different initial water contents as follows:

- Distance blocks and transition blocks: 21 ± 1 %
- Supercontainer end blocks: 17 ± 1 %
- Supercontainer ring-shaped blocks: 11 ± 1 %

As such, the initial relative humidity values measured with the capacitive hygrometers differ as a function of their position.

- Distance blocks and transition blocks: In drift section 2, the wireless hygrometers measured 83.5 % and the wired hygrometers measured 84.5 %. The wireless hygrometers are located in the inner part of the block. In drift section 7, the hygrometers measured between 81.9 and 83.5 % independent of whether they were wired or wireless. In drift section 9, only the wired sensors provided signals at the beginning of the test which were between 84.3 and 83.5 %.
- Supercontainer end blocks: In drift section 5 the wired sensors measured 73.9 % but the wireless sensors measured 83 % (see Figure 6-2).
- Supercontainer ring-shaped blocks (section 4): In drift section 4 all of the sensors are wired and measured relative humidities between 52.2 and 52.8 %.

The psychrometers (WP) started to be in range at different times but in general they correlated very well with the capacitive hygrometer (WC) sensors. WP sensors come into range after the corresponding WC sensor indicates saturation. Table 7-1 indicates which psychrometer sensors came into range fastest and slowest for each section.

Table 7-1. Evolution of psychrometer sensors (WP) to measurement range (time in days) in different sections along the drift indicating which responded fastest and slowest.

Section	Fastest in-range	Time [d]	Slowest in-range
S2	WP-1722-5	300	WP-1722-4
S5	WP-1008-1	> 500	WP-1008-2
S7	WP-0820-5	> 500	WP-0820-4
S8	WP-0480-6	> 600	WP-0480-4
S9	WP-0286-6	> 700	WP-0286-4

Based on the information in Table 7-1, it can be stated that the psychrometer sensors did not reach the measurement range before day 300 at the back end of the drift and took much longer when moving towards the plug, in some cases with times longer than 700 days. Full saturation of the entire blocks will take much more time because the sensors listed in Table 7-1 were located at the periphery of the blocks. The inner psychrometer sensors are not yet in range. The sensors in S-4, located between the canister and the block, are not yet in range either.

The pore pressure sensors in the blocks need to have free water in the chamber of the sensor (inside the filter) in order to measure pressure. Due to the low hydraulic conductivity of the bentonite blocks this process will require a substantial amount of time. Therefore, there will be a gap between the time that the psychrometer sensors measure zero suction and the time that the pore pressure sensors start to provide some signal.

Presumably only those pore pressure sensors with ready access to water through some preferential pathway through the blocks would provide early signals (see Figures 6-5 and 6-6). The presence of preferential pathways is corroborated by the WC sensors (see Figure 7-6), where the relative humidity signals jump suddenly after DAWE wetting.

The signals from selected soil moisture sensors are presented in Figure 7-7. In almost all cases, signal decreases are observed at the beginning of the test, possibly due to initial cracking/expansion of the blocks. After some time, all signals begin to increase due to wetting of the blocks.

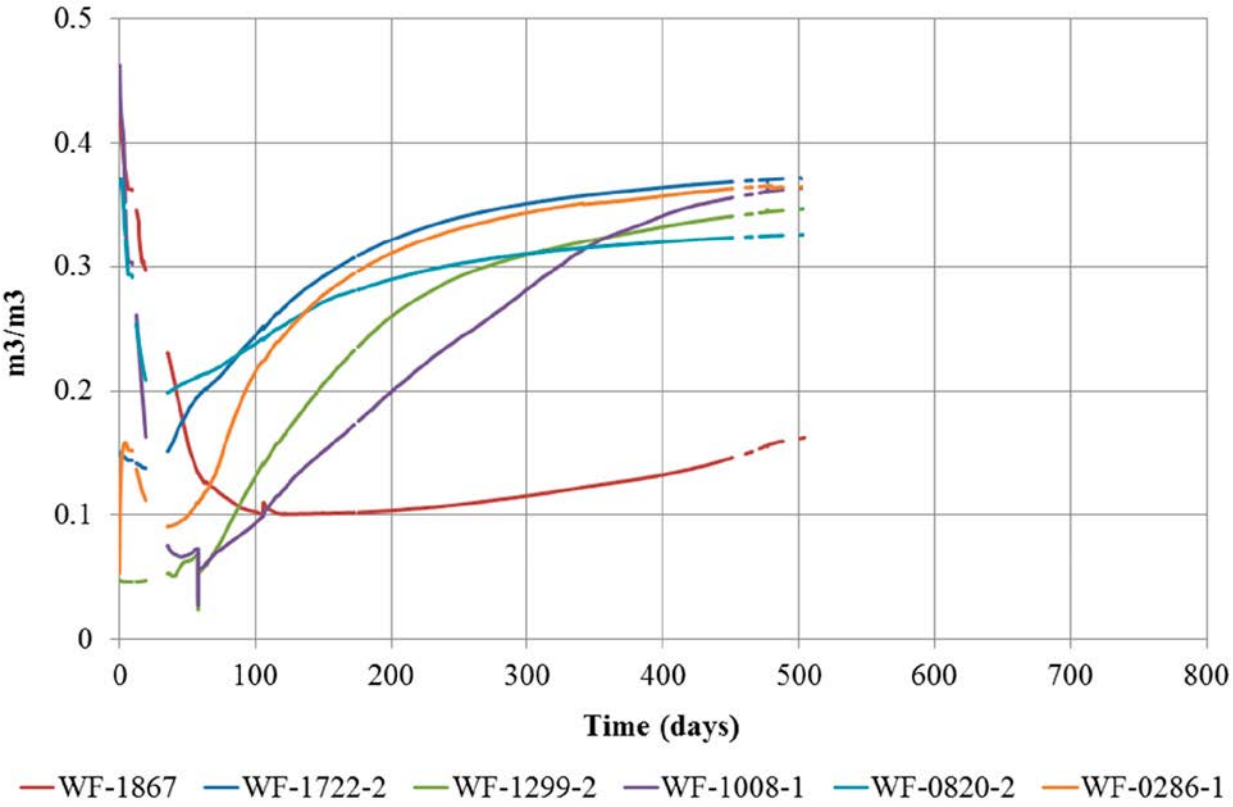

Figure 7-7. *Evolution of the soil moisture sensor signals in different drift sections. 1722 corresponds to S-2, 1008 to S-4, 1299 to S-5, 0820 to S-7, 0480 to S-8 and 0286 to S-9.*

7.4 Pore pressure in the gap between drift components and the rock wall

The pore pressure in the gap between drift components and the rock wall is an important value to assess the swelling pressure of the bentonite against the rock wall. The total pressure sensors at the rock wall measure the total pressure (swelling pressure + pore pressure), so if it is possible to measure the pore pressure in gap, it should be possible to extract the swelling pressure. The initial gas pressure sensors with 250 kPa range were exchanged to pore pressure sensors with 3 MPa range as described in Chapter 3. It appears that the sensors are not connected hydraulically now because different values are measured over the length of the drift (see Figure 7-8). The highest pressure is measured at the end of the drift and the smallest is measured at the middle of the drift in the Supercontainer location.

7.5 Movements

An assessment of the movements of the different components may help to better understand the system behavior as well, especially if there is any asymmetry in the saturation process.

Plug displacements were too small to be accurately measured by the sensors installed on the face. The thickness of the plug is 40 mm and the pressure from the pellet-filling zone should not be more than 1 MPa, so any displacements of plug could be quite small and sensors with lower detection limits should have been installed. The strain gauges on the plug face did measure increasing levels of strain.

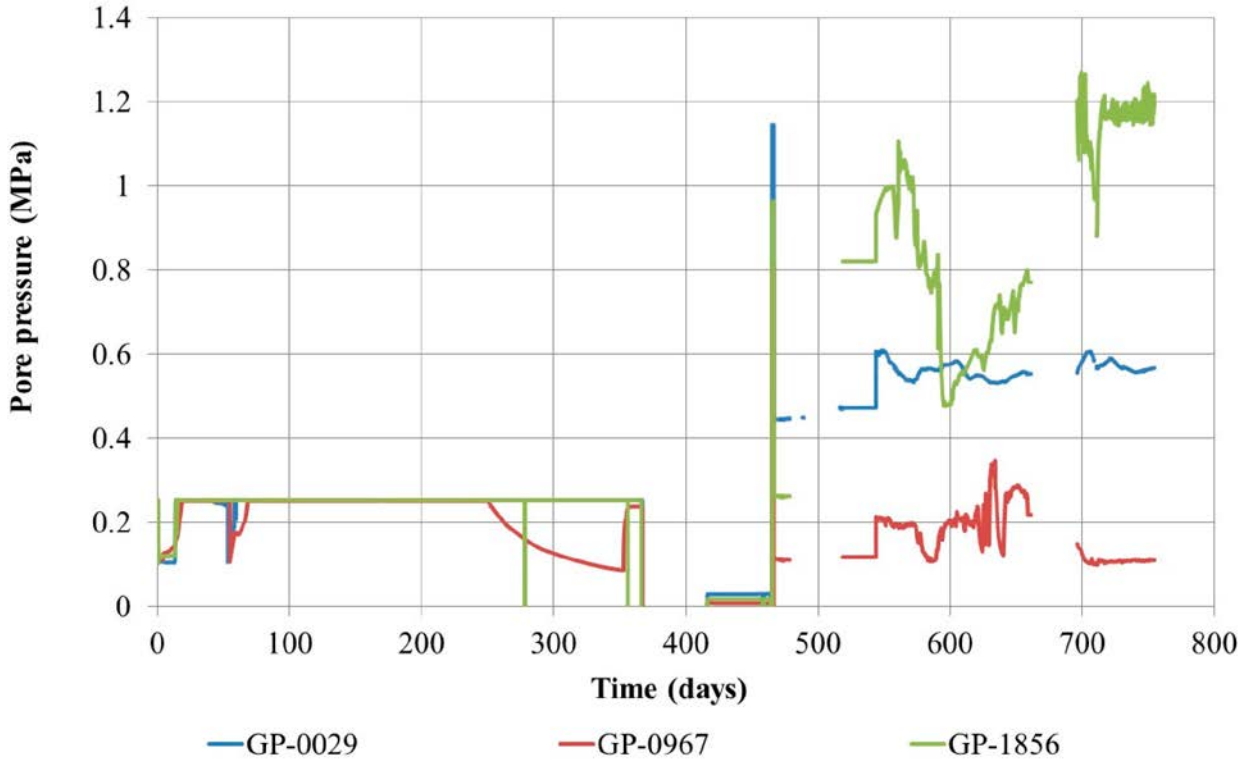

Figure 7-8. *Pore pressure evolution in the gap between the drift components and the rock wall at S-1 (GP-1856), S-5 (GP-0967) and S-10 (GP-0029).*

The sensors for measuring displacements of the Supercontainer have a measurement range of ±25 mm. As the initial, installed baseline measurements of DS-1082-1, DS-1082-4 and DS-1275-4 were more than 20 mm and DS-1275-3 more than 25 mm, it may be that the sensor range was too small to begin with. If the sensors were out of the range, it is possible that the signals are no longer linear with the displacements. This issue can be checked after dismantling. In other locations the displacements measured by the sensors, e.g., DS-1275-2 and DS-1275-4, were contradictory. The measured displacements could be due to movements of the sensors within their original block positions rather than any displacement of the Supercontainer itself. DS-1275-2 showed a sudden displacement on day 418 which was not detected by the other two displacement sensors.

The sudden rotations indicated by the inclinometers in very early stages could be due to adjustments of the blocks due to swelling once the gap was water filled.

In any case, given the limited dataset and associated uncertainties, accurate interpretation of component movement is difficult.

7.6 Strains

No significant or abrupt strains on the Supercontainer were measured near one end of the structure from two strain gauges during the time (almost 300 days) that signal was recorded.

The strains measured on the plug ideally would serve to complement measurements from the total pressure sensors and the displacements sensors. Unfortunately, given the difficulties described above with respect to the displacement sensors and the fact that the total pressure sensors may not be properly grounded, measurable signal was detected only with the strain gauges. The strains are an indirect measure of the pressure against the plug. It is possible to estimate pressure values from the measured strains with additional analysis (Bendito and Pintado 2016).

8 Wireless system status

The wireless transmitters were encapsulated in Äspö on October 2013. After installation (Figure 8-1), nodes 3 to 7 were functioning and nodes 1 and 2 were not. Node 1 has an RS-485 cable for sending data to the MP-40 unit, so this node does not have wireless transmission problem. Receivers 2 and 3 were also functioning.

Nodes 3 and 4 failed on December 7, 2013 at 22:25, a few hours after filling the gap and the pellets with water. The reason could be due to the difficulty in transmitting wireless signal through water but only the gap was filled with water and the nodes were sending signal for some hours after the filling process.

Receivers 1 (R-1) and 2 (R-2) were inspected on January 2014 and the conclusions were that the relays did not suffer any electrical shorts, so the problem lies in the receiver/transmitter links. Receiver 3 (R-3) was also assessed to be functioning adequately.

An attempt was made to recover the signal from the nodes by inserting an antenna through the pellet-filling hole (Figure 8-2) on the plug face and connecting it to a new external receiver. Two antenna lengths were checked using two different rod lengths (0.85 and 1.2 m). No signals were detected. The 1.2 m length antenna was left in place and the hole was resealed. Additionally, two boreholes (200 mm deep and 20 mm diameter) were drilled into the rock near the plug face (see Figure 8-2 for locations) and antennas were inserted. These antennas were also connected to the external receiver. Signals were detected with limited success.

Nodes 5, 6 and 7 were working and sending signal for 103 days (until 20.03.2014). Node 4 started to send signal on 07.03.2014 but then stopped on 20.03.2014.

Node 2 started providing signal on 29.01.2014 and stopped on 05.02.2014.

The fuse of the MP-40 unit failed on 20.03.2014. The fuse was changed but the unit was not functioning correctly. It was sent to AITEMIN and returned to Äspö after repairs. However, no signal is currently being recorded. The reasons for this malfunctioning are not evident. The battery capacity should be sufficient because the transmission frequency was 12 hours and the battery duration should be four years at this frequency. R-3 was working but is now disconnected due to short-circuiting.

No additional activity has been performed and the status of the wireless units remains as described above.

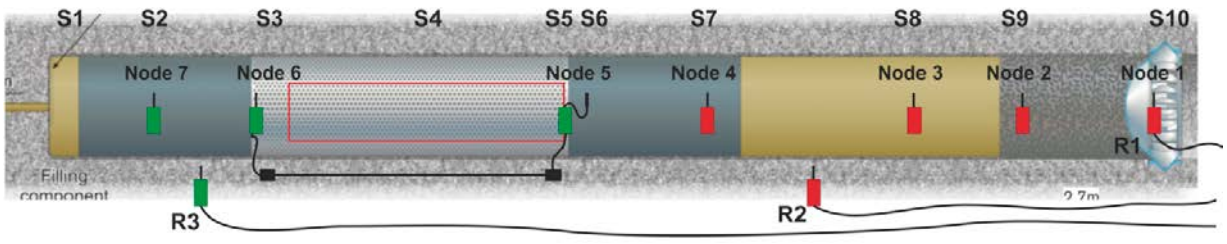

Figure 8-1. *Location of wireless transmitters (or nodes) and receivers in the MPT experiment (red-colored device locations correspond to those from which signal was lost after DAWE).*

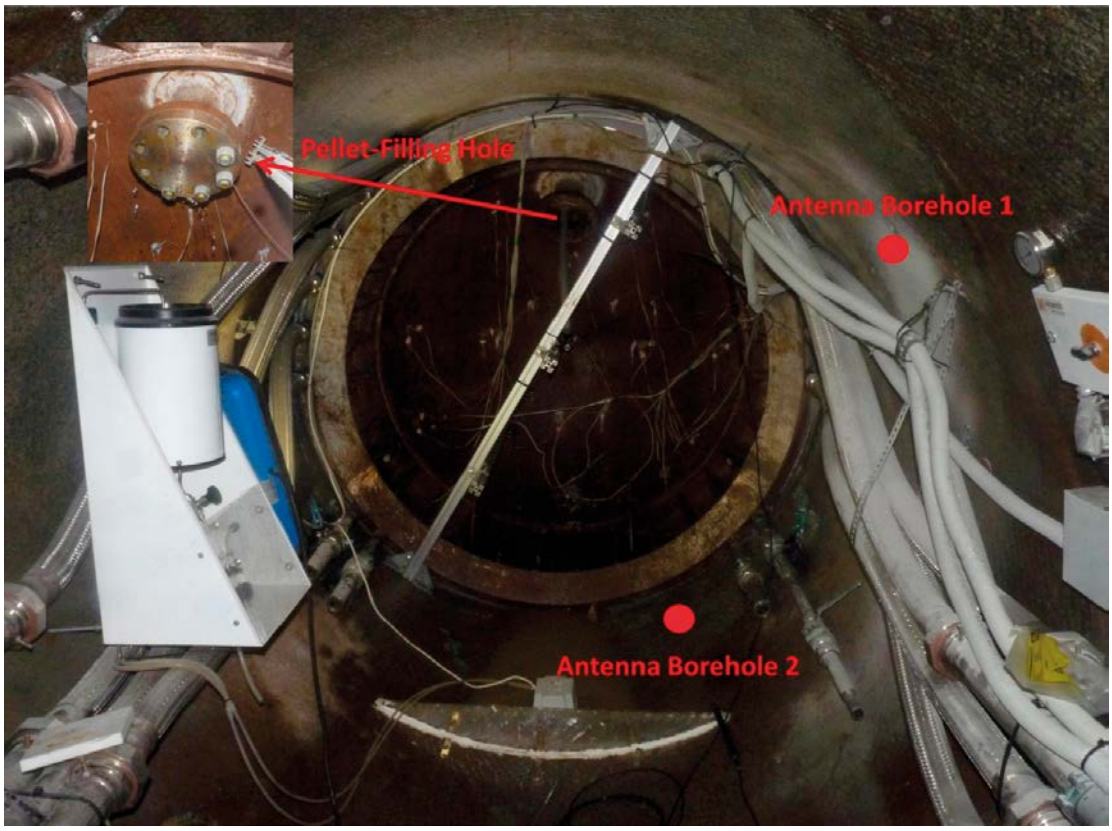

Figure 8-2. *Photographic image of plug face showing locations of pellet-filling hole (through which an antenna was inserted) and additional antenna boreholes.*

9 Conclusions

The total pressure sensors in the rock, the pore pressure sensors in the rock, the capacitive hygrometers, the psychrometers and the soil moisture sensors were all functioning adequately to around day 500. After that time, approximately when the power supply in the datalogger failed and was changed, the signals from the WF sensors became unstable. Other sensors showed signal oscillations which could be due to the new power supply or due to the damaged power supply affecting the sensors before its failure. In any case, most of the signals are still being recorded.

The use of both capacitive hygrometers and psychrometers has demonstrated itself to be a useful technique to capture the full saturation process. Information has been obtained which will allow both qualitative and quantitative analysis of the saturation process as well as model verification. Unfortunately, sensor performance close to the pellet filled zone was deficient.

Initially, the total pressure sensors at the rock wall started measuring appreciable signals in parallel with the pore pressure sensors at the rock wall. After longer times (100 days), the signals started to differentiate from one another and pressures due to swelling bentonite became discernible. The density of the bentonite close to the sensors can be determined during the dismantling process and compared to data from swelling pressure measurements in oedometer cells, the Big Bertha tests (Sandén et al. 2008, SKB 2012) and perforation hole tests (Asensio Sánchez 2013, Pintado et al. 2016).

It appears that the saturation process and therefore the swelling development were faster at the back end of the gallery and slower when moving towards the plug (longitudinal direction). This result is in accord with the fact that the back of the gallery was the wettest section as measured before the emplacement of the test components (see Figure 1-4).

Differences in saturation behavior were detected within the blocks themselves. Saturation was faster at the right hand side and the bottom and slower at the top of the blocks most likely due to the accumulation of water on the drift floor by gravity. Some rapid saturation recorded by a few of the sensors at the beginning of the test could be explained by the presence of cracks or damage in the blocks leading to direct contact between the sensors inside the blocks with the gap. This contact was then lost when the bentonite swelled, thus sealing preliminary flow paths.

There are clear differences in the evolution of the total pressure measurements between the pellet filling and the bentonite blocks. The total pressures measured in the pellet-filling zone should be lower than in the distance and transition block sections and those pressures that are measured in the pellet-filling zone are probably due to water pressure rather than swelling pressure.

The total pressures measured at the rock wall in section 1 vary from 1.5 to 4.2 MPa over the surface of the distance block/drift end interface. This variation is probably due to the heterogeneity of the rock/block contacts.

The total pressure measured at the rock wall at the Supercontainer position is higher than expected. The Big Bertha tests ongoing at Clay Technology demonstrate that swelling pressures measured around the Supercontainer are strongly dependent, at the beginning of the test at least, on the position of the sensors with respect to the perforation holes. The exact positions of the MPT Supercontainer holes in terms of the position of the total pressure cells are not known. The pressures registered at the beginning of the test are due to water pressure and are not affected by the presence of the Supercontainer. Sections 1–5 comprise the part of the drift where there is more inflow from the rock and the evolution of the total pressure in these sections was faster.

The pore pressure sensors in the buffer are not yet generally measuring positive pressures. This expected lag is due to the long time necessary for filling all the experiment gaps with water, including the bentonite pores and the sensor cavities. The bentonite has an extremely low hydraulic conductivity and the saturation of the pores and sensor cavities will likely require some years.

The sensors for measuring movements of the blocks and the Supercontainer have provided some information but due to the complexity of the potential movements of KBS-3H components, it is difficult to analyze the data. The installation of the KBS-3H components is quite intricate and the sensors could have become over-ranged after the installation. The use of larger displacement range sensors could mitigate this problem in future tests. During the dismantling process, it may be possible to determine the position of the canister and compare it with the position predicted from the measurement of the inclinometers and displacement sensors.

The signals from the total pressure sensors in the blocks, which were manufactured by ÅF / Geokon is not satisfactory. The cable shielding was removed due to practical problems with the lead-throughs during installation of these sensors in the blocks, and the sensors may not be properly grounded as a result. The two sensors on the plug also showed significant noise development until finally, the signals were lost.

The use of strain gauges is novel for "in situ" tests in nuclear waste management applications. They can provide useful information from the early stages of the test but it is clear that the corrosion of the plug and the saturation process in the Supercontainer will be problematic for relying on these sensors over the long-term if they cannot be properly protected.

The displacement sensors on the plug have not measured any displacement yet because the inner total pressure is likely still rather low in the adjoining pellet-filled chamber. It is possible that small displacements of the plug have occurred and were not detected because the range of the current sensors is too high. The use of displacement sensors with lower ranges in parallel with the higher range sensors could be considered. More thorough study regarding the expected displacements of the plug should have been performed before the dimensioning of the test.

The wireless system was working as intended only at the very beginning of the test. Although the transmitters were encapsulated and their batteries calculated to run for 4 years at a measuring interval of 12 hours, most signals were lost during the early stages of the test. The potential advantages offered by this kind of system justify the attempt to use it. The main conclusion is that added redundancy is needed, e.g., the inclusion of additional receivers or antennas connected to redundant receivers. It is also the case that some data could be recovered from the memory cards inside the transmitters after dismantling.

For future experiments, transmitter operation could be improved if signals are collected over discrete periods of time and transmitted only once per week or per month, thus decreasing the battery consumption and extending operational lifetimes. As the measuring frequency of the transmitters can be adjusted remotely, the best approach could be to set a relatively high frequency (every 10 minutes for example) during the early stages of the test and then change later to a lower frequency in order to preserve the duration of the batteries. If the transmitters do not receive any order from the receivers during a certain period of time (one day for example), the measuring period could be increased to 12–24 hours automatically.

The current status of the sensors is listed in Table 8-1. There are 90+ sensors functioning normally and it is quite likely that these sensors could remain so over several additional years.

Table 8-1. Status of the MPT sensors.

		Status					
Sensors	**Tot**	**Up (normal)**	**Up (noisy)**	**Over-ranged**	**<LOD**	**Down (wired)**	**Down (wireless)**
TP rock	27	27					
TP plug	3					2	1
TP buffer	13					13	
PP rock short	9	5				4	
PP rock borehole	18	18					
PP buffer	23	6			1	4	12
WC	34	2		13		4	15
WP	32	13	8	2	7	2	
WF	13					11	2
DS	8	6				2	
DB	2						2
DC	3				3		
IS	2	1				1	
IB	4	3					1
GP	3			3			
SG	32	9				23	
FM	1				1		
Total	**227**	**90**	**8**	**18**	**12**	**66**	**33**

GP sensors were replaced by PP pressure. The three sensors are running. FDR sensors were working till day 500 approximately.

SG in supercontainer are faulty. Some now SG have been installed in plug.

LOD: Limit Of Detection.

10 Future actions

Maintenance should be performed on the datalogging system and sensor connections to try and ascertain the reasons for the increased noise levels. In particular, the power supply of the sensors should be inspected and, if necessary, isolated to avoid interference from failed sensors.

The sensors measuring displacements on the plug face should be changed to those with lower range.

The pressures measured in the boreholes of section 9 should be compared with pressures measured separately in other boreholes as close to the drift as possible. It should be taken into account that the boreholes in section 9 are close to a drain (i.e. the drift) and it is possible that these pressures may not follow the water pressure evolution of other boreholes which lie farther away.

The strain gauge data could be used to estimate the inner pressure on the plug face. It is necessary to develop a computational approach for performing such estimates but this approach can be used for future analyses as well (Figures 10-1 and 10-2). As the total pressure sensors at the plug are not functioning, strain gauge measurements offer the only data available for determining pressure against the plug.

The pore pressure in the gap should be measured in order to calculate the swelling pressure. It is proposed to increase the water pressure to around 200 kPa during a short period of time (a one-hour pulse) in order to check the response of the total pressure sensors and the pore pressure sensors in the gap. This test will also be useful for checking if the cracks in blocks are sealed. The measured results from this water pressure increase should be followed-up by B+Tech and Aitemin immediately and the test should be done only after checking the dataloggers and purging the pore pressure sensors. It is also proposed that the pressure drop be analyzed as well. This analysis could provide additional information about the hydraulic conductivity of the medium.

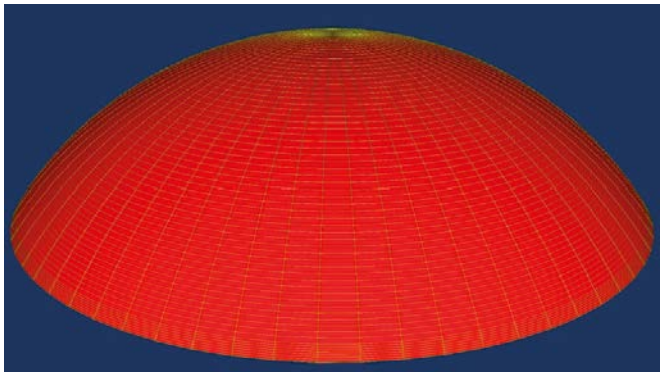

Figure 10-1. *Plug discretization.*

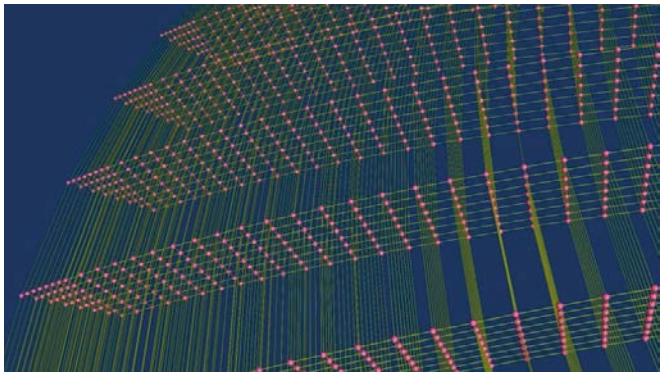

Figure 10-2. *Detailed mesh.*

References

SKB's (Svensk Kärnbränslehantering AB) publications can be found at www.skb.com/publications.

Asensio Sánchez L, 2013. Hydro-mechanical elastoplastic model of expansive bentonite behaviour in free swelling conditions. PhD thesis. Universidad de Castilla-La Mancha, Ciudad Real, Spain.

Bendito E, Pintado X, 2016. Monitoring of swelling pressure in bentonite. Environmental Geotechnics 3, 334–345.

Delta-T Devices, 1999. ThetaProbe soil moisture sensor. User manual ML2x-UM-1.21. Cambridge: Delta-T Devices Ltd. Available at: https://www.upgmbh.com/fileadmin/produkte/support/ML2x_Theta_ProbeUserManual_v1.21.pdf

Eriksson M, Lindström L, 2008. KBS-3H post-grouting. Mega-Packer test at –220 m level at Äspö HRL. SKB R-08-42, Svensk Kärnbränslehantering AB.

ENRESA, 2000. FEBEX project. Full-scale engineered barriers experiment for a deep geological repository for high level radioactive nuclear waste in crystalline rock. Publicación Técnica 1/2000, ENRESA, Spain.

Gensler W G (ed), 1986. Advanced agricultural instrumentation: design and use. Dordrecht: M. Nijhoff.

Johanesson L-E, 2014. KBS-3H. Manufacturing of buffer and filling components for the Multi Purpose Test. SKB P-14-07, Svensk Kärnbränslehantering AB.

Karnland O, Olsson S, Nilsson U, 2006. Mineralogy and sealing properties of various bentonites and smectite-rich clay materials. SKB TR-06-30, Svensk Kärnbränslehantering AB.

Kiviranta L, Kumpulainen S, 2011. Quality control and characterization of bentonite materials. Posiva Working Report 2011-84, Posiva Oy, Finland.

Kiviranta L, Kumpulainen S, Pintado X, Karttunen P, Schatz T, 2016. Characterization of bentonite and clay materials 2012–2015. Posiva Working Report 2016-05, Posiva Oy, Finland.

Kronberg M, 2016. KBS-3H Preparations, assembly and installation of the Multi Purpose Test. SKB P-14-27, Svensk Kärnbränslehantering AB.

Martikainen J, Schatz T, 2011. Laboratory tests to determine the effect of Olkiluoto bounding brine water on buffer performance. Posiva Working Report 2011-68, Posiva Oy, Finland.

Pintado X, Schatz T, García-Siñeriz J-L, 2015. Initial data report for the Multi Purpose Test. LUCOEX project. Deliverable D-N°: D4:06, European Comission.

Pintado X, Kristensson O, Malmberg D, Åkesson M, Olivella S, Puig I, 2016. TH and THM modelling of a KBS-3H deposition drift. Posiva Working Report 2016-25, Posiva Oy, Finland.

Posiva, 2015. YJH-2015. Olkiluodon ja Loviisan voimalaitosten ydinjätehuollon ohjelma vuosille 2016–2018. Finland: Posiva Oy. (In Finnish.)

Sandén T, Börgesson L, Dueck A, Goudarzi R, Lönqvist M, Nilsson U, Åkesson M, 2008. KBS-3H. Description of buffer tests in 2005–2007. SKB R-08-40, Svensk Kärnbränslehantering AB.

SKB, 2012. KBS-3H Complementary studies, 2008–2010. SKB TR-12-01, Svensk Kärnbränslehantering AB.

SKB, 2013. RD&D Programme 2013. Programme for research, development and demonstration of methods for the management and disposal of nuclear waste. SKB TR-13-18, Svensk Kärnbränslehantering AB.

Wescor, 2014. PSYPRO User's manual. Logan, UT: Wescor, Inc.

Section 9 – Packers description

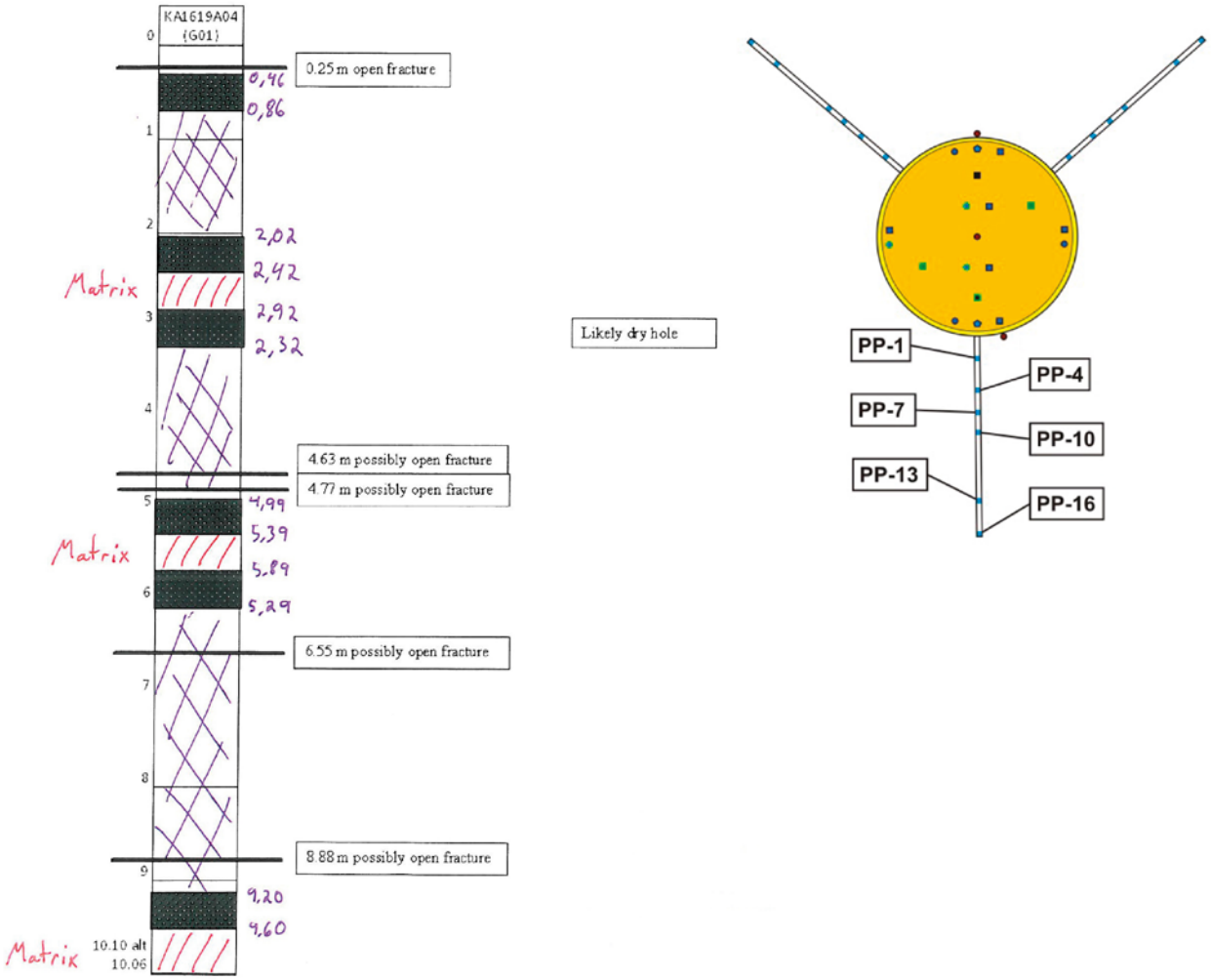

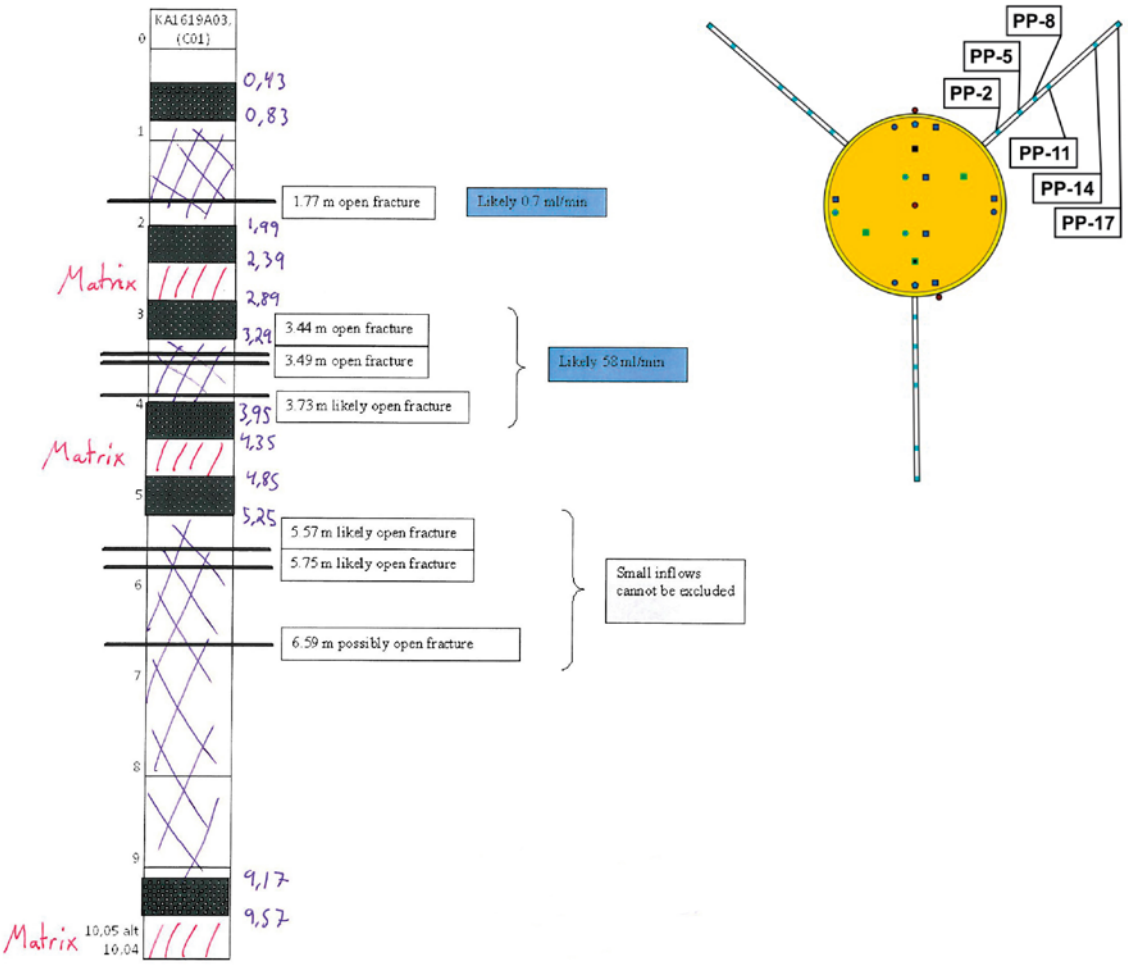
KA1619A03.
(C01)
0,43
0,83
1.77 m open fracture
Likely 0.7 ml/min
1,99
2,39
Matrix
2,89
3.44 m open fracture
3,29
3.49 m open fracture
Likely 58 ml/min
3.73 m likely open fracture
3,95
4,35
Matrix
4,85
5,25
5.57 m likely open fracture
5.75 m likely open fracture
Small inflows
cannot be excluded
6.59 m possibly open fracture
9,17
9,57
Matrix
10.05 alt
10.04
PP-8
PP-5
PP-2
PP-11
PP-14
PP-17

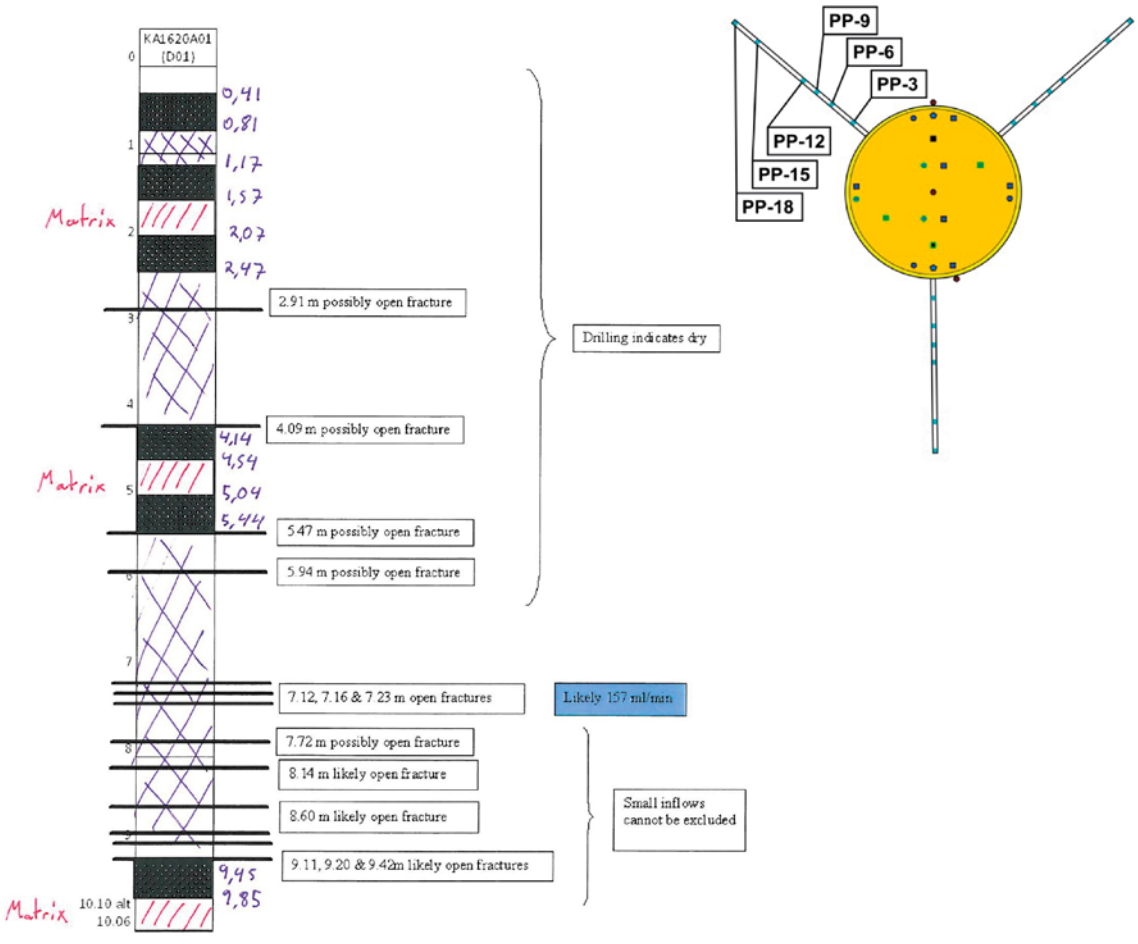
KA1620A01
(D01)
0,41
0,81
1,17
1,57
Matrix
2,07
2,47
2.91 m possibly open fracture
Drilling indicates dry
4.09 m possibly open fracture
4,14
4,54
Matrix
5,04
5,44
5.47 m possibly open fracture
5.94 m possibly open fracture
7.12, 7.16 & 7.23 m open fractures
Likely 157 ml/min
7.72 m possibly open fracture
8.14 m likely open fracture
Small inflows
cannot be excluded
8.60 m likely open fracture
9.11, 9.20 & 9.42m likely open fractures
9,45
9,85
Matrix
10.10 alt
10.06
PP-9
PP-6
PP-3
PP-12
PP-15
PP-18

Arkitektkopia AB, Bromma, 2017

SKB is responsible for managing spent nuclear fuel and radioactive waste produced by the Swedish nuclear power plants such that man and the environment are protected in the near and distant future.

skb.se